Semifluorinated Polymers and Hydrophilic High Capacity Ion-Exchangers as Ion-Sensing Membranes for Measurements in Harsh Sample Conditions

A DISSERTATION
SUBMITTED TO THE FACULTY OF
UNIVERSITY OF MINNESOTA
BY

Jesse L Carey III

IN PARTIAL FULFILLMENT OF THE REQUIREMENTS
FOR THE DEGREE OF
DOCTOR OF PHILOSOPHY

Philippe Bühlmann, Adviser

January 2016

Acknowledgements

During my doctoral studies I have had the benefit of receiving assistance and support from the following people:

First and foremost, I must thank my advisor Phil Bühlmann. His strong dedication to the fundamental principles of science, never ending search for knowledge and strong work ethic have been inspiring. The guidance and support that I have received from Phil have helped me grow not only as a scientist but as a person.

I must also give special thanks to Dr. Eric Olson, Dr. Xu Zou and Elizabeth Lugert-Thom whose guidance and friendship were instrumental in getting me started in the lab.

I would also like to thank the following people for their contributions to the work in this thesis:

Dr. Thomas P. Krick, Dr. Joseph Dalluge and Sean E. Murray from the University of Minnesota Mass Spectroscopy facilities, for their assistance with the MALDI Mass Spectroscopy in Chapter Three and several other projects.

Dr. Letitia Yao of the University of Minnesota Chemistry NMR Lab, for her assistance in many projects.

Shogo Ogawara and Dr. Xu Zou, whose work with many of the potentiometric measurments with hydrophilic high capacity membranes and many conversations on the subject made Chapter Four possible and led the way for the current pulse reference electrode disscused in Chapter Six.

Dr. David R. Whitcomb and his colleages at Carestream Health, whose knowledge on the subject of nanoparticle synthesis was fundamental for the succes of the sensor and nanoparticle synthesis described in Chapter Five.

Professor Lee Penn, whose knowledge on the subject of nanoparticle synthesis and her expertise in micoroscopy was fundamental for the succes of the sensor and nanoparticle synthesis described in Chapter Five.

Suyue Chen, for taking the transmission electron microscopy images presented in Chapter Five, as well as for the many hours of insightful discussion on the topic of nanoparticle synthesis and using potentiometric sensors to monitor them.

Ronald Bystrom of the University of Minnesota Physics Machine Shop, for his assistance in designing and creating the electrode bodies used in Chapter Three and Chapter Five.

Dr. Jon Thompson, Dr. Conor Smith and Dr. Doug Fryer of United Science, for allowing me to use their ion-chromatography system used in Chapter Five and aiding me in its setup.

The University of Minnesota Research Analytical Laboratory, for performing the colorimetric measurements in Chapter Five.

Dr. David Giles, for his aid in interpretation of differential scanning calorimetry spectra in Chapter Three and Chapter Five.

I would also like to thank my colleagues in the Bühlmann research group and the Chemistry department in general, whose support and friendship have made my time in graduate school truly enjoyable and have taught me much about the world.

I owe a great deal to my family, especially my parents, who have always supported me in my academic efforts. Without their love, devotion, and generosity I would not be where I am today.

Lastly, I must thank Laurel, as without her love and support in all aspects of my life this would have not been possible.

Dedication

This thesis is dedicated to my parents,

Jesse L Carey jr. and Linda Carey

And to

Laurel Elaine Hundley

Abstract

The research presented in this thesis is focused on the development and use of ion-selective electrodes (ISEs) in harsh conditions, such as measurements in organic solvents, biological media, and samples containing lipophilic ions and at high temperatures. This thesis focuses on the study of two classes of ISE membranes to overcome challenges presented by these conditions, semifluorinated polymer membranes and hydrophilic high capacity ion-exchanger (HHCIE) membranes. First, a brief overview of the working mechanism and components of ISEs, as well as the problems caused by harsh sample conditions is given. Also, included is a discussion on fluorous membrane ISEs, which show resistance to biofouling, HHCIE membranes and polymer background relevant to ISEs. Semifluorinated polymers were synthesized by attachment of fluorinated side chains to the lipophilic polymer, poly(4-vinylphenol). However, the percent conversions of these reactions are not high enough to produce polymers that are suitable for use as ISE membranes. Several semifluorinated monomers were synthesized, polymerized into semifluorinated polymers and then fabricated into ISEs. These electrodes can utilize both fluorophilic and lipophilic ionophores, allowing for a wider range of possible analyte ions then previously available to fluorous membrane ISEs. Ion-exchanger electrodes made from these polymers show a wide selectivity rage, up to 14 orders of magnitude. Study of HHCIE membranes found them to be highly resistant to the effect of Donnan failure (co-ion interference). HHCIE membranes were used to make a sensor that could monitor the concentration of NO_X^- species *in situ* during nanoparticle synthesis reactions at 150 °C in propylene glycol. It is also shown that nitrate ions present in this reaction are reduced to nitrite. A current pulse

reference electrode with a HHCIE membrane was developed which should have advantages over similar electrodes made with lipophilic membranes when measuring in biological media.

Table of Contents

List of Tables

List of Figures

List of Symbols and Abbreviations

A	Membrane surface area
a	Activity
AIBN	Azobisisobutyronitrile
$a_J(BG)$	Activity of the interfering ion J in the background
$a_I(\ DL\ )$	Activity of the primary ion I at the detection limit
Bu_4NHSO_4	Tetrabutylammonium hydrogen sulfate
C_{RX}	Chain transfer constant
D	Diffusion coefficient
DBS	Dibutyl sebacate
DHB	Gentisic acid
DMA	Dimethylacetamide
DMF	*N*,*N*-Dimethylformamide
DMI	Methylpyrrolidone
DMSO	Dimethyl sulfoxide
DOS	Dioctyl sebacate
E°	Standard potential
EDS	Energy-dispersive X-ray spectroscopy
emf	Electromotive force

F	Faraday's constant
f	Initiator efficiency
F113	1,1,2-Trichloro-1,2,2-trifluoroethane
HFE-7100	Methoxyperfluorobutane, mixture of n- and iso-butyl isomers
HHCIE	Hydrophilic high capacity ion-exchanger
ISEs	Ion-selective electrodes
k_d	Rate constant for the decomposition of the initiator
k_p	Rate constant for polymerization
$K_{I,J}^{pot}$	Selectivity coefficient
k_t	Rate constant of termination
KTpClPB	Potassium tetrakis(4-chlorophenyl)borate
MALDI-MS	Matrix-assisted laser desorption/ionization-mass spectrometry
M_n	Molecular weight (number-average)
M_w	Molecular weight (weight-average)
Mn(III)TPPCl	5,10,15,20-Tetraphenyl-21*H*,23*H*-porphine manganese(III) chloride
NaTFPB	Sodium tetraphenylborate
n_i	degree of polymerization
NMP	Dimethylimidazolidinone
o-NPOE	*o*-Nitrophenyl octyl ether
PEEK	Polyether ether ketone

PDI	Polydispersity index
PVC	Polyvinylchloride
PVP	Polyvinylpyrrolidone
R	Gas constant
SEC	Size exclusion chromatography
T	Temperature
t	Current pulse time
TDDMACl	Tridodecylmethylammonium chloride
TEM	Transmission electron microscopy
T_g	Glass transition temperature
THF	Tetrahydrofuran
$\bar{v}$	Kinetic chain length
$\bar{v}_{tr}$	Kinetic chain length with chain transfer
z_I	Charge of the ion
ϕ	Electrical potential
μ_I	Chemical potential
μ_I°	State chemical potential
μ_I'	Electrochemical potential
γ_S^D	Dispersive surface energy

1 CHAPTER ONE:

Introduction

1.1 Ion-Selective Electrodes (ISEs)

1.1.1 ISE Overview

Ion-selective electrodes (ISEs) are widely used analytical devices, making over a billion measurements every year.[1] A large amount of this use is in the medical field measuring ion concentrations in blood. In fact, a vast majority of clinical laboratories in the United States use ISEs to measure sodium and potassium concentrations.[2] In 1991, 200 million clinical analyses of potassium ion concentrations by polymeric ISEs were made in the United States alone.[3] ISEs are also widely used in industrial and food processes, and for environmental monitoring.[1, 4, 5] ISEs have been developed for a wide range of ions. Several approaches, such as buffering the concentrations of ions in the inner filling solution or solid contact electrodes, have been developed to allow ISEs to achieve low limits of detection, reaching as low as ppt levels.[6-9] ISEs can mostly be divided into three main groups: glass electrodes, such as the ubiquitous glass pH electrode, crystalline electrodes, such as fluoride selective electrodes that utilize lanthanum fluoride crystals, and polymeric membrane ISEs, such as those based on plasticized PVC, commonly used to measure the concentration of potassium in blood. The rest of this discussion will focus on ISEs of the third type, polymeric membrane ISEs.

While ISEs have found great success in the clinical environment, their function is often still degraded when used in biological media, especially for prolonged periods of time. This problem is called biofouling. Also, polymeric ISEs have found only limited use in organic solvents and at high temperatures. They can also suffer from interferences caused by highly lipophilic ions. The principles of basic ISE function and composition are

detailed below, as well as details about the use of ISEs in harsh sample environments and background on strategies to overcome these problems. Also discussed are reference electrodes commonly used with ion-selective electrode measurements and the problems that can occur when they are used in such sample matrixes. Additionally, background on polymerization techniques useful for synthesizing polymers for ISE membranes is included.

1.1.2 The Nernstian Response

ISEs are a type of potentiometric sensor which respond to the activity of ions in a solution. One of the most important components of the ISE is its membrane. ISEs function under near zero current conditions.[1] To use an ISE, three major components are necessary: the ISE, an external reference electrode, and a potentiometer (Figure 1.1). The cell diagram and potentials can be written as:

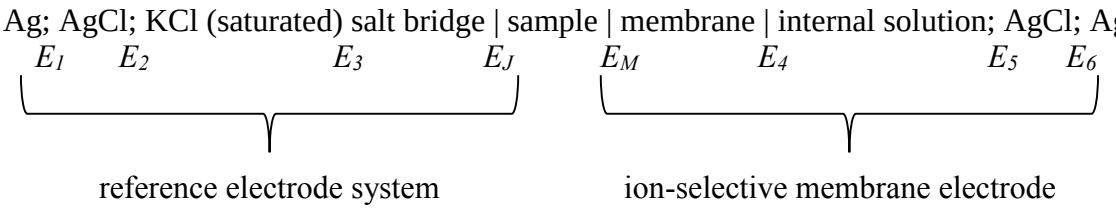

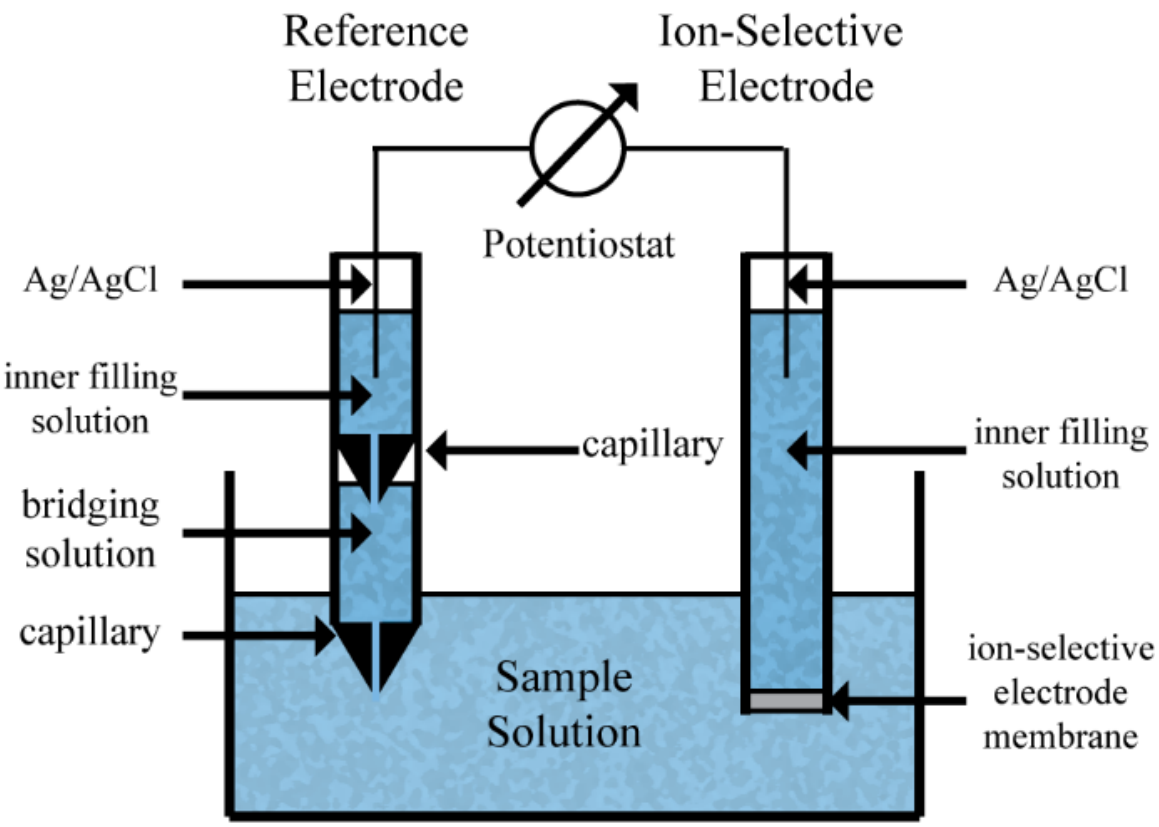

Figure 1.1: Diagram of typical ISE setup.

The electromotive force (emf) of the system is the sum of the individual potentials at each of the interfaces. Only two of the potentials, the membrane potential, E_M, and the liquid junction potential of the sample/bridge junction, E_J, are dependent on the sample. The other potentials, which are independent of the sample, can be combined into one constant, E_{const}. The emf measured by the potentiometer is therefore:[1]

$$emf = (E_1 + E_2 + E_3 + E_4 + E_5 + E_6) + E_J + E_M = E_{const} + E_J + E_M \qquad (1.1)$$

E_J is due to the difference in the ionic composition of the salt bridge and the sample solution, and can be held at a small constant value by using a concentrated electrolyte with ions of similar mobilities, or estimated by use of the Henderson formalism:[10]

$$E_{\text{junction}} = \frac{\sum_{\text{i}} \frac{|z_{\text{i}}|u_{\text{i}}}{z_{\text{i}}}\left[c_{\text{i,bridge}} - c_{\text{i,sample}}\right]}{\sum_i |z_{\text{i}}|u_{\text{i}}\left[c_{\text{i,bridge}} - c_{\text{i,sample}}\right]} \frac{\text{R}T}{\text{F}} \ln \frac{\sum_{\text{i}}|z_{\text{i}}|u_{\text{i}}c_{\text{i,sample}}}{\sum_i |z_{\text{i}}|u_{\text{i}}\, c_{\text{i,bridge}}} \tag{1.2}$$

where z_{i} is the charge of the ion, u_{i} is the mobility of the ion, $c_{\text{i, bridge}}$ is the concentration of the ion in the bridging solution, $c_{\text{i, sample}}$ is the concentration of the ion in sample solution, R is the gas constant, T is the temperature and, F is Faraday's constant (96,485.3365 C/mol). Therefore the main contributor to the emf is the membrane potential, E_M, which can be broken down into three parts. The first part, the phase boundary potential at the membrane/inner filling solution interface, is usually independent of the sample.[11, 12] The second part, the diffusion potential, is negligible as long as there is no concentration gradient within the membrane.[11] The last part, the phase boundary potential, E_{PB}, at the membrane/sample interface is sample dependent. The first two portions of E_M can therefore be included into E_{const} giving:

$$emf = E_{const} + E_{PB} \tag{1.3}$$

where E_{PB} is the phase boundary potential of the sample/membrane interface. E_{PB} can be derived though thermodynamics. The electrochemical potential of an ion, I, in the aqueous phase, ${\mu_I}'_{(aq)}$, can be described by the equation:

$${\mu_I}'_{(aq)} = \mu_{I(aq)} + z_I \text{F}\phi_{(aq)} \tag{1.4}$$

where z_{I} is the charge of the ion, $\phi_{(aq),}$ is the electrical potential, F is Faraday's constant and $\mu_{I(aq)}$ is the chemical potential of the ion in the aqueous phase. This can be written as:

$$\mu_{I(aq)} = \mu_I^{\circ}{}_{(aq)} + \mathrm{R}T \ln\left(a_{I(aq)}\right) \quad (1.5)$$

where $\mu_I^{\circ}{}_{(aq)}$ is the state chemical potential, R is the gas constant, T is the temperature and $a_{I(aq)}$ is the activity of the ion, I, in the aqueous phase. Substituting (1.4) into (1.5) gives:

$$\mu_I'{}_{(aq)} = \mu_I^{\circ}{}_{(aq)} + \mathrm{R}T \ln\left(a_{I(aq)}\right) + z_I \mathrm{F}\phi_{(aq)} \quad (1.6)$$

This process can be repeated for the organic phase of the membrane, giving:

$$\mu_I'{}_{(org)} = \mathrm{R}T \ln\left(a_{I(org)}\right) + z_I \mathrm{F}\phi_{(org)} \quad (1.7)$$

At equilibrium, the electrochemical potentials are equal; thus E_{PB} can be calculated as the difference between the electrical potential of the phases, giving:

$$E_{PB} = \phi_{(org)} - \phi_{(aq)} = \frac{\mu_I^{\circ}{}_{(org)} - \mu_I^{\circ}{}_{(aq)}}{z_I \mathrm{F}} + \frac{\mathrm{R}T}{z_I \mathrm{F}} \ln\left(\frac{a_{I(aq)}}{a_{I(org)}}\right) \quad (1.8)$$

Substituting equation (1.8) into (1.3) yields:

$$emf = E_{const} + \frac{\mu_I^{\circ}{}_{(org)} - \mu_I^{\circ}{}_{(aq)}}{z_I \mathrm{F}} + \frac{\mathrm{R}T}{z_I \mathrm{F}} \ln\left(\frac{a_{I(aq)}}{a_{I(org)}}\right) \quad (1.9)$$

When the concentration of the ion in the organic phase remains constant, all of the sample independent portions of the potential are included in a new constant, E°, giving the well-known Nernst equation:

$$emf = E^{\circ} + \frac{\mathrm{R}T}{z_I \mathrm{F}} \ln\left(a_{I(aq)}\right) \quad (1.10)$$

Therefore at 20 °C, an ISE would ideally display a so-called "Nernstian" response slope of 58.1 mV per 10-fold change in the activity of a monocation.[13]

1.1.3 Selectivity

1.1.3.1 Selectivity Definition

The most important characteristic of an ISE is its selectivity towards ions. Selectivity is the preference for the primary ion, I, over an interfering ion, J. This is

controlled by two factors, the free energy of transfer, and the strength that the ionophore binds to the ion. The free energy of transfer is the difference of the dehydration and solvation energy of the ion moving from the aqueous phase of the sample to the membrane phase. The lower the free energy of transfer of an ion, the more favored this process is and therefore the higher the selectivity towards the ion. For an electrode with no ionophore, the selectivity follows the Hofmeister series of free energy of transfer. For a cation-exchange electrode this is $Cs^+ > Rb^+ > K^+ > Na^+ > Li^+$.[13] By adding an ionophore the free energy of transfer for the target ion is reduced, thus increasing the selectivity for that ion.

The selectivity is quantified by the selectivity coefficient, $K_{I,J}^{pot}$, which is always less than one if the electrode has a higher selectivity for the primary ion, I, than the interfering (or discriminated) ion, J. This constant originated from the semiempirical Nicolskii-Eisenman equation, in which the activity term in the Nernst equation (1.10) is replaced by the selectivity-weighted activities of the two ions.

$$E = E^\circ + \frac{\mathrm{R}T}{Z_1\mathrm{F}} \ln\left(a_I(\,IJ\,) + K_{I,J}^{pot} a_J(IJ\,)^{\frac{Z_I}{Z_J}}\right) \tag{1.11}$$

This gives the potentiometric response of an ISE exposed to a sample containing ions I and J, where $a_I(\,IJ\,)$ and $a_J(IJ)$ are the activities of I and J in the mixed solution. This equation fails, however, when the charges of the ions are not the same and both of the ions' activities significantly contribute to the emf, giving different results depending on which ion is treated as the primary ion.[14] Setting equation (1.11) equal to the Nernst equation (10) can relate the activity of the ions in the mixture to the activity of the primary ion by itself giving:

$$a_I(I) = a_I(IJ) + K_{I,J}^{Pot} a_J(IJ)^{z_I/z_J} \tag{1.12}$$

If two solutions, one with only ions I and one with only ions J, give the same emf then $a_I(IJ)$ becomes zero and $a_J(IJ)$ is equal to $a_J(I)$. Therefore equation (1.12) can be rearranged to:

$$K_{I,J}^{Pot} = \frac{a_I(I)}{a_J(J)^{z_I/z_J}} \tag{1.13}$$

The Nernst equation (1.10) can be solved for the activity of each of the ions giving:

$$a_I(I) = \exp\left\{\frac{z_I \mathrm{F}(E - E_I^\circ)}{\mathrm{R}T}\right\} \text{ and } a_J(J) = \exp\left\{\frac{z_J \mathrm{F}(E - E_J^\circ)}{\mathrm{R}T}\right\} \tag{1.14}$$

where E_I° and E_J° are standard potentials for ions I and J. These equations (1.14) can be substituted into (1.13) giving:

$$K_{I,J}^{pot} = \exp\left[\frac{(E_J^\circ - E_I^\circ) z_I \mathrm{F}}{\mathrm{R}T}\right] \tag{1.15}$$

The Nernst equation (10) can be solved for both E_I° and E_J° and inserted into (1.15) to give:

$$K_{I,J}^{pot} = \frac{a_I(I)}{a_J(J)^{z_I/z_J}} \exp\left[\frac{(E_J - E_I) z_I \mathrm{F}}{\mathrm{R}T}\right] \tag{1.16}$$

where E_I and E_J are the emf responses observed for solutions containing only I or J at the activity $a_I(I)$ or $a_J(J)$, respectively. When the activity of both solutions is 1 M then equation (1.16) reduces back to (1.15). These equations are useful for experimentally determining $K_{I,J}^{pot}$. There are two ways to experimentally determine $K_{I,J}^{pot}$, the separate solution method and the fixed interference method.[1] Both of these methods should, ideally, give equal values for $K_{I,J}^{pot}$.

1.1.3.2 Separate Solutions Method

In the separate solutions method the calibration curves for ions I and J are determined independently by using solutions only containing one of the ions. These calibration curves can be extrapolated to 1 M and the values of E_I° and E_J° can be determined, as at 1 M, E_I° and E_J° are equal to E_I and E_J respectively. Then $K_{I,J}^{pot}$ can be determined with equation (1.15).[1, 14] The response slope for both ions I and J must be Nernstian to yield an accurate selectivity coefficient.

Exposure to the primary ions before measurements of the discriminated ions can have a large effect on the determined selectivity coefficients, especially in highly selective systems where low levels of the primary ion displaced from the membrane into the sample solution can determine the potential at the membrane.[15] This can also cause sub-Nernstian slopes for the discriminated ions due to the discriminated ions' inability to fully displace the primary ion from the membrane. To avoid these problems when determining selectivity coefficients, the inner filling and conditioning solution of the electrode should therefore be one of the discriminated ions and the electrodes should not be exposed to the primary ion until after the measurements of the discriminated ions.[14, 15]

1.1.3.3 Fixed Interference Method

In the fixed interference method, the calibration curve for the primary ion, I, is determined in a solution with a constant background concentration of the interfering ion, J.[14] The response in solutions containing only ions I or only ions J should be Nernstian. The background concentration of ion J should fall within this Nernstian response range. In the solution with both ions, when the concentration of I is high the response should be

Nernstian, at low concentrations of I the potential is constant due to the constant concentration from J. $K_{I,J}^{pot}$ can be determined by the fixed interference method by using the equation:

$$K_{I,J}^{pot} = a_I(DL)/a_J(BG)^{\frac{z_I}{z_J}} \quad (1.17)$$

where $a_I(DL)$ is the activity of the primary ion I at the detection limit. This is determined by extrapolating the Nernstian portion of the plot to the emf of the background interference, and $a_J(BG)$ is the activity of the interfering ion J in the background (Figure 1.2). This method is particularly useful for determining the selectivity for pH electrodes as the response to the interfering ions can only be determined in the presence of the analyte. The complement of the fixed inference method is the fixed primary ion method. The underlying principles for this method are the same as for the fixed inference method, the difference being that the primary ion's concentration is held constant and the concentration of the interfering ion is varied.[4]

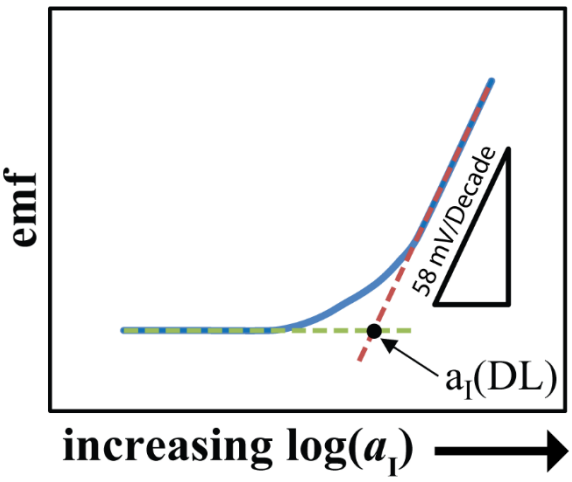

Figure 1.2: Example of fixed interference method: the blue line denotes the electrode's response at various concentrations of the primary ion, I. The dashed lines represent the extension of the linear portion of the Nernstian range (red) and the potential at the detection limit (green).

1.1.4 Membrane Components

1.1.4.1 Polymer Matrix and Plasticizer

The main component of the membrane is the polymer matrix. The main purpose of the polymer is to provide the mechanical support of the membrane.[1] Polyvinylchloride (PVC) is the most popular polymer for use in ISE membranes due to its stability.[1] Other polymers such as polyurethane, silicone rubber and polyacrylates are popular as well; see Figure 1.3 for structures.[16-19] The glass transition temperature (T_g) is an important property of polymers used as ISE membranes. At or below the glass transition temperature (T_g) the polymer is hard, rigid and amorphous. Only some polymers have a glass transition temperature, but other polymers may crystallize. Above this temperature the polymer is

soft and flexible.[20] Although many of the physical properties of the polymer are like that of a solid, on a molecular scale the polymer is more like a liquid. Several factors influence the T_g of a polymer. For example, increased backbone flexibility decreases T_g, large rigid side chains increase T_g and polymers with weak interactions tend to have a lower T_g.[21] The glass transition temperature can also be lowered by adding low molecular weight molecules, called plasticizers. For a polymer to be used as an ISE membrane its T_g must be below the operating temperature of the ISE to allow for the ionic species to move through the membrane allowing for suitable conductivities.[20] If the T_g is too high above the operating temperature, the electrical resistance will be too large for the material to be used with an ISE. For example it has been shown in the literature that near the T_g the electrical resistance of poly(methyl methacrylate) membrane drops by six orders of magnitude.[22]

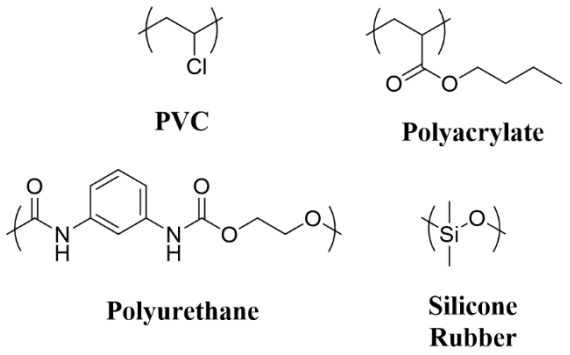

Figure 1.3: Commonly used polymers for ISEs.

If the T_g of the polymer is too high, a plasticizer may be used to lower it to an appropriate value. Plasticizers are low weight organic molecules which must be soluble in the membrane. They should also have a high boiling point to avoid evaporation.[1] The plasticizer should be free of functional groups that could bind with ionic species, as this

would affect the selectivity of the membrane.[1] The polarity of the plasticizer can also affect the selectivity of the membrane, so this should also be taken into account when choosing a plasticizer.[1] For these reasons the selectivity coefficients of ISEs made with PVC and different plasticizers, such the commonly used *o*-nitrophenyl octyl ether (*o*-NPOE), dibutyl sebacate (DBS), chloroparaffin, or dioctyl sebacate (DOS)—see Figure 1.4 for structures—can vary by orders of magnitude.[1,23] Typically the plasticizer will make up the majority of the membrane; often the sensor has optimal properties when the weight percent of the membrane that is plasticizer is about 66%, while the PVC is only about 33%.[1, 24] Other polymer systems have also been used, such as silicone rubber or acrylate copolymers, which do not need plasticizers to function due to the suitable glass transition temperature of these polymers.[16, 25] The choice of plasticizer also effects the working range of the electrode. However, it is not simply determined by the polarity of the plasticizer, but also complexation of the ions by the plasticizer and or ionic sites.[1] For example, the working range of pH selective sensors made with PVC plasticized with *o*-NPOE in a 0.1 M KCl background is larger than that of membranes made with PVC plasticized with the less polar DOS.[26, 27]

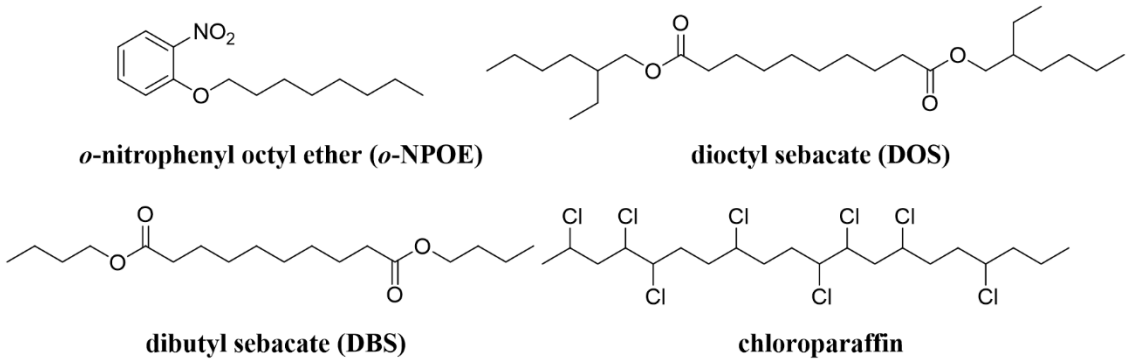

Figure 1.4: Commonly used plasticizers for ISEs.

1.1.4.2 Ionic Site

Ionic sites provide the ion exchange capabilities of the membrane and reduce the resistance of the membrane. They serve as the counter ion for the analyte ion, causing the membrane to have permselectivity and stopping counter ions from entering the membrane in significant quantities. This is often referred to as Donnan exclusion.[1, 28] Ionic sites keep the total ion concentration in the membrane constant over the linear range of the electrode, allowing for the Nernstian response. In ionophore-free membranes and membranes with electrically neutral ionophores anionic sites are used to create ISEs that are selective to cations and cationic sites are used to create ISEs that are selective to anions. The ionic sites should not significantly interact with the analyte or interfering ions, as to not affect the selectivity of the sensor. Tetraphenylborate derivatives are commonly used to create sensors that respond to cations, and tetraalkylammonium salts are commonly used for sensors that respond to anions, see Figure 1.5.[1] The ion sites must be highly lipophilic so that they do not leach out of the ISE membrane into the sample solution. Ionic sites with low lipophilicity will limit the lifetime of the sensor. Covalently attaching the ionic sites to the polymeric substrate has been shown to increase the lifetime of the sensor, due to reduced leaching of the ionic sites into the sample solution.[1, 29]

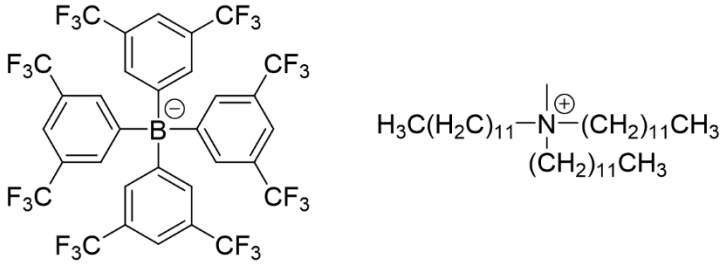

Figure 1.5: Commonly used lipophilic ionic sites, anionic site (left), cationic site (right).

1.1.4.3 Ionophore

Ionophores determine the selectivity of the ISE by reducing the free energy of transfer of the target ion from the sample solution into the membrane.[13] Ionophores ideally selectively bind the target ion. This binding can occur by ion–dipole interactions, hydrogen bonds, ligation to metal cations, and the formation of covalent bonds.[4] The ionophore must be soluble in the polymer membrane, and should strongly yet reversibly complex with the ion of interest. A greater selectivity improves the detection limit of the ISE. It does not, however, necessarily improve the working range of the electrode. Very strong binding of the ion can result in interference due to the co-ion extracting into the membrane. This is referred to as Donnan failure.[30]

The ratio between the ionic site and the ionophore also has an important effect on the selectivity of the sensor. The ideal ratio is determined by the stoichiometry in the formed complex between the target analyte and the ionophore, the charge of the analyte ion, as well as the stoichiometry in any formed complex between any interfering ions and the ionophore and the charge of the interfering ion.[1] In cases with neutral ionophores the concentration of the ionophore should be higher than that of the analyte ion that can transfer into the membrane which is determined by the ionic site concentration. This allows for a majority of the target ion in the membrane to exist in its complexed form. Generally, if the target ion complexes with multiple molecules of the ionophore a higher amount of ionophore will be needed.[4] The ionophore only makes up a small amount of the membrane, typically only about 1% by weight.[1] Both neutral and charged ionophores have been

utilized in ISEs. However, it should be noted that in many cases when using charged ionophores the added ionic sites should have the same charge sign as the analyte ion, the opposite of ISEs made with neutral ionophore and ion-exchangers, to ensure that the analyte ion will be predominantly in its complexed form. However, there are some situations, such as a primary divalent ions and an interfering monovalent ions both complexing in a one-to-one ratio with the ionophore, where sites with the same charge as the primary ion should be used to give the best selectivity.[1, 31]

Covalently attaching the ionophore to the polymeric substrate has been shown to increase the lifetime of these sensors due to inhibition of leaching of the ionophore into the sample solution, as well as improving the detection limit of the sensor by reducing ion fluxes.[1, 29, 32]

1.1.5 Harsh Sample Matrixes for Ion-Selective Electrode Measurements

1.1.5.1 Biofouling

Biofouling occurs when ISEs are exposed to biological samples such as blood, urine or cheese. It causes a loss of selectivity, increases signal drift, and reduces the lifetime of the ISE.[33] This effect is due to partitioning of neutral lipophilic compounds into the membrane of the ISE and the leaching of membrane components, such as the ionic site, ionophore and plasticizer, into the sample media, as well as by adsorption of cells or proteins onto the membrane.[33, 34] Biofouling limits the use of ISEs in fields such as manufacturing and food processing. For example, when an ISE is exposed to cheese, a decrease in the selectivity of H^+ ISE by up to 4 orders of magnitude has been observed and when a K^+ ISE made with commercially available K^+ ionophore, valinomycin, was exposed

to urine a 6-fold increase in Na^+ interference was observed.[33, 35] While most neutral compounds do not cause interference in potentiometric sensors, those that are highly lipophilic can. Several of these compounds can be found in urine. Chloroparaffin-PVC ion-exchangers that have been exposed to urine extracts have been shown to have observed drifts of 240 mV over a 3 hour time period.[33] pH modification experiments have shown that these interferents are basic compounds that are extracted as neutral species and interfered as cationic species.[36]

One method that has been shown to be effective at reducing biofouling in urine is to remove the interfering compounds using several extraction techniques before measurement; this reduced the signal drift and improved selectivities when compared to the pure urine.[37] However removing the compounds is not always ideal, practical or possible, such as when dealing with inline manufacturing or if using ISEs as long term implantable sensors. Sensors utilizing polymeric membranes (silicone rubber, PVC or polyurethane) that continually release nitric oxide have been shown to reduce blood platelet adhesion as well as the formation of fibrous tissue around the sensors.[38, 39] Covalently attached ionic sites and ionophores have been shown to improve the lifetime of sensors as they stop leaching of the membrane components into the lipophilic biological media.[29, 40, 41] It has also been shown that buffering the inner filling solution at a biologically relevant pH can help substantially reduce the drift due to some inferents, such as cholic acid.[42] In some cases, ISEs made with higher polarity plasticizers, such as *o*-NPOE, have higher drift due to charged species (proteins) adsorbed on the electrodes' surface during blood serum measurements than those made with lower polarity plasticizers, such as DOS.[1, 23] The use

of ISEs with fluorous membranes looks to be a promising way to reduce the effects of biofouling; this will be covered in more detail in a later section.

1.1.5.2 High Temperature Measurements

Polymeric membrane ISEs are most typically used at ambient temperatures. Plasticized PVC membrane ISEs are not often used in applications with temperatures higher than 50 °C, although they have been on rare occasions used in systems as hot as 70 °C.[43-45] ISEs are likely not utilized at elevated temperatures due to weakening of the mechanical strength of the membrane, increased leaching of membrane components due to decreased viscosity of the membrane and increased solubility of the components in water, or thermal degradation of membrane components. Covalently attaching membrane components, as well as utilizing membranes that are plasticizer free or cross-linked may help improve the performance of ISEs at high temperatures.

At high temperatures the response slope of ISEs increases as described by the Nernst equation (Equation 1.10). It should be noted that the phase boundary potentials that make up E° are also dependent on temperature, and it is unlikely that the temperature response is consistent throughout the entire electrochemical cell. Therefore it is easy to predict the change in emf due to change in concentration when the temperature is constant, but difficult to predict the change in emf due to temperature change when the concentration is constant.

1.1.5.2 Organic solvents

While polymeric ISEs have found broad use in aqueous systems, their use in organic solvents has been rather limited; most potentiometric measurements in organic

liquids are performed with glass or crystalline electrodes.[46] The main difficulty with measuring in organic liquids with polymeric ISEs is the leaching of membrane components into the sample media, as well as weakening of the membrane due to swelling with solvent. Plasticizers used for most ISEs are miscible with many organic liquids. Use of polymeric ISEs based on PVC in organic solvents are limited within most of these reports to measurements in water/alcohol mixtures, usually with less than 50% alcohol.[45, 47-49] There have been several reports of electrodes based off silicone rubber for anions that have measured ions in 90% alcohol/water mixtures, 40% isopropanol/water mixtures, 60% acetone/water and 60% DMF/water mixtures. However, above these values the silicone rubber swells continuously and does not give a satisfactory response.[17, 46] ISEs for CN^- and F^- based on poly(acrylamide) showed Nernstian responses in propylene carbonate, acetonitrile, *N*,*N*-dimethylacetamide and *N*,*N*-dimethylformamide.[50] The success of these sensors is likely due to several factors that prevent the leaching of membrane components into the organic solvent. They do not utilize a plasticizer, and the ionophore and ionic sites are covalently attached to the polymer. Highly cross-linked polymers may be suitable for use in organic solvents as they are less likely to be soluble in these media.

The activity of ions is much more difficult to accurately calculate in organic solvents than in water. Of the many methods available for determining activity, only the most simple, the Debye–Hückel limiting law, is suitable for solvents other than water. This in turn causes difficulty in predicting changes in the liquid junction potential between the sample and reference electrode. This liquid junction potential can be quite large if the sample solvent and the solvent used in the bridging solution of the reference electrode are

not the same.[46] Therefore it is recommended that the same solvent be used for both, although this is not always possible if the reference electrode is incompatible with the solvent. Calibrations in organic liquids can be affected by extraction of impurities from the organic solvents into the sample membrane.[46]

1.1.5.4 Donnan Failure

When measuring in samples containing hydrophobic co-ions with ISEs, deviation from linearity at the upper detection limit occurs; this is known as Donnan failure.[51, 52] Many real world samples contain organic hydrophobic co-ions, such those of biological origin, limiting the use of ISEs in many applications. Donnan failure can be looked at in two different ways, the failure of co-ion exclusion from the membrane caused by the high lipophilicity of the co-ion, or high levels of salts consisting of the analyte ion and a co-ion in the membrane exceeding the ion exchange capacity of the membrane.[11, 52] Ionophores which tightly bind the analyte ion can lead to coextraction at high primary ion concentrations in the sample, increasing Donnan failure.[1] Once all of the ionophore is bound to primary ions the membrane contains ionophore–primary ion complex which can act as lipophilic ionic sites, and extract sample co-ions. The membrane is now permselective towards the co-ions giving the electrode a response to co-ions; see Figure 1.6. This limits the ability to use ionophores that bind the target ion extremely strongly. The makeup of the membrane and therefore, in many cases, the plasticizer used, also has an effect on the extent of Donnan failure, with more polar plasticizers more likely to suffer from Donnan failure.[1]

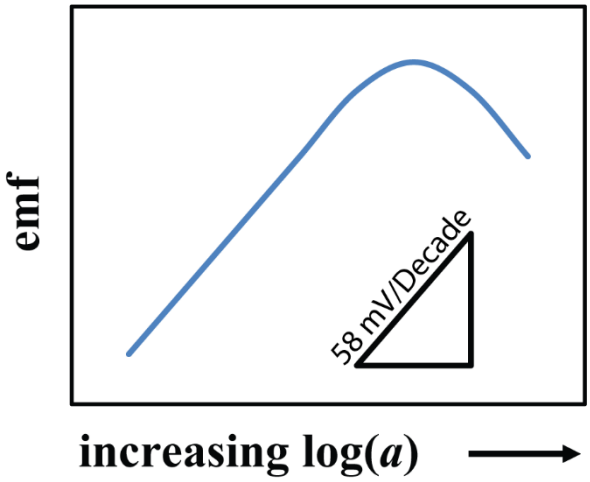

Figure 1.6: Depiction of response of cation selective ISE suffering from Donnan failure, i.e., showing response to co-ions at high activities.

1.2 Fluorous Membrane ISEs

1.2.1 Fluorous Compounds

Perfluorinated compounds have an extremely low polarity and polarizability.[53] This is shown well by the π^* scale for solvent polarity and polarizability, where cyclohexane defines 0, dimethyl sulfoxide defines 1, and water has a value of 1.09.[53] Perfluorinated compounds have negative values on this scale, such as perfluorotributylamine at -0.36 or perfluorooctane at an even lower -0.41.[53] This is due to the symmetry of the molecules and the extremely low polarizability of C-F bonds resulting from the high electronegativity of fluorine. These compounds have such low polarizabilities and polarities that they are not only immiscible with water but also many lipophilic compounds, such as hydrocarbons. The term "fluorous" is often used when these compounds are immiscible with their hydrocarbon counterparts.[54] The term "fluorophilic" refers to compounds that

preferentially solvate in the fluorous phase. Fluorophilic ions that allow for electrochemical experiments to be readily preformed in the fluorous phase have only fairly recently been developed.[55-57]

Fluorous polymers tend to have good thermal and chemical stability as well as low surface energy, relative permittivity, refractive indices, friction coefficients and dielectric constants.[58-61] This has led to a wide variety of uses for fluorous polymers and small molecules, including uses in biomaterials, batteries, coatings, contact lenses, drug delivery, electronics, fiber optics, full cells, lubricants and surfactants.[62-66] A variety of polymerization techniques can now be used to create fluorous polymers, narrow distribution of molecular weights.[67]

1.2.2 Fluorous Membrane ISEs

Recently, fluorinated polymers have been used as membranes in ISEs.[68] These fluorous membrane ISEs not only hold promise to reduce the effect of biofouling, but to also greatly improve selectivities over conventional PVC sensors. Interfering lipids and proteins are unable to dissolve in the extremely low polarity of the fluorous phase, preventing them from reducing the selectivities. Several ionophores that are soluble in the fluorous phase have been developed and used in ISEs; see Figure 1.7. Fluorous membrane ISEs have utilized both neutral and charged ionophores.[69, 70] Current fluorous membrane ISEs have been used to detect Ag^+, and carbonate, as well H^+ for pH measurements.[69-71] Fluorous ion-exchange electrodes have been used to measure perfluorinated acids such as perfluorocarboxylates and perfluorosulfonates.[55, 72,73] Ion pair formation in fluorous membrane based ISEs has been shown to be very strong, with ion pair formation constants,

K_{ip} (M^{-1}), five orders of magnitude larger than that of values previously reported organic solvents.[68] The main strategy employed for creation of the fluorophilic salts and fluorophilic ionophores is to attach several perfluoroalkyl chains, often referred to as ponytails, to existing suitable salts and ionophores. Both fluorophilic anionic and cationic sites have been synthesized to create sensors that respond to cations and sensors that respond to anions, see Figure 1.7.[55, 70, 72, 74] Fluorophilic electrolytes have also been synthesized, see Figure 1.7, and can be used to reduce the electrical resistance of the fluorous membrane, which is often quite high.[72, 74] Most of these membranes have utilized liquid compounds such as perfluoroperhydrophenanthrene or a linear perfluorooligoether as the main component of the membrane, however plasticized Teflon AF has been used as well.[68, 69, 75]

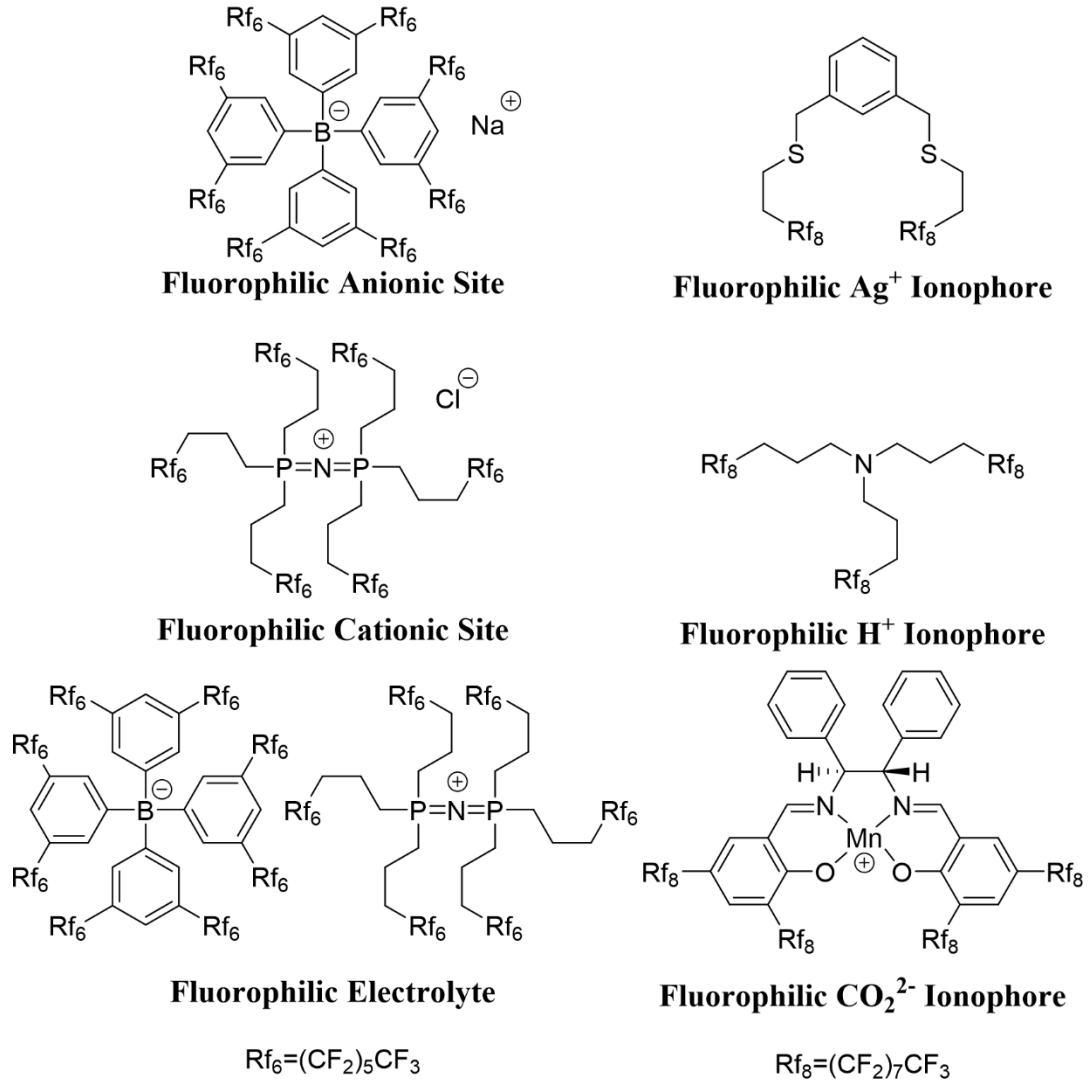

Figure 1.7: Fluorophilic membrane components: anionic site (top left), cationic site (middle left), electrolyte (bottom left), Ag^+ ionophore (top right), H^+ ionophore (middle right), and CO_2^- ionophore (bottom right).

1.2.3 Fluorous ISEs and Selectivity

Fluorous membrane ISEs have been shown to have improved selectivity characteristics compared to those of other lipophilic ISEs due to their low polarity.

Fluorous ion-exchange electrodes have shown extremely broad selectivity ranges (16 orders of magnitude) compared to that of more traditional lipophilic membranes based on PVC (8 orders of magnitude).[68] This is due to the high free energy of transfer for ions into the fluorous phase compared to more lipophilic membranes.[68] Because of the high transfer energy of hydrophilic ions, fluorous membrane ion-exchange electrodes have very high selectivities for fluorous ions such as perfluorooctanoate and perfluorooctanesulfonate, and can be used to measure trace amounts of these compounds in environmental samples.[73] Fluorous membrane ISEs utilizing fluorophilic ionophores have also shown excellent selectivity coefficients. An ISE for pH measurement based off of a fluorous membrane with the H^+ ionophore, $[CF_3(CF_2)_7(CH_2)_5]_3N$ showed selectivities that were greater than those of an equivalent non-fluorous ISE, and were of the same order of magnitude as the best ionophore-based sensor for pH that has been developed.[71] Fluorous membrane ISEs for silver and carbonate have shown some of the best selectivities for these ions as well.[69, 70] For example, a fluorous membrane based Ag^+ ISE has shown logarithmic selectivity coefficients of -9.4, -11.6, -12.9 and -13.0 versus Cs^+, K^+, Na^+, and Cu^{+2}, respectively.[69] This sensor has also shown very low limits of detection, 4.1 ppt.[69]

1.2.4 Fluorous ISEs and Biofouling

Fluorous membranes show great promise for reducing the effects of biofouling. Their extremely low polarity should reduce the amount of species that can adsorb on the surface of the membrane. Compounds that are prevalent in biological samples, such as amino acids, carboxylic acids, and sugars have low solubilities in fluorous compounds.[76] The solubility of linear alkane alcohols in fluorous solvents has been shown to drop with

increasing chain length.[36] Fluorous membrane ISEs have been shown to have much lower drift when exposed to extracts from urine than ISEs with lipophilic PVC based sensing membranes.[36] Fluorous ISEs have also been used to monitor silver ion concentrations in bacteria growth media while monitoring silver nanoparticle toxicity, as well as to show the effect that natural organic matter plays in this process due to its ability to complex silver ions.[77, 78]

1.2.5 Limitations of Fluorous Membranes ISEs

The majority of these sensors depend on a fluorous liquid membrane, such as perfluoroperhydrophenanthrene or a linear perfluorooligoether, supported on a porous Teflon disk.[71, 72] However, this limits the mechanical stability and life time of the membrane, thus hampering the development of a miniaturized version of the electrode which would be needed if the ISE was to be used for long term implantable sensors inside the body. The development of a self-supported fluorous membrane ISE would aid in miniaturization of the ISE. This would open a variety of new possible ways to use and implement ISEs with fluorous membranes, such as printing the membrane for micro fabrication. As mentioned above, plasticized Teflon AF has been used as an ISE membrane, however the selectivity of these sensors has been limited by impurities in those membrane.[75]

Currently, fluorous electrodes rely on the use of fluorophilic ionophores to achieve selectivity toward specific ions. Therefore, there is not a wide selection of suitable ionophores available, limiting their use to certain ions, unlike sensors that make use of the traditional lipophilic ionophores, which have been more thoroughly explored and are

available for a wide range of ions.[13] The range of fluorophilic ionophores could be expanded but this would require significant work in ionophore development. Also while both fluorophilic cationic and anionic sites have been developed, membranes made with the existing phosphonium cationic sites suffer from a short lifetime due to decomposition of the phosphonium ion in alkaline solutions.[55] This also limits the development of miniaturized fluorous ISEs, as a better fluorous electrolyte is needed to maintain sufficiently low resistance that is necessary for the sensors to function.

1.3 Polymers for ISEs

1.3.1 Molecular Weight

An important aspect when characterizing polymers is the molecular weight of the polymers. Synthetic polymers are synthesized in a method that results in molecules with varying degrees of polymerization, the number of repeat units in the polymer. Therefore the average molecular weight of the polymers in a given sample is always reported. There are two types of averages, the number-average molecular weight (M_n) and the weight-average molecular weight (M_w). M_n is defined as the sum of the mole fractions of polymers with a degree of polymerization i (x_i) times the mass of polymer chains with the degree of polymerization i (M_i); it can also be described as the sum of the number of polymers of a certain degree of polymerization (n_i) times the mass of a polymer of that degree of polymerization divided by the total number of polymers (18). This average would be achieved by picking each polymer and determining its molecular weight, and is the characteristic molecular weight for when the number of polymers is important. M_w is

defined as the weight fraction of polymers with a degree of polymerization i (w_i) times the mass of a polymer with the degree of polymerization i; it can also be described as the sum of the number of polymers of a certain degree of polymerization times the mass of a polymer of that degree of polymerization squared, divided by the sum of the number of polymers of a certain degree of polymerization (n_i) times the mass of a polymer of that degree of polymerization (1.18). This average would be obtained by picking a repeat unit at random and determining the molecular weight of the polymer it is a part of and is the characteristic molecular weight for when the size of the polymers is important.

$$M_n = \sum_i x_i M_i = \frac{\sum_i n_i M_i}{\sum_i n_i} \qquad M_w = \sum_i w_i M_i = \frac{\sum_i n_i M_i^2}{\sum_i n_i M_i} \tag{1.18}$$

M_n and M_w together give information on the distribution of the size of the polymers, or the polydispersity. The polydispersity index (PDI) is the ratio of M_w to M_n.

$$\text{PDI} = \frac{M_w}{M_n} \tag{1.19}$$

As M_w is always greater then M_n, the minimum value of the polydispersity index is one and would occur when all of the polymers are the same size. Polymer distributions with polydispersity indexes greater than 2 are considered broad and polymer distributions with polydispersity indexes less the 1.5 are considered narrow; however polymer distributions with PDI below 1.1 can be achieved.[21]

Common ways to determine the molecular weight of polymers include matrix-assisted laser desorption/ionization-mass spectrometry (MALDI-MS), end group analysis and size exclusion chromatography (SEC).[21] MALDI-MS can be used to determine both M_n and M_w of polymers. Due to their extremely low polarity, fluoropolymers are more difficult to analyze by MALDI then most polymers.[79] Few matrixes have been shown to be

effective for analyzing fluoropolymers with MALDI-MS, however gentisic acid (DHB) has shown to be an effective matrix, allowing for a strong signal to be obtained.[79]

End group analysis can be used to determine the M_n of the polymers. This is most often done by comparing the ratio of a ^{1}H-NMR signal from the polymer end group and a signal from the repeat unit.[21] This can be difficult for polymers with high molecular weight due to the small signal from the end group compared to the repeat unit or when there is peak overlap. Also, this method gives no information on M_w.

SEC can also be used to determine the molecular weight of fluorous polymers.[80] In SEC, polystyrene standards are often used to calibrate the column; therefore, all molecular weight data will be relative to polystyrene. The M_n values obtained by SEC will likely be affected by the differences in the hydrodynamic radius of the fluorous polymer and polystyrene in the solvent.[21, 80] Fluoropolymers are not likely to be soluble in most common solvents due to their fluorous nature. Unfortunately, most fluorous solvents are prohibitively expensive for use in chromatography. One possible solvent for fluoropolymers is supercritical carbon dioxide, as fluorous polymers tend to be soluble in it, and it has been used as a solvent for SEC before; however, such a system would be difficult and time consuming to set up.[81, 82]

1.3.2 Polymerization

There are many different methods of polymerization, including condensation reactions, free radical polymerization, stable free radical polymerization, anionic polymerization, and atom transfer polymerization. Anionic, stable free radical, and atom transfer polymerization are types of living polymerizations.[21] A living polymerization is a

chain-growth polymerization which ideally occurs without irreversible chain-termination or chain transfer reactions.[83] Living polymerizations can be used to create polymers with low polydispersity indexes (often less than 1.04) as well as block-copolymers, graft and star polymers.[84-87]

While living polymerizations are very useful, the simpler free radical polymerization is sufficient for many applications, such as when the polydispersity is not very important or well-defined polymeric structure is not needed. This type of polymerization is widely utilized in industry, making up a large amount of produced polymers. 40 billion of the 110 billion pounds of polymers made in the United States were formed by free radical polymerization in 2001.[88] In free radical polymerization, an initiator is used to start the polymerization by forming radicals which react with monomers.[21] These monomers then gain a radical and then react with another monomer, adding to the polymer chain (Figure 1.8, top). This process, called propagation, continues, causing the chain to grow until termination occurs. Free radical polymerization is not a living polymerization technique, meaning that the active polymer chains can self-terminate, leading to much larger polydispersity than a living polymerization. Termination can occur in several ways. The first, called combination, is when two polymer chains with radicals react with each other to form one chain (Figure 1.8, middle). The second, called radical disproportionation, is when two polymer chains with radicals react with each other and one chain abstracts a hydrogen from the other, leaving no radicals; one chain is left with a saturated end group and the other one with an unsaturated end group (Figure 1.8 bottom). These two types of termination can also occur with the initiator. If all termination occurred by combination,

the polydispersity would be 1.5. If it all occurred by disproportionation then the polydispersity would be 2.[21] For these reactions, the chain length, and therefore the average molecular weight, of the polymer is directly proportional to the monomer concentration and inversely proportional to the inverse of the square root of the initiator concentration, as shown by the kinetic chain length, $\bar{v}$:[21]

$$\bar{v} = \frac{k_p[\mathrm{M}]}{2(f k_t k_d[\mathrm{I}])^{1/2}} \tag{1.20}$$

where k_p is the rate constant for polymerization, k_t is the rate constant of termination, k_d is the rate constant for the decomposition of the initiator, f is the fraction of initiator that reacts with the monomer (initiator efficiency), [M] is the concentration of the monomer and [I] is the concentration of the initiator. The higher the monomer concentration the more likely the radical chains are to react with them before terminating, increasing the average length of the polymer chains. Increasing the initiator concentration increases the number of radical chains, giving the chains less time to react with monomers before they self-terminate, decreasing the molecular average length of the polymer. The final method of termination is reaction with impurities or inhibitors which are purposefully added to give short chain lengths.

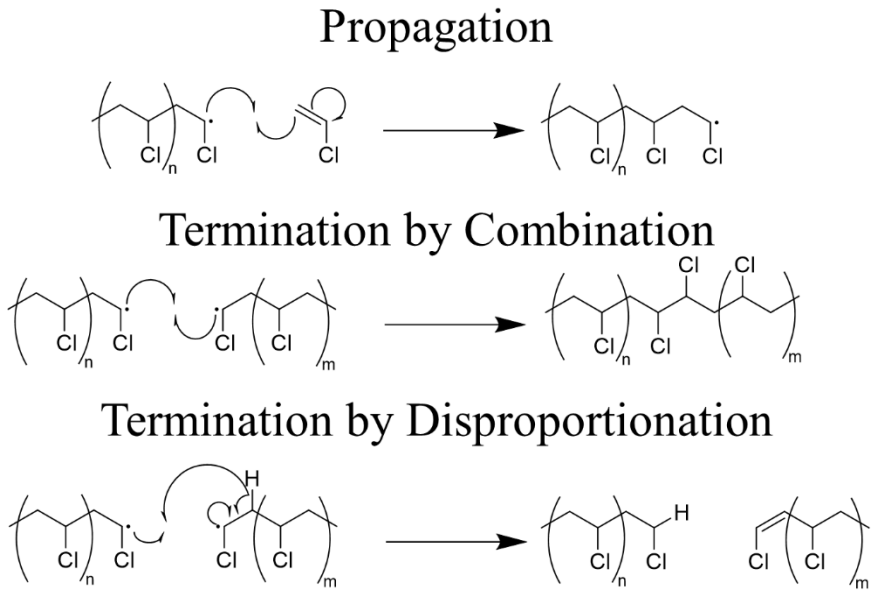

Figure 1.8: Example scheme of polymer chain propagation (top), termination by combination (middle), termination by disproportionation (bottom).

The radical chains can undergo another processes during propagation called chain transfer. In chain transfer, the radical is transferred from the growing chain to either a monomer, unreacted initiator, solvent molecule or compounds added to promote chain transfer, by extraction of hydrogen or other atoms. The polymer chain is then terminated and the radical, now on a monomer, initiator, or solvent molecule, can continue to grow a new polymeric chain. Chain transfer can also occur with other polymeric chains, resulting in one terminated chain and one branched chain. The radical chain can also chain transfer to a different part of the chain, resulting in a branched polymer; this process is referred to as back biting. The rate of chain transfer is dependent on the structure of monomer, polymer, initiator and the solvent molecules. Chain transfer reduces the molecular weight

of the polymer and increases polydispersity. Branching does not reduce the average molecular weight, but creates polymers with low density and increased polydispersity. The kinetic chain length taking chain transfers into account can be described by the following equation:[21]

$$\frac{1}{\bar{\nu}_{tr}} = \frac{1}{\bar{\nu}} + \sum_{\text{all RX}} C_{\text{RX}} \frac{[\text{RX}]}{[\text{M}]} \tag{1.21}$$

where $\bar{\nu}_{tr}$ is the kinetic chain length taking into account chain transfer, $\bar{\nu}$ is the kinetic chain length without chain transfer described by equation (1.20), [M] is the concentration of monomer, [RX] is the concentration of the species that the radical is transferred to (solvent, initiator, monomer, etc.), and C_{RX} is the chain transfer constant. C_{RX} is the ratio of the rate constants for transfer to the specific species RX, $k_{\text{tr,R}}$, and the rate constant of polymerization, k_{p}. These values vary from system to system and should be determined experimentally on an individual basis for each system.

Many types of monomers can be polymerized by radical polymerization. A wide array of initiators are available. A popular initiator azobisisobutyronitrile (AIBN) can form radicals both when heated (thermal decomposition) and when exposed to UV-light (photolysis).[21] Also, the end groups formed by this initiator should not significantly interact with most ions and, therefore, should not affect the selectivity of ISEs with polymers made from this initiator. It is often used in polymerization of polymers for ion-selective electrodes.[16]

1.3.3 Cross-Linked Polymers

Cross-linked polymers are polymers were the polymer chain has been connected by covalent bonds, or other strong interactions, to form an interconnected network. Increasing

the extent of crosslink causes an increase in the glass transition temperature, however the magnitude of this change differs depending on the type of cross-links that are formed.[89] A cross-linked polymer with a glass transition temperature below room temperature is called an elastomer. It is usually soft, deformable, and elastic. The long chains of the polymer allow it to reconfigure itself, distributing an applied stress. The cross-linkages allow it to return back to its original configuration when this stress is removed.[21] A common example of an elastomer is a rubber band. A cross-linked polymer that is rigid is called a thermoset.[21] Epoxy adhesive is an example. When the polymer is highly crosslinked so that it contains no unconnected polymer chains and forms a network extending through the entire bulk material, it is refer to as a rubber.[21] If this polymer is highly crosslinked so that the network extends through the entire bulk material but there are still significant amounts of solvent or low molecular weight polymer chains, it is called a gel. Gels can be swelled with solvents allowing them to find many uses, such as hot melt adhesives, soft contact lenses and absorbents. Higher amounts of crosslinking reduce the amount the gel can swell.[21]

Cross-linked polymers have been used as ISE membranes. Cross-linked methacrylate polymers have been used to create ISEs that can be microfabricated using photolithography.[90] Cross-linked polymers have been used in ISEs for poly-ions, such as heparin.[91] The cross-linking allows for control of the viscosity and therefore the diffusion through the membrane. This is important for polyion ISEs because of their nonequilibrium response, which is dependent on the diffusion of the polyion, and is used to determine the concentration of the ions.

1.4 Hydrophilic High Capacity Ion-Exchange Electrodes (HHCEI)

1.4.1 Composition of Hydrophilic High Capacity Ion-Exchange (HHCEI) Membranes

Ion-exchange resins were first developed in the 1930s for ion-exchange separations.[92] They are commonly used in electrodialysis, fuel cells, separations and batteries.[93] They are also sometimes referred to as hydrophilic high capacity ion-exchange (HHCEI) membranes, ion-exchanger based Donnan exclusion membranes (IEDEM), or as simple ion-exchange resins.[94, 95] Today, most hydrophilic high-capacity ion-exchange membranes used consist of an often highly cross-linked polymer to which ion-exchange sites (often referred to as ionic sites) are covalently attached. These membranes contain a high concentration, often greater than 1 mol equivalent per kg, of ion-exchange sites. This makes the membranes hydrophilic and gives them a low resistance. Due to the high concentration of ion-exchange sites, the polymer self assembles to form nanometer-scale pores or channels with high charge density, which swell with solvent.[93, 96] The size of these pores varies based upon the degree of cross-linking, with high crosslinking resulting in smaller pore sizes.[93, 95, 97] Sulfonate groups are commonly used as anionic sites, and tetraalkylammonium groups are often used as anionic sites.[93, 95]

1.4.2 Hydrophilic High Capacity Ion-Exchange (HHCIE) Electrodes in Sensing

HHCIE membranes were used to potentiometrically measure ion concentrations in aqueous samples as early as the 1950s.[98, 99] As the state of solvation of the exchangeable ions is very similar in the nanopores and in the sample solutions, HHCIE membranes exhibit a very narrow range of selectivity, as the free energy of transfer for most ions into

the pores is close to the same.[94] HCCIE membranes' use in potentiometric sensing was greatly reduced with the development of lipophilic ion-exchange membranes, such as those based on plasticized PVC. These lipophilic membranes which have broader selectivity ranges due to differences of free energy of transfer of ions into the membrane, which can easily be modified to be selective toward a target ion with the addition of ionophores to the membrane making them very useful in many applications. However, recently there has been some renewed interest in using HCCIE membranes in potentiometric sensing. Due to their narrow selectivity ranges, HHCIE based sensors don't suffer from interference from low concentrations of lipophilic ions like those based on lipophilic membranes do. Also, they suffer less from biofouling because their ionic sites are covalently attached to the polymer. Commercially available HHCIE membranes have recently been used to prepare potentiometric sensors for the measurement of chloride in blood.[94] Their low resistance also makes them useful in chronopotentiometry, where they have been used as both a working electrode in blood and as a counter electrode.[100, 101]

1.5 Reference Electrodes

1.5.1 General Characteristics of Reference Electrodes

Reference electrodes are critically important to electrochemical measurements. To have an accurate and precise electrochemical sensor, a stable reference electrode is necessary. They must be insensitive to any changes in the sample solution and maintain a constant potential. A reference electrode needs to be non-polarizable, meaning that if current passes across the electrode/electrolyte interface, this should cause no change in the

potential. It should also have high current exchange density. These features allow for the exchange of charges at the interface of the electrode without significantly affecting the potential. The electrode should also be resistant to potential fluctuations caused by random charge injection at the interface.[102] The reaction of the electrode should have fast kinetics so that it can quickly reach equilibrium. The potential given by the electrode should have a low temperature dependence. The solution in contact with the reference electrode should be saturated so that the potential, which is determined by the concentration of ions in the solution, does not change due to solution evaporation. The absolute potential of an electrode (half-cell) cannot be measured. Therefore, the potential of the standard hydrogen electrode has been arbitrarily defined as zero and potentials are often reported relative to this.

1.5.2 Ag/AgCl Reference Electrodes

Ag/AgCl chloride reference electrodes are popular choices for reference electrodes used in potentiometric systems. They are much easier to maintain than the more traditional standard hydrogen electrode or saturated calomel electrode. They also have the benefit of suffering less from fouling than the standard hydrogen electrode, which can foul easily due to the high adsorption activity of the platinum electrode, and do not contain toxic components such as mercury in the saturated calomel electrode. These electrodes are often comprised of a Ag/AgCl wire immersed into a AgCl-saturated KCl-saturated solution connected to the sample by a salt bridge. The potential of the electrode is determined by the following redox reaction:

$$\mathrm{AgCl}_{(s)} + e^{-} \rightarrow \mathrm{Ag}_{(s)} + \mathrm{Cl}^{-}_{(aq)} \tag{1.22}$$

In this reaction, the concentration of reactive species, Cl^-, determines the potential as described by the Nernst equation.[103] When the filling solution is saturated with Cl^-, current flow does not significantly affect the concentration, resulting in high potential stability. Under these conditions at 25 °C, 0.199 V is the commonly used potential for Ag/AgCl electrodes. In many older publications it was common to use 0.01 M HCl as the filling solution, resulting in a potential of 0.222 V at 25 °C.[104] The potential is also dependent on the temperature of the solution, changing almost 90 mV from 25 to 125 °C.[105, 106] Miniaturization of Ag/AgCl electrodes with liquid filling solutions has been achieved by microfabrication etching of silicon substrate as well as by use of thin planar porous glass, a hydrogel layer, or a membrane with a pinhole.[107-109] However, these electrodes are limited by evaporation due to the small amount of solution. Miniaturized solid state Ag/AgCl reference electrodes have been developed by spin-coating or screen printing a KCl saturated agar gel on a Ag/AgCl film.[110, 111] These electrodes result in a reference electrode with a limited working range but give a constant potential from pH 4 to 10 and at Cl^- concentrations between 10^{-6} to 0.3 M.

1.5.3 Free Flow Liquid Junctions for Reference Electrodes

There are several different methods for contacting the bridging solution to the sample solution. Free flow liquid junctions are the most common used in aqueous solutions with Ag/AgCl reference electrodes. These junctions allow a small amount (0.5-2 μL/h) of bridging solution to flow into the sample solution.[112] Although there are several geometries for free flow liquid junctions, those with ground glass sleeves tend to be the most stable and reproducible liquid junction potentials.[112] It is important to choose a bridging solution

that will not interfere with measurements as the sample is being contaminated with small amounts of the bridging solution. The bridging solution should also utilize an equal transference salt, i.e., a salt composed of a cation and an anion with equal mobility, such as potassium chloride or lithium acetate, to minimize the liquid junction potential.

Although widely used, free flow reference electrodes have several problems. In biological samples they often suffer from clogging by proteins and lipids.[113, 114] They can also become contaminated by sample components and they can considerably contaminate small volume samples. Additionally, because of the continuous flow of the solution, the filling solution can eventually run out; this is especially problematic for miniaturized electrodes. Although many of these problems can be overcome in the laboratory setting by flushing with cleaning solutions and refilling the filling solutions, this is not always feasible in many applications.[112]

1.5.4 Glass Frit Liquid Junction for Reference Electrodes

Nanoporous glass frits and microporous ceramic plugs are also used to separate filling solutions of reference electrodes from the sample.[115-117] This setup is especially popular for measurements in organic solvents.[118-120] While microporous ceramic plugs have a pore size of approximately 0.1−3 μm, nanoporous glass frits are popular because their smaller pore size, ranging from 4−100 nm, further restricts liquid flow.[115-117] However, it has recently been found that at ionic strengths under 100 mM, the half-cell potentials of these reference electrodes are not always sample independent, and depend on the ionic sample composition.[121] These changes in potential can be upwards of 50 mV. This effect is due to electrostatic screening of ion transfer into the glass pores by the surface

charge density on the glass surface when pore dimensions are comparable to or smaller than the Debye length of the ions.[121] This effect is very similar to the response given by ion-exchange resins (HHCIE membranes), nanoporous opal films and nanopore based sensors.[95, 122, 123] In addition, the surface charge density of the glass pores is dependent on pH, causing this effect to vary by pH, with a more pronounced effect observed at higher pH.[121, 124, 125] This can cause rather large errors in measurements when using reference electrodes with these frits. Therefore, care should be taken to assure that the half-cell potential is constant at ionic strengths and pH being used.

1.5.5 Pulse Reference Electrodes

Recently, in an effort to address the issues with free flow liquid junction base reference electrodes, reference electrodes without liquid junctions that instead utilize current pulses to define the potential have been developed.[126] These electrodes have utilized hydrophobic ion-doped polymeric membranes. By applying a current pulse the transmembrane ion fluxes can be controlled to obtain a sample independent reference electrode potential. Similar current pulse techniques have be used with ISEs to control transmembrane ion fluxes, yielding lower limits of detection.[127-129] However, in this case the pulse is being used to effectively do the exact opposite, raising the limit of detection, giving a constant potential across a wide concentration range.[126] The potentiometric measurement is made immediately after the current pulse. At this time the potential at the reference electrode is determined by the concentration of the ions released by the pulse which have not had time to diffuse away from the electrode. The electrode gives a much more stable potential when measuring in blood over two days when the current is applied

than when it is not. These electrodes give a stable potential up to about 0.1 mM, at which point they start responding to changes in the ion concentration.[126] Current pulses of a maximum of approximately 2 μA have been used with these electrodes. It is likely that using a larger current would increase the range that the potential is stable, allowing for this electrode to be useful in many more applications. Unfortunately, the high electrical resistance of the hydrophobic membranes necessitates a relatively large voltage to be applied to achieve these currents, limiting the ability to increase said current.

1.6 Conclusion

ISEs are widely used potentiometric sensors. However, their performance still suffers when applied in harsh conditions. In biological systems they can suffer from large amounts of drift, shortened lifetime and reduced selectivity. Fluorous membrane ISEs have previously been developed to combat this problem. However, most of these sensors have membranes composed of fluorous liquids, limiting their application. The next two chapters discuss the development of semifluorinated polymers and ISEs, utilizing them to address this issue. The remaining chapters discuss the use of hydrophilic high capacity ion-exchange (HHCEI) membranes in ISEs. First, the effect of Donnan failure on these, as well as on more traditional lipophilic ISE and ion-exchange electrodes is discussed, showcasing the ability of HHCEI membranes to measure in backgrounds of lipophilic co-ions. Next, the development of a HHCEI membrane based sensor that can measure in organic solvents and at high temperature is detailed, along with its use to monitor NO_x^- concentrations

during nanoparticle synthesis. Finally, the development of a pulse based reference electrode utilizing HHCEI membranes is also discussed.

2 CHAPTER TWO:

Synthesis of Semifluorinated Polymers by Modification of Lipophilic Polymers for Use as ISE Membranes

Ion-selective electrodes based off fluorous liquid membranes have shown resistance to biofouling and extraordinary selectivity ranges. However, due to their liquid nature they are not very robust and have a limited lifetime. Most commercially available fluorous polymers lack the appropriate glass transition temperatures or have functional groups that would affect the selectivity towards ions. In attempts to create semifluorinated polymers for use in ion-selective membranes, the polymer poly(4-vinylphenol) was modified to have perfluoroalkyl and alkyl substituents using a Williamson ether synthesis. High percent conversions were obtained for the alkyl substitutions, however, for the perfluoroalkyl chains the percent conversion was less than 50%.

2.1 Introduction

Fluorous membrane based ion-selective electrodes (ISEs) have been shown to have several improved characteristics as compared to ISEs with typical lipophilic membranes, including improved selectivity and resistance to biofouling.[36, 69, 70, 130] Fluorous membrane ISEs utilizing fluorophilic ionic sites and ionophores have been used to measure pH as well as silver and carbonate.[69-71] These electrodes have been based on fluorous liquids such perfluoroperhydrophenanthrene or a linear perfluorooligoether.[68, 69] However, because these compounds are liquids they must be supported on porous disks, are not very robust, have a limited lifetime, and are difficult to miniaturize. A fluorous polymer would be an ideal candidate to use as a self-supported ISE membrane. Unfortunately, most commercially available fluorous polymers lack the appropriate glass transition temperatures or have functional groups that would negatively affect the selectivity over

interfering ions. ISEs with self-supported membranes have previously been made from Teflon AF2400 plasticized by a linear perfluorooligoether, however low levels of carboxylic acid impurities affect the selectivity of these membranes.[75]

Here I have worked toward developing semifluorinated polymers for use as ISE membranes by modifying existing lipophilic polymers to be more fluorophilic by addition of perfluoroalkyl chains. Lipophilic polymers are commercially available in a wide array of well-defined properties. Achieving a variety of desired properties, such as low polydispersity, is more difficult in fluorous polymers than for most other polymers.[67] Also, the synthesis and purification of large amounts of monomers for fluorous or semifluorinated polymers is often difficult and involves several steps.[131] Therefore, modifying non-fluorinated polymers into semifluorinated polymers may be a valuable tool for the synthesis of semifluorinated polymers for use as ISE membranes. A further benefit of having synthetic control over the polymer structure is the future possibility of covalently attaching ionic sites and ionophores. A high percent conversion of each repeat unit will be needed to produce polymers with the necessary fluorophilicity that, when used in ISEs, would give similar characteristics as those seen in ISEs made with fluorous liquids. The chosen target polymer (Figure 2.1) should be fluorophilic when high conversion is achieved. Based on similar polymers in the literature it is hypothesized that this polymer would exhibit a glass transition temperature that is low enough for the polymer to have sufficient ion mobilities without the aid of a plasticizer.[132, 133]

2.2 Experimental

2.2.1 Materials

1-Bromoheptane, cesium fluoride, dimethylacetamide (DMA), *N*,*N*-dimethylformamide (DMF). dimethylimidazolidinone (NMP), dimethyl sulfoxide (DMSO), iodomethane, methylpyrrolidone (DMI), poly(4-vinylphenol) (M_W c.a. 11,000), sodium hydride (60% purity), tetrahydrofuran (THF) and toluenesulfonyl chloride were purchased from Sigma Aldrich (St. Louis, MO). 2-Perfluorohexylethyl alcohol, 1-iodo-2-(perfluorohexyl)ethane and 1-bromo-2-(perfluorohexyl)ethane was purchased from Alfa Aesar (Ward Hill, MA). THF was distilled over sodium metal and benzophenone before use. All other solvents were dried with molecular sieves before use. HFE7100 and perfluorohexane were purchased from 3M (St. Paul, MN). 1,1,2-Trichloro-1,2,2-trifluoroethane (F113) was purchased from Spectrum Chemical (New Brunswick, NJ).

2.2.2 Synthesis of tosyl$(CH_2)_2(CF_2)_5CF_3$ with a modified literature procedure[134]

2-Perfluorohexylethyl alcohol ($C_6F_{13}CH_2CH_2OH$) (2.18 g, 6.0 mmol, 10 mL), 4-toluenesufonyl chloride (1.20 g, 6.3 mmol) and NaOH (0.280 g, 7 mmol) were added to a round bottom flask with 10 mL of THF, and the solution was stirred for 48 h. The solvent was evaporated. The resulting solid was dissolved in dichloromethane and washed with 1 M HCl until a neutral pH was reached. The organic layer was then dried with magnesium sulfate, and the solvent was removed by rotary evaporation. The solid was then purified by chromatography on a silica gel column with an eluent of a 10:1 v/v mixture of petroleum ether and ethyl acetate. White solid 2.48 g, 80% yield. ^{1}H NMR (500 MHz, Varian, $CDCl_3$

δ in ppm from TMS): 7.82 (d, 2H, -Ph), 7.40 (d, 2H, -Ph), 4.32 (t, 2H, -SO_3CH_2-), 2.54 (m, 2H, -CF2-CH2-), 2.47 (s, 3H, -Ph-CH3).

2.2.3 Reaction of poly(4-vinylphenol) with 1-bromoheptane

NaH (0.110 g, 60% purity, washed with hexanes before use, 2.8 mmol) was suspended into 5 mL of *N*,*N*-dimethylformamide (DMF). Poly(4-vinylphenol) was dried under vacuum at 150 ºC for 1 hour (0.5 g, 4.1 mmol of repeat units) and was then added to the NaH suspension, which was then stirred for 30 minutes. Next, 1-bromoheptane (1.47 g, 8.2 mmol) was added and the solution was stirred for ~36 hours at 70° C under nitrogen. The resulting polymer was obtained by precipitation from methanol, and its identity was verified by ^{1}H NMR (300 MHz, Varian, $CDCl_3$ δ in ppm from TMS) giving broad peaks at 6.2-6.8 (aromatics, 4H); 3.85 (2H, OCH2), 1.747 (3H CH_2), 1.311(10H, alkyl chains and backbone) and 0.896 (3H, CH_3). Comparison of the peak area of the aromatics to the OCH_2 peaks indicated a 98% conversion.

2.2.4 Methylation of poly(4-vinylphenol)

0.25 g (2 mmol) of poly(4-vinylphenol) was dried under vacuum at 150 ºC for 1 hour. It was then dissolved in 2 ml of dimethylformamide (DMF). Next, 1 equivalent 0.083 g (2 mmol) of 60% purity NaH was washed with hexanes 3 times. It was then added to the poly(4-vinylphenol)/DMF solution and allowed to stir for 30 minutes. Then 4 equivalents (2.27 g, 8 mmol) of ICH_3 was added, and the reaction solution was stirred and heated at 40 ºC in an oil bath with a condenser and nitrogen balloon for 2 days. The solution was added to water, causing a precipitate to form. The solid was filtered, dissolved in ethyl acetate and washed several times with water. The solution was then dried over magnesium sulfate,

filtered, and the solvent was evaporated. This procedure was repeated with the resulting product to increase the percent conversion. ^{1}H NMR (500 MHz, Varian, deuterated acetone δ in ppm from TMS) giving broad peaks at 6.2-6.8 (aromatics, 4H); 3.741 (3H, OCH_3), 1.878 and 1.515 (3H polymer backbone). Comparison of the peak area for aromatics and the OCH_3 indicated a conversion greater than 99%.

2.2.5 Synthesis of semifluorinated polymer by modification of poly(4-vinylphenol)

First, 0.46 g (3 mmol) of CsF was dried under vacuum for 1 hour and dissolved in 3 ml of dimethylformamide (DMF). Then 0.18 g (1.5 mmol of monomer equivalents) of poly(4-vinylphenol) was dried under vacuum at 150 ºC for 1 hour and then dissolved in the solution. This was allowed to stir for 30 minutes. Then 2 equivalents (1.28 g, 3 mmol) of $Br(CH_2)_2(CF_2)_5CF_3$ was added, and was stirred and heated at 150 ºC in an oil bath with a condenser and nitrogen balloon for 2 days. The DMF was removed by heating while under vacuum; the resulting solid was washed with methanol. The solid was once again dried under vacuum. ^{1}H NMR (500 MHz, Varian, deuterated DMF δ in ppm from TMS) 6.2-6.8 (aromatics, 4H); 4.07(2H, OCH_2); 2.81 (2H, CH_2CF_2); 1.878 and 1.515 (3H polymer backbone); 48% conversion. This procedure was also performed with dimethylacetamide (DMA), methylpyrrolidone (DMI), dimethyimidazolidinone (NMP), and dimethyl sulfoxide (DMSO) in place of DMF with percent conversions of 0%, 24%, 42%, and 0%, respectively.

2.3 Results and Discussion

Modifying lipophilic polymers into fluorophilic semifluorinated polymers may be a valuable tool for the synthesis of semifluorinated polymers for use as ISE membranes. The non-fluorous polymers to be modified would require a functional group that could be used to attach perfluoroalkyl chains to increase the fluorophilicity of the polymer. Poly(4-vinylphenol) would be a suitable polymer to be modified. A Williamson ether synthesis with the phenol groups of poly(4-vinylphenol) and a perfluoroalkyl halide after phenol deprotonation with sodium hydride to give a semifluorinated polymer, as shown in Figure 2.1, could be used to add perfluoroalkyl side chains to the polymer. The drawback, however, is that any remaining hydroxyl groups could negatively affect the selectivity of the ISE. Therefore it would be necessary to achieve a very high level of conversion for the polymer to be useful as an ISE membrane. If a suitably high percentage of conversion to fluorinated groups is achieved to give sufficient fluorophilicity, any remaining alcohol groups could be methylated to reduce the effects of functional groups on selectivity.

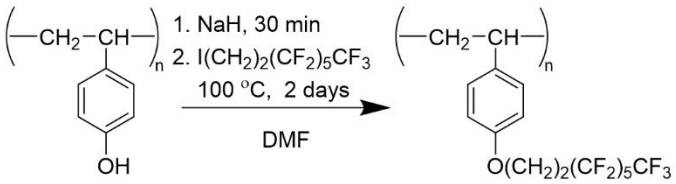

Figure 2.1: Reaction scheme for the synthesis of a semifluorinated polymer.

A test reaction with non-fluorinated reagents to determine the validity of this strategy, using poly(4-vinylphenol) and 1-bromoheptane, was performed. ^{1}H NMR results

indicated a 98% conversion after a reaction time of approximately 36 h. After the attachment of the fluorinated chains to the polymer, any remaining alcohol groups will need to be methylated, to ensure the polymer can function as an ISE membrane without affecting selectivity coefficients. To test the methylation reaction, poly(4-vinylphenol) was methylated using ICH_3, see Figure 2.2. Repeating the reaction can significantly raise the percent conversion. This can achieve conversion rates greater than 99%, which would be sufficient to minimize the remaining alcohol groups' effects on the selectivity.

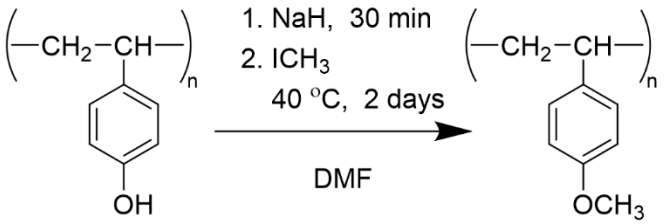

Figure 2.2: Methylation of poly(4-vinylphenol).

After the success of these test reactions, several attempts were made to produce a semifluorous polymer using $I(CH_2)_2(CF_2)_5CF_3$. However, these reactions were unsuccessful, leaving mostly starting materials and none of the desired product. The reaction was conducted several times at higher temperatures (100 °C) and over longer time periods (up to 3 days), but none gave the desired product. Since CsF has been used to produce aryl ethers in the literature,[135] CsF was used in place of the NaH. However, the results were similar and none of the desired product was formed. It seems likely that $I(CH_2)_2(CF_2)_5CF_3$ is not reactive enough or is not sufficiently soluble in DMF to undergo this reaction, even with the aid of the CsF. The reaction was then attempted with the more

reactive $Br(CH_2)_2(CF_2)_7CF_3$ and NaH. This was slightly more successful, with a conversion of less than 15%. By using CsF in conjunction with $Br(CH_2)_2(CF_2)_7CF_3$ the conversion was improved to 23%. Using excess $Br(CH_2)_2(CF_2)_7CF_3$ and CsF improved the conversion to 48% (see Figure 2.3). Using more than a twofold excess did not further improve the percent conversion. Reacting the resulting semifluorinated polymer under the same reaction conditions for a second time also did not further increase the percent conversion as it had with the methylation reaction. The resulting polymer seemed to be no longer soluble in DMF and this may be limiting the percent conversion. Reaction with $Tos(CH_2)_2(CF_2)_5CF_3$ (where Tos stands for the tosyl group) was less successful (36%). Reactions with several other combinations of reagents and solvents (Figure 2.4) were also performed (Table 2.1), however the resulting percent conversion for each of these trials was less than 48%. Reactions performed with DMA showed no evidence of the desired products. The reaction with DMSO showed signs of solvent decomposition and no desired products.

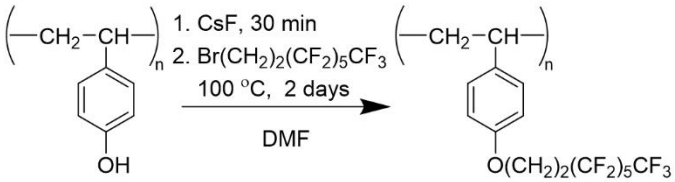

Figure 2.3: Alternative reaction scheme for the modification of poly(4-vinylphenol) into a semifluorinated polymer.

Table 2.1: Synthesis of semifluorinated polymers from polyvinyl phenol in various solvents

Solvent	Catalyst/ Base	Polymer poly(4-vinylphenol)	Reagent	Percent conversion
DMF	NaH 1 eq.	1 eq.	$Br(CH_2)_2(CF_2)_5CF_3$ 1 eq.	<15
DMF	CsF 1 eq.	1 eq.	$Br(CH_2)_2(CF_2)_5CF_3$ 1 eq.	23
DMF	CsF 2 eq.	1 eq.	$Br(CH_2)_2(CF_2)_5CF_3$ 2 eq.	48
DMF	CsF 2 eq.	1 eq.	$Tosyl(CH_2)_2(CF_2)_5CF_3$ 2 eq.	36
DMA	CsF 1 eq.	1 eq.	$Br(CH_2)_2(CF_2)_5CF_3$ 2 eq.	NR
DMA	NaH 1 eq.	1 eq.	$Br(CH_2)_2(CF_2)_5CF_3$ 2 eq.	NR
DMI	CsF 2 eq.	1 eq.	$Br(CH_2)_2(CF_2)_5CF_3$ 2 eq.	24
NMP	CsF 2 eq.	1 eq.	$Br(CH_2)_2(CF_2)_5CF_3$ 2 eq.	42
DMSO	CsF 2 eq.	1 eq.	$Br(CH_2)_2(CF_2)_5CF_3$ 2 eq.	Solvent decomposition

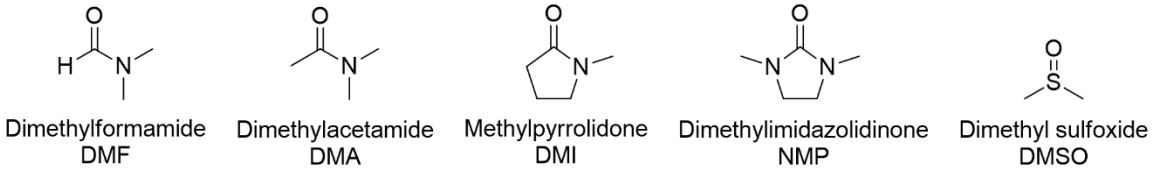

Figure 2.4: Structures and abbreviations of solvents used in the synthesis of semifluorinated polymers.

While the methylation reaction with polyvinyl phenol is with a conversion greater than 99% highly successful and would allow for sufficient elimination of alcohol functional groups, the percent yield of the attachment of fluorous chains to polyvinyl phenol is too low, as even the highest conversion values are less than 50%. The resulting polymers will be unlikely to exhibit the fluorophilicity necessary to give improvements to selectivity and the resistance to biofouling as seen with fully fluorous membranes. It is likely that as fluorinated groups are added to the polymer, the polymer becomes less soluble in solvents that are suitable for the reaction to occur. Therefore, it was determined that due to the low percent conversion, modifying non-fluorinated polymers would be a less successful strategy for producing semifluorinated polymers useful as ion-selective electrode membranes than polymerizing semifluorinated monomers.

2.4 Conclusion

Reactions adding lipophilic modifications to polyvinyl phenol, such as methylation, were highly successful, giving high percent conversions (<99%). However, attempts to convert non-fluorinated polymers into semifluorinated polymers for use as ISE membranes were substantially less successful, as a sufficiently high percent introduction of fluorinated groups was not obtained, despite considerable effort and variation of numerous reaction parameters. These low conversion values (<50%) could possibly be due to the limited solubility of the more highly fluorinated intermediate polymer products in solvents required for the reaction to proceed further. Because of the low conversion rate of the phenol groups to fluorinated ether side groups, these polymers lack the fluorophilicity

necessary to show any of the benefits seen by ISEs utilizing fluorous membranes. Modification of monomers before polymerization may therefore be a better method for synthesizing polymers with the desired properties.

3 CHAPTER THREE:

Semifluorinated Polymers for Ion-Selective Electrodes

Most commercially available fluorous polymers are ill suited for use as ion-selective electrode (ISE) membranes; therefore, we have synthesized semifluorinated polymers for use as ISE membranes. Ion-exchanger electrodes made with several of these polymers show a wide selectivity range (~14 orders of magnitude), approaching that of previously developed fluorous liquid ion-exchange electrodes. These polymers have also been used to create ISEs using fluorophilic silver ionophores. Although these electrodes are less selective compared to their fluorous liquid counterparts, these polymers can utilize both fluorophilic ionophores as well as traditional lipophilic ionophores, such as the silver ionophore Cu(II)-I (o-Xylylenebis(N,N-diisobutyldithiocarbamate)). We have cross-linked these polymers to produce durable membranes that retain broad selectivity ranges and are compatible with both fluorophilic and hydrophilic ionophores. K^+ ISEs made with the cross-linked semifluorinated polymer and the ionophore valinomycin show selectivity coefficients comparable to similar PVC membrane electrodes as well as superior thermal stability at high temperatures, with a majority of the electrodes still giving a Nernstian response after being exposed to a boiling aqueous solution for 10 h.

3.1 Introduction

Ion-Selective Electrodes (ISEs) have become a widely used analytical technique in a variety of fields including clinical chemistry, environmental analysis, physiology, and process control. ISEs made with fluorous membranes have been developed over the past decade for a variety of ions.[70, 71, 73, 136] These sensing membranes have shown considerable improvement in selectivity as compared to conventional (e.g., PVC based) electrode

materials,[70, 71, 73, 136] as well as promise in reducing the effects of biofouling.[137] This is due to the extremely low polarity and polarizability of fluorous compounds. For example on the π^* scale for solvent polarity, where cyclohexane defines 0, dimethyl sulfoxide defines 1, and water has a value of 1.09, perfluorooctane has an incredibly low value of -0.41.[53] This causes a large increase in the free energy of transfer of interfering ions into the membrane. This is showcased by the large selectivity range of ion-exchange electrodes made with perfluoroperhydrophenanthrene (16 orders of magnitude selectivity range),[68] as compared to those with membranes made from plasticized PVC (~8 orders of magnitude).[68] These electrodes have used fluorophilic salts as ionic sites and fluorophilic ionophores to achieve high selectivity towards specific ions such as the silver, carbonate, and protons,[70, 136,138] achieving the best selectivity coefficients for these ions to date.

Biofouling occurs when ISEs are exposed to biological samples such as blood or urine. It causes a loss of selectivity, increases signal drift and reduces the lifetime of the ISE.[33] This effect is due to partitioning of neutral lipophilic compounds into the membrane of the ISE as well as by adsorption of cells or proteins onto the membrane and the leaching of membrane components into the sample media.[33] Due to the extremely low polarity of fluorous membranes it is unlikely that lipophilic sample components will adsorb onto the surface of the membrane or absorb into the membrane.

Most of these fluorous membrane ISEs made to date use fluorous liquids such as perfluoroperhydrophenanthrene or a linear perfluorooligoether deposited on a porous Teflon disc.[68, 136] While this has allowed fluorous membrane ISEs to find use in several applications, such as monitoring the toxicity of silver nanoparticles[77] and the detection of

perfluorooctanoate and perfluorooctanesulfonate in environmental samples,[73] the use of a liquid limits the mechanical stability of these membrane, hampering the development of a miniaturized fluorous membrane ISE. The development of a self-supporting fluorous membrane ISEs would enable the miniaturization of these ISE. It would also allow for solvent free casting of the fluorous ISE membranes. This would open a variety of new possible ways to use and implement ISEs with fluorous membranes, such as printing of these membranes in microfabrication. Unfortunately, available suitable commercial polymers would need to be plasticized to have the correct glass transition temperature, and there are only few reports of appropriately plasticized fluorous polymers. In one such case, fluorous polymers have been plasticized using a highly fluorinated compound containing polar functional groups (i.e. carboxylic acid), which would drastically affect the selectivity of a sensor.[139] Another study showed that Teflon AF2400 could be successfully plasticized with a linear perfluorooligoether.[140] This plasticized Teflon AF2400 was used to create a self-supported fluorous membrane; however, low levels of carboxyl impurities have limited the selectivity of those membranes.[75]

Possible candidates for use as ISE membranes need to meet several criteria. First, they need to be free of interfering functional groups, such as carboxylic acids, which would bias the selectivity of the electrodes by interacting with ionic species. Second, the glass transition of the polymer need to be lower than the operating temperature of the ISE, so that ions have sufficient mobility in the membrane for the sensor to function. The previously synthesized polymer **P1** (see Figure 3.1) was shown to have a glass transition temperature of (17-18 °C).[132, 133] While there are no examples of the homopolymer **P2** (see

Figure 3.1) in the literature, a block-*co*-polymer with a block that corresponds to **P2** has been previously synthesized, showing a glass transition at -44 °C corresponding to the **P2** block.[80] These values would allow for these polymers to be used in an ISE without the need for a plasticizer. Finally, the polymers should also be sufficiently fluorinated such that the ISE exhibits characteristics similar to those observed with ISEs made with fluorous liquids (broad selectivity range and resistance to biofouling). The previously synthesized polymer **P1** has shown a low dispersive surface energy (γ_S^D = 10.7 mNm^{-1})[132] and high contact angle (advanced contact angle of 69.0° with decane),[132] characteristics commonly observed in fluorous polymers.[67] The block-co-polymer with a **P2** block had a measured contact angle of 107°, indicative of a highly hydrophobic surface.[80] It can be assumed that a **P2** homopolymer would be at least as hydrophobic, if not more so.

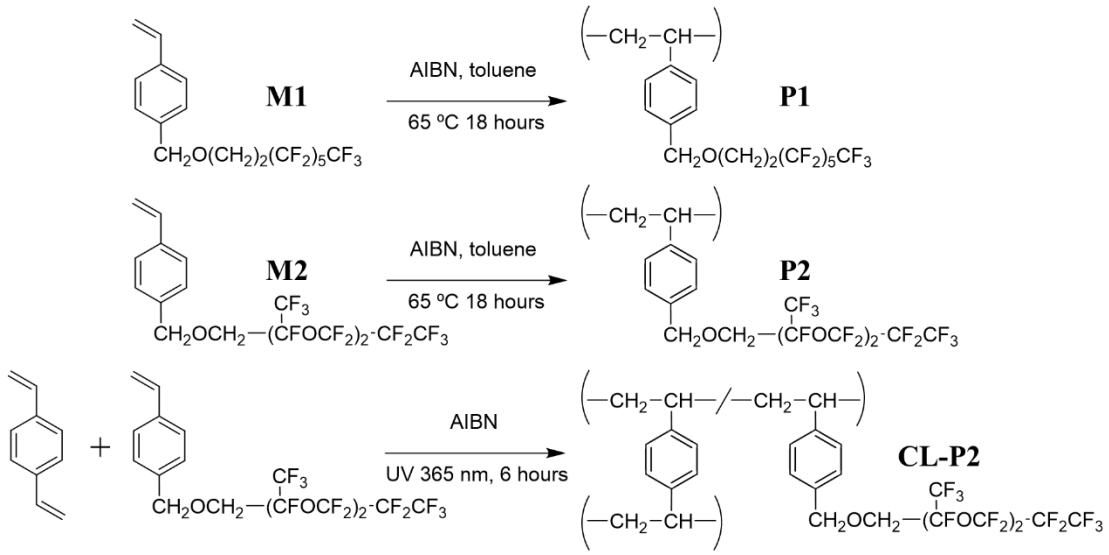

Figure 3.1: Reaction scheme for the free radical polymerization of (top) **M1** to **P1**, (middle) **M2** to **P2**, and (bottom) **M2** and divinylbenzene to **CL-P2**.

In this work, we have synthesized semifluorinated monomers (**M1** and **M2**, see Figure 3.2) that were then polymerized into semifluorinated polymers (**P1** and **P2**, see Figure 3.1). These polymers have allowed for fabrication of fluorophilic polymeric membrane ISEs that function without a plasticizer, due to their low glass transition temperature. With the addition of a cross-linker, they become robust enough to be used as self-supporting membranes. Although they are less fluorophilic than previous fluorous liquid membranes, they still can produce sensors with broad selectivity ranges and should still provide resistance to biofouling. Due to their slightly lower fluorophilicity, they allow for use of a wider range of ionophores, which should expand the range of possible applications for these sensors.

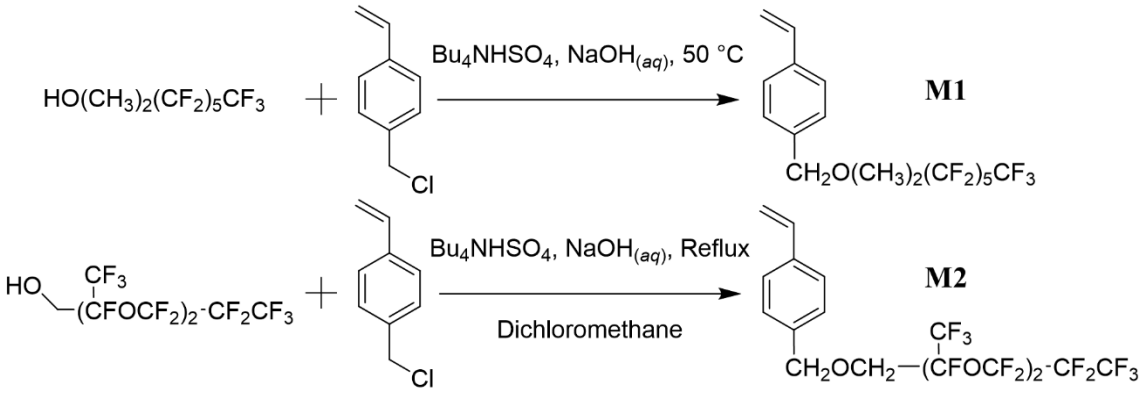

Figure 3.2: Reaction scheme for the synthesis of (1*H*,1*H*,2*H*,2*H*-perfluorooctan-1-yl)styrene, **M1** (top) and the fluorinated oligoether monomer, **M2** (bottom).

3.2 Experimental Section

3.2.1 Materials

Azobisisobutyronitrile (AIBN), 4-chloromethylstyrene, Cu(II)-I iononophore (o-Xylylenebis(N,N-diisobutyldithiocarbamate), 2-nitrophenyl octyl ether (*o*-NPOE), polyvinylchloride (PVC) (Selectophore, high molecular weight), sodium tetraphenylborate (NaTFPB), and valinomycin were purchased from Sigma Aldrich (St. Louis, MO). 2-Perfluorohexyl-ethanol was purchased from Alfa Aesar (Ward Hill, MA). 1H,1H-Perfluoro(2,5-dimethyl-3,6-dioxanonan-1-ol and 1H,1H-perfluoro(2,5,8-trimethyl-3,6,9-trioxadodecan)-1-ol was purchased from Synquest Laboratories (Alachua, FL). Salts for selectivity measurements of the highest purity available (≥99.999% trace metals basis or Puratronic) were purchased either from Sigma Aldrich or Alfa Aesar (Ward Hill, MA). Tetrabutylammonium hydrogen sulfate (Bu_4NHSO_4) was purchased from Thermo Fisher (Waltham, Massachusetts). Perfluorohexane and Novec Engineering Fluid HFE-7100 (Methoxyperfluorobutane, mixture of n- and iso-butyl isomers) were purchased from 3M (St. Paul, MN). Divinylbenzene (*m*- and *p*- mixture) was purchased from TCI America (Portland, OR), and stabilizers were removed by flash chromatography on a silica column before use. THF was distilled over sodium metal and benzophenone before use. All other solvents were used without further purification. AIBN was recrystallized from ethanol before use. The fluorophilic ionic site, sodium tetrakis[3,5-bis(perfluorohexyl)phenyl]borate, was synthesized as described in the literature.[68] The fluorophilic silver ionophores, 1,3-bis(perfluorooctylethylthiomethyl)-benzene (**Ag-R_{f8}**) and 1,3-bis(perfluorodecylethylthiomethyl)benzene (**Ag-R_{f10}**) were synthesized as

described in the literature.[141] Fluoropore membrane filters (pure Teflon, 47 mm diameter, 0.45 μm pore size, 50 μm thick, 85% porosity) were obtained from EMD Millipore (Billerica, MA).

3.2.2 Synthesis of Monomers for Semifluorous Polymers Synthesis of the Monomer (1*H*,1*H*,2*H*,2*H*-Perfluorooctan-1-yl)styrene, (M1)

The monomer **M1** was synthesized with slight modification of a literature procedure.[132] A higher yield was obtained with this method than with attempts to use other methods. 2-Perfluorohexyl-ethanol ($C_6F_{13}CH_2CH_2OH$) (4.0 g), tetrabutylammonium hydrogen sulfate (Bu_4NHSO_4) (0.28 g) and 6 M NaOH (4.28 mL) were added to a round-bottom flask and stirred at 50 ºC with a condenser under N_2 for 10 min. Then 4-chloromethylstyrene (1.66 g) was added (the mixture turned bright yellow), and the reaction mixture was stirred at 50 ºC with a condenser under N_2 overnight (18h). The mixture was allowed to cool to room temperature and 25 mL of dichloromethane was added. This was washed several times with 0.1M HCl and water. The solvent was dried over magnesium sulfate and the solvent was removed by evaporation. The monomer was purified over a silica gel column (100 g) with ethyl acetate/hexanes (1/30 v/v) as the eluent. Yield: 50%, clear liquid, ^{1}H-NMR (500 MHz, Varian, $CDCl_3$ δ in ppm from TMS) giving signals at 7.42 (d, 2H, aromatics) and 7.31 (d, 2H, aromatics), 6.79 (dd,1H, CH=), 5.79 and 5.263 (d, 2H CH2=), 4.54 (s, 2H $PhCH_2O$), 3.375 (t, 2H, OCH_2), 2.43 (m, 2H, CH_2CF_2,) which corresponds well to data given in the literature.[132]

3.2.3 Synthesis of the Monomer 1-((2,3,3,3-Tetrafluoro-2-(1,1,2,3,3,3-hexafluoro-2-(perfluoropropoxy)propoxy)propoxy)methyl)-4-vinylbenzene, (M2)

NaOH (6.9 g, 0.173 mol) dissolved in water (14 mL) was placed in a round-bottom flask. The alcohol, 1H,1H-Perfluoro(2,5-dimethyl-3,6-dioxanonan-1-ol) (3.00 g, 6.22 mmol) was then added under vigorous stirring. Bu_4NHSO_4 (1.69 g, 5.0 mmol), dichloromethane (140 mL), and 4-vinylbenzyl chloride (0.90 g, 5.90 mmol) were added, and the mixture was refluxed overnight. The aqueous and organic layers were separated with a separatory funnel. The organic layer was washed three times with 0.1 M HCl_{aq}, and three times with water. The monomer was purified over a silica gel column (100 g) with ethyl acetate/hexanes (1/30 v/v) as the eluent. Yield: 30%, clear liquid, ^{1}H-NMR (500 MHz, Bruker, $CDCl_3$ δ in ppm from TMS) giving signals at 7.4 (d, 2H aromatics), 7.3 (d, 2H, aromatics), 6.79 (dd, 1H, CH=), 5.79 and 5.263 (d, 2H, CH2=), 4.66 (s, 2H, $PhCH_2O$), and 4.00 (d, 2H, OCH_2), which corresponds well to data given in the literature.[80]

3.2.4 Thermal Free Radical Polymerization of M1 to Poly(1*H*,1*H*,2*H*,2*H*-perfluorooctan-1-yl)styrene (P1)

Typical reaction: **M1** (1*H*,1*H*,2*H*,2*H*-perfluorooctan-1-yl)styrene; 0.40 g), azobisisobutyronitrile (AIBN; 0.024 g or 20 mol%), and toluene (2.64 mL) were added to a 50 mL round-bottom flask. The solution was then degassed by using the pump-freeze-thaw-method, i.e., the flask was submerged in liquid nitrogen to freeze the solution, a vacuum was applied on the flask for 10 min, the connection to the vacuum was closed, and the flask was removed from the liquid nitrogen and placed in a cool water bath. The solution was then allowed to melt and after 5 min the process was repeated several times.

The flask was then purged with argon gas run through a drierite column. The solution was then stirred for 18 h at 60 ºC. Upon cooling of the solution to room temperature, the polymer was precipitated by addition of the reaction solution into methanol. The polymer was collected by centrifugation, followed by dissolution in THF and reprecipition by addition into methanol; this process was repeated 4 times. Yield: 25%, ^{1}H-NMR (500 MHz, Varian, $CDCl_3$ δ in ppm from TMS) giving broad signals at 6.9-.6.5 (4H, aromatics), 4.4 (2H $PhCH_2O$), 3.68 (2H, OCH_2), 2.48 (2H, CH_2CF_2), polymer backbone from 1.8-1.2 (4H CH_2) and 1.431 (1.3 H, end-groups, CH_3), which corresponds well to data given in the literature.[132] The molecular weight of the polymer was determined using MALDI-MS with THF as the solvent and dithranol as the matrix. As the ratio of initiator to monomer decreases, the molecular weight of the polymer increases, see table 3.S1.

3.2.5 Thermal Free Radical Polymerization of M2 to Poly(1-((2,3,3,3-tetrafluoro-2-(1,1,2,3,3,3-hexafluoro-2-(perfluoropropoxy)propoxy)propoxy)methyl)-4-vinylbenzene). P2

These reactions were conducted in the same manner as for **P1**. Yield: 25%, ^{1}H-NMR (500 MHz, Bruker, $CDCl_3$ δ in ppm from TMS) giving broad signals at 6.9-.6.5 (4H, aromatics), 4.68 (2H $PhCH_2O$), 4.11 (2H, OCH_2), polymer backbone from 1.8-1.2 (4H CH_2). The molecular weight of the polymer could not be successfully determined by using MALDI-MS. The polymer resulting from solvent-free reactions resulted in polymers that were not soluble in THF, referred to as (**HMW-P2**). In these cases, after precipitation the polymer was dissolved in perfluorohexane and washed several times with THF, and then the perfluorohexane was evaporated.

3.2.6 Cross-linked Semifluorinated Polymer (CL-P2)

Typical reaction: **M2**, (0.5 g,), AIBN (0.002 g for 1 mol%) and divinylbenzene (3.3 mg, 3 mol% inhibitor previously removed by silica column) were added to a 3 cm diameter glass casting dish. The mixture was placed in a reaction box with a UV lamp (Blak-Ray, B-100A, 100W, 365 nm long wave UV, Ultra-Violet Products, Upland, CA), with nitrogen gas flowing through the box. The membrane was exposed to UV light for 6 hours. The resulting membranes were washed 3 times with 3 ml of THF, 3 times with 3 ml of perfluorohexane, and 3 times with 3 ml of HFE-7100 to remove impurities. The resulting membranes were measured to be 0.35 mm thick.

3.2.7 Differential Scanning Calorimetry (DSC)

Glass transition temperatures of the polymers were determined using differential scanning calorimetry using a TA Instruments Q1000 (TA Instruments, New Castle, DE, USA). The temperature was cycled several times from –50 ºC to +100 ºC, using a scan rate of 10 ºC/min.

3.2.8 MALDI Mass Spectroscopy

MALDI mass spectroscopy was used to determine the number average and weight average molecular weight of polymers using a Applied Biosystems-SCIEX 4800 MALDI-TOF/TOF Mass Spectrometer (SCIEX, Framingham, MA) in positive ionization mode with dithranol as the matrix.

3.2.9 Electrode Construction for Homopolymer Membranes

Electrodes were constructed using custom-made electrode bodies[68] made of Kel-F (polychlorotrifluoroethylene) with Fluoropore membranes, cut to 13 mm diameter circle,

as a support. 25 mg of the homopolymers **P1** made with 20% initiator,**P2** made with 20% initiator or **HMW-P2** made with 1% initiator, were dissolved in 0.5 ml of THF (perfluorohexane was used for **HMW-P2**, which was insoluble in THF) along with the appropriate amount of the fluorophilic ionic site. For the silver selective electrodes, the ionophore was dissolved as well. This solution was then applied to the Fluoropore support 50 μL at a time. The solvent was allowed to evaporate in between applications, repeating applications until all 0.5 mL of the solution was applied to the electrode. The inner filling solution of the ion-exchanger electrode was 10 mM KCl. A Ag/AgCl wire was used as an internal reference electrode. The electrodes were conditioned in 10 mM KCl for 18 h prior to use. Silver selective electrodes were constructed with an additional compartment by inserting into the top of the Kel-F electrode body a cotton-packed pipette tip containing the Ag/AgCl wire as an internal reference electrode, and closing with a septum, see Figure 3.S2. The outer filling solution was 10 mM KOAc and the inner filling solution (the upper compartment) was 10 mM NaCl. Electrodes were conditioned in 10 mM KOAc for 18 h and all electrode bodies, beakers, pipettes, and the reference electrode were soaked in 1 M HNO_3 prior to use to remove any traces of silver ions.

3.2.10 Electrodes Made With Cross-Linked Semifluorinated Polymer (CL-P2)

The ionic site (10.3 mg), and in the case of the silver or potassium selective ISE the appropriate amount of ionophore (13.2 mg of the **Ag-Rf$_{10}$**, 10.9 mg of the **Ag-Rf$_8$**, 3.59 mg of Cu(II)-I, or 7.7 mg of valinomycin) were dissolved in HFE-7100. This solution was then placed in the casting dish with the **CL-P2** membrane and allowed to evaporate. The membranes were then cut to the appropriate size, removed from the casting dish and placed

in the Philips body electrodes[142] for the ion-exchanger electrodes, or in custom-made bodies with two compartments (shown in Figure 3.6) for the silver selective electrodes. These custom bodies consist of the cap and plunger of a Philips body electrode held to a glass tube with Tygon tubing. An upper compartment consisting of a cotton packed pipette tip containing the Ag/AgCl wire as an internal reference electrode and closed with a septum was inserted into the glass tube and held in place with more Tygon tubing. Silver ISEs were conditioned in 1 mM KOAct prior to selectivity measurements. All electrode bodies, beakers, pipettes and the reference electrode were soaked in 1 M HNO_3 prior to use. Ion-exchange electrodes used 1 mM KCl as inner filling and conditioning solution, and potassium ISEs used 1 mM NaCl for inner filling solution and conditioning solution. All electrodes were conditioned for 18 h prior to use.

3.2.11 ISE and Ion-Exchange Electrode Measurements.

For all measurements the external reference electrode was a double-junction Ag/AgCl electrode with a 1 M LiOAc bridge electrolyte and an AgCl saturated 3 M KCl reference electrolyte. EMF Suite 1.03 software (Fluorous Innovations, Arden Hills, MN) was used with an EMF 16 potentiometer (Lawson Labs, Malvern, PA). The liquid junction potential was calculated using the Henderson Equation[143] and activities were calculated using a two-parameter Debye-Hückel approximation.[144] The separate solutions method was used to determine the selectivity coefficients.[15, 40] Unless noted, the electrodes' response was near Nernstian for all ions (between 50 and 62 mV for mono-cations and between 25 and 32 mV for di-cations). The resistance of membranes were measured using the known shunt method.[145]

3.2.12 Temperature Endurance Tests

The temperature stability of cross-linked **CL-P2** membrane electrodes and of potassium selective PVC membrane electrodes were measured in parallel for comparative purposes. PVC-based membranes were prepared for this purpose by dissolving 46.1 mg of PVC, 92.1 mg of *o*-NPOE, 0.79 mg of NaTFPB, and 1.66 mg of valinomycin in 2 mL of freshly distilled THF. The solution was placed in a 3 cm diameter casting dish and the THF was allowed to evaporate overnight. This yielded a membrane with a thickness of 0.10 mm. Membranes with a 1 cm diameter were cut from the master membrane and placed in Philips body electrodes that contained a Ag/AgCl wire as an internal reference and an inner filling solution of 1 mM KCl. These electrodes were conditioned in 1 mM KCl overnight before use.

To test the ability of the electrodes to function after being exposed to high temperatures, the potassium ISEs made from PVC and from **CL-P2** were placed in a 1 mM KCl solution inside of a water-jacketed flask that was connected to a temperate-controlled water bath. The emf was monitored in 5 °C intervals from 25 °C to 90 °C for 5 minutes each. The electrodes' response to K^+ at room temperature was measured after heating to 40, 60, 75, and 90 °C. The electrodes were then held at 90 °C in 1 mM KCl for five hours while monitoring the emf. The electrodes' response to K^+ at room temperature was measured after one, three and five hours. The electrodes were then placed in a boiling solution. The electrodes' response to K^+ at room temperature was measured after 3 and 5 hours and every 2.5 hours after that, up to 17 .5 hours total.

3.3 Results and Discussion

3.3.1 Synthesis of Fluorinated Homopolymers

Before synthesis of the polymers to be used as ISE membranes, the corresponding monomers had to be synthesized. The monoether **M1,** used for the synthesis of the semifluorinated homopolymer **P1**, was synthesized from 2-(perfluorohexyl)ethanol and 4-chloromethylstyrene using tetrabutylammonium hydrogen sulfate as a phase transfer catalyst (see Figure 3.2). Synthesis of two semifluorinated oligoether monomers was also attempted (see Figure 3.2 and Figure 3.S1). The shorter of the fluorinated oligoether monomers, **M2**, was successfully synthesized using a modified literature procedure similar to that used for **M1**,[80] using dichloromethane as a solvent (see Figure 3.2). Using larger amounts than those used in the literature of the phase transfer catalysis proved necessary to obtain an acceptable yield of **M2**. The identity of **M1** and **M2** was confirmed by ^{1}H-NMR (see Figures 3.S3 and 3.S4). The fluorous oligoether chain of the fluorinated oligoether monomer was used to increase the fluorophilic character of the resulting polymer and still maintain a low glass transition temperature in the corresponding polymer. This design takes advantage of the fact that long chain perfluoroalkanes are crystalline solids at room temperature while perfluorooligoethers are liquids.[80, 133, 146] Difficulties arose in the synthesis of the longer chained fluorinated oligoether monomer, **M3** (See Figure 3.S1). The longer chain oligoether alcohol is not soluble in dichloromethane. Synthesis of **M3** was attempted using 1,1,2-trichloro-1,2,2-trifluoro-ethane as solvent. This was unsuccessful, likely due to the low solubility of tetrabutylammonium hydrogen sulfate

in 1,1,2-trichloro-1,2,2-trifluoro-ethane. Additional experiments using mixtures of HFE-7100, perfluorohexane, trichloro-trifluoro-ethane and dichloromethane as a solvent were performed, but unfortunately none yielded the desired product, even when extending the reaction time to two days.

First, homopolymers were synthesized from the monomers to test the viability of these polymers as the polymer matrix of ISE membranes. **M1** was polymerized into the semifluorinated homopolymer, **P1**, by free radical polymerization with toluene as the solvent, using several concentrations of the initiator azobisisobutylonitrile (AIBN), see Figure 3.1. To remove impurities from the polymer, it was repeatedly dissolved in THF and precipitated by addition of the THF solution into methanol. Only minimal impurities were detected by ^{1}H-NMR spectroscopy after this purification (see Figure 3.S5).

End group analysis by ^{1}H-NMR spectroscopy of **P1** as prepared with 20% initiator and using the integral of the peak due to the methyl groups of the AIBN end groups at 1.43 ppm compared with that of Ar-CH_2 (peak F, Figure 3.S5) at 4.42 ppm suggested that the average degree of polymerization was 8.4. However, the peak due to the AIBN end group has significant overlap with the peaks fom the backbone of the polymer (A and B) and, therefore, this value likely slightly underestimates the degree of polymerization. MALDI mass spectroscopy was used to independently determine the molecular weight of the **P1** polymer, using dithranol as a matrix (see Table 3.1 for the results and Figure 3.S7 for an example of a typical mass spectrum). The degree of polymerization for **P1** as prepared with 20% initiator and determined by MALDI was 9.8, only slightly larger than the value

determined by end group analysis using the ^{1}H-NMR spectra (8.4). This difference can be explained by the peak overlap in the ^{1}H-NMR spectrum.

Decreasing the concentration of initiator only saw a very small increase in the degree of polymerization of **P1** (see Table 3.1). Therefore, over the range of tested concentrations, the concentration of the initiator used to make **P1** should have little effect on the performance of the ISE. The PDI of **P1** is above 1.5 for all initiator concentrations as expected for a free radical polymerization. All polymers of type **P1** are are soluble in THF, 1,1,2-trichloro-1,2,2-trifluoro-ethane and chloroform, but have limited solubility in perfluorohexane. The solubility does not vary significantly by mass, which is not surprising given the small variation in molecular mass with initiator concentration. The PDI of **P1** is above 1.5 for all initiator concentrations as expected for a free radical polymerization. Decreasing the oncentration of initiator only saw a very small increase in the degree of polymerization of **P1**. Therefore, over the range of tested concentrations, the concentration of the initiator used to make **P1** should have little effect on the performance of the ISE.

Table 3.1: Analysis of **P1** Polymers by MALDI Mass spectrometry.

Initiator	M_n (g/mol)	M_w (g/mol)	N	PDI
50% AIBN	4700	8600	9.8	1.83
20% AIBN	4700	8700	9.8	1.85
5% AIBN	5900	9500	12.3	1.63
0.1% AIBN	5300	11300	11.0	2.15

M2 was polymerized into a fluorinated oligoether homopolymer, **P2** by free radical polymerization (see Figure 3.1) in toluene using several concentrations of the initiator, AIBN, as with **P1**. After purification of the polymer as with **P1**, minimal impurities were

detected by ^{1}H-NMR. MALDI mass spectroscopy was used to attempt to determine the molecular weight of the **P2** polymers as with **P1**, using dithranol as a matrix. However, such attempts were unsuccessful. Trials with other matrices, such α-cyano-4-hydroxycinnamic acid and pentafluorobenzoic acid, which has shown prior success as a matrix for fluorous polymers,[79] were also unsuccessful. Reactions performed in a neat solution of **M2** (i.e., without solvent) with 1 % initiator produced a polymer that was not soluble in THF or chloroform, but was soluble in perfluorohexane, indicating that this polymer is more fluorophilic. Due to the higher concentration of monomer, this polymer is expected to have a higher molecular weight (therefore this will be referred to as high molecule weight **HMW-P2** below) as the chain length of the polymer should be directly proportional to the monomer concentration, as shown by the kinetic chain length:[21]

$$\bar{v} = \frac{k_p[\mathrm{M}]}{2(f k_t k_d[\mathrm{I}])^{1/2}} \tag{3.1}$$

where k_p is the rate constant for polymerization, k_t is the rate constant of termination, k_d is the rate constant for the decomposition of the initiator, *f* is the fraction of initiator that reacts with the monomer, [M] is the concentration of the monomer and [I] is the concentration of the initiator. Unfortunately, attempts to confirm this by determining the mass of the **HMW-P2** by MALDI were unsuccessful as in the case of MALDI analysis of **P2**, despite trials with several matrices. This is likely due to the difficulties associated with ionizing fluorous polymers of sizable molecular weight.[79] While other methods, such as size exclusion chromatography, may allow the determination of the molecular weight of **P2** and **HMW-P2**, due to the high cost of fluorous solvents this was determined to be nonessential. In any case, it appears that the increased chain length of **HMW-P2** increased

the fluorophilicity of the polymer, as the end group makes up a smaller portion of the polymer chain. ^{1}H-NMR spectroscopy of **HMW-P2** was performed using perfluorohexane as solvent with a capillary of C_6D_6 for signal locking; the resulting spectrum is shown in Figure 3.S6. The peak from the methyl groups from the end groups are not visible by ^{1}H-NMR, likely masked by the signals due to the polymer backbone and impurities in the perfluorohexane, suggesting a high degree of polymerization.

The glass transition temperatures, *T*g, of the semifluorinated polymers were determined by DSC. The *T*g of **P1** was determined to be 18.0 ºC for all tested initiator concentrations, similar to values found in the literature (17-19 ºC), even though the polymers reported in the literature are of slightly higher molecular weight (M_n= 15 and 36 kg/mol),[132, 133] and -43.0 ºC for **P2** polymers, which matches well the *T*g of -44 ºC for the **P2** block as reported in the literature for a polystyrene-**P2** block-*co*-polymer.[80] These values make **P1**, **P2**, and **HMW-P2** suitable for use as polymer matrixes for ISE membranes as they are below the typical operating temperatures of ISEs.[20]

3.3.2 Homopolymer Ion-Exchange Electrodes

Minor concentrations of impurities in the membrane matrix can affect the response of ISEs.[28, 75] If there are hydrophobic ionic impurities, then the ISE will respond to ions of the opposite charge when no additional ionic sites are added as these impurities act as ion exchanger sites. Because the ratio between ionic sites and the ionophore affects the selectivity of an ISE, lipophilic ionic impurities can also affect the selectivity of membranes with added ionic sites.[1] To test for ionic impurities that would interfere in an ISE, an electrode was first constructed using **P1** (prepared with 20% initiator) and no added

ionic sites. This electrode was conditioned in 1 mM KCl. It showed a slow sub-Nernstian (~24 mV/decade) response to cations, and a large drift upon exposure to differing concentrations of KCl, indicative of a high resistance membrane with a low concentrations of ionic impurities. Indeed, attempts to measure the resistance by the know shunt method indicated that the membrane resistance was much larger than 10 GΩ.

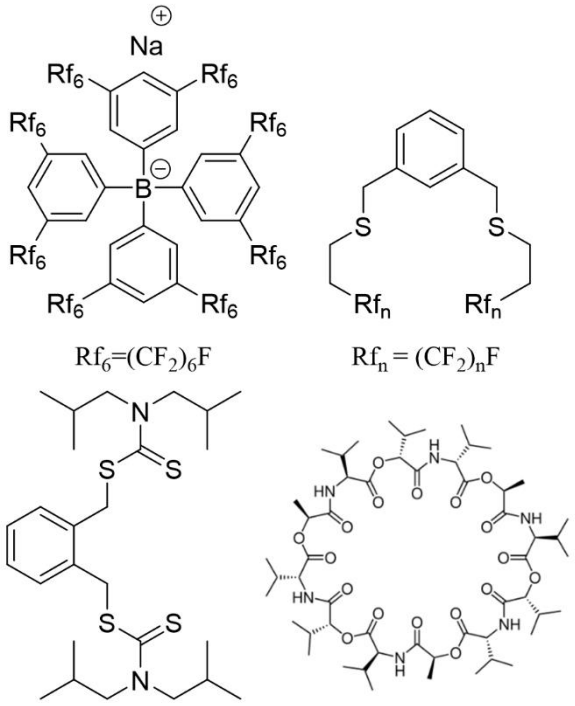

Figure 3.3: Membrane components: fluorophilic ionic site, sodium tetrakis[3,5-bis(perfluorohexyl)phenyl]borate (top left); fluorophilic Ag^+ ionophores **Ag-Rf$_8$** (n = 8) and **Ag-Rf$_{10}$** (n = 10; top right); Ag^+ ionophore, Cu(II)-I (bottom left); K^+ ionophore, valinomycin (bottom right).

To assess the ion selectivity made possible with the homopolymer **P1** as ISE membrane matrix, ion-exchange membrane electrodes were made with this polymer

(prepared with 20% initiator) and the fluorophilic, sodium tetrakis[3,5-bis(perfluorohexyl)phenyl]borate (Figure 3.3) to provide ion exchanger sites (10 mmol per kg of polymer). The resistance of the resulting membranes was determined to be 1.4 ± 0.2 GΩ, confirming that the addition of the fluorophilic borate significantly lowers the membrane resistance. These electrodes gave Nerstian (58 mV/Decade) responses to changes in the cation concentrations. Selectivities coefficients are shown Figure 3.4 and Table 3.2. The electrodes' selectivities follow the Hofmeister series. The selectivity range of the **P1** ion-exchange electrodes is not as broad as for fluorous membrane ISEs made with the same ionic site (over 15 orders of magnitude),[68] and is closer to that of more conventional polymeric membrane ISEs (8 orders of magnitude).[68] A partially fluorinated polymer may need a higher fluorous content than **P1** to provide a larger selectivity range,[68] which may be achieved by increasing the chain length of the fluorous ponytail, however for long chain perfluoroalkanes increasing the chain length has been shown to increase the glass transition temperature to values that would not be suitable for ISE membranes.[133] Alternatively, it is possible that the functional groups introduced by the initiator are responsible for some of the selectivity loss. Therefore, testing of alternative initiators may be useful.

Electrodes constructed from **P2** and **HMW-P2** with added ionic sites showed similar results to those observed with **P2**. Ion-exchange membrane electrodes were also made with **P2** (20% initiator) and **HMW-P2** (1% initiator) and the fluorophilic ionic site in the same manner as those made with **P1**. The resistance was determined to be 16 ± 1 MΩ in case of the low molecular weight **P2** membrane and 160 ± 20 MΩ for the **HMW-**

P2 membrane . This difference is consistent with the increase in fluorophilicity of **HMW-P2** as displayed by its solubility in perfluorohexane. The fact that both the **P2** and **HMW-P2** membranes exhibit a substantially lower resistance than the **P1** membranes shows that the fluorophilic site and its counter ion in the ISE membrane are much more mobile in in the fluorous environment provided by the perfluorooligoether side chains of **P2** and **HMW-P2** than this is the case for the perfluorohexyl groups of **P1**.

Membranes made from these polymers showed near Nernstian response slopes to all ions tested. The selectivity coefficients of these electrodes are shown in Figure 3.4 and Table 3.2. The selectivity range of ion-exchange electrodes made from **P2** and **HMW-P2** showed a substantially broader selectivity range (13 and 14 orders of magnitude respectively) than those made by **P1** (8 orders of magnitude) and that of typical PVC ion-exchangers (8 orders of magnitude). The **HMW-P2** has a broader selectivity range than the lower molecular weight polymer, likely due to its increased fluorophilicity. The **HMW-P2** selectivity range is approaching that of ion-exchange electrodes made by fluorous liquids (16 orders of magnitude). Because these polymers are not perfluorinated, membranes made with these polymers are not be expected to match the selectivity range shown by the ISEs with perfluorinated sensing membranes.

Table 3.2: Selectivity coefficients for various ion-exchange membranes made with PVC, **P1**, **P2**, **HMW-P2**, **CL-P2**, or a fluorous liquid (perfluoroperhydrophenanthrene).

	$Log(K^{POT}_{Cs+,J+})$						
Ion J	PVC *o*-NPOE	**P1**	**P2**	**HMW-P2**	**CL-P 2** 6% CL	**CL-P2** 3% CL	Fluorous liquid[68]
$N(Bu)_4^+$	4.41	6.0 ± 0.3	8.4 ± 0.3	10.1 ± 0.2	5.5 ± 0.8	9.5 ± 0.6	11.41
Ag^+	-0.25	1.4 ± 0.3	3.9 ± 0.2	1.3 ± 0.1	0.9 ± 0.3	1.5 ± 0.7	1.4
K^+	-1.07	-0.9 ± 0.3	-1.6 ± 0.1	-1.6 ± 0.1	-1.4 ± 0.6	-1.9 ± 0.8	-2.59
Na^+	-2.90	-1.9 ± 0.1	-2.4 ± 0.3	-3.0 ± 0.1	-2.5± 0.4	-2.4 ± 0.4	-3.75
Li^+	-3.66	-2.3 ± 0.3	-3.3 ± 0.2	-3.2 ± 0.1	-2.5 ± 0.5	-3.1 ± 0.1	-4.01
Ca^{2+}	-3.79	-	-4.4 ± 0.2	-3.8 ± 0.2	-3.6 ± 0.9	-3.9 ± 0.8	-4.35

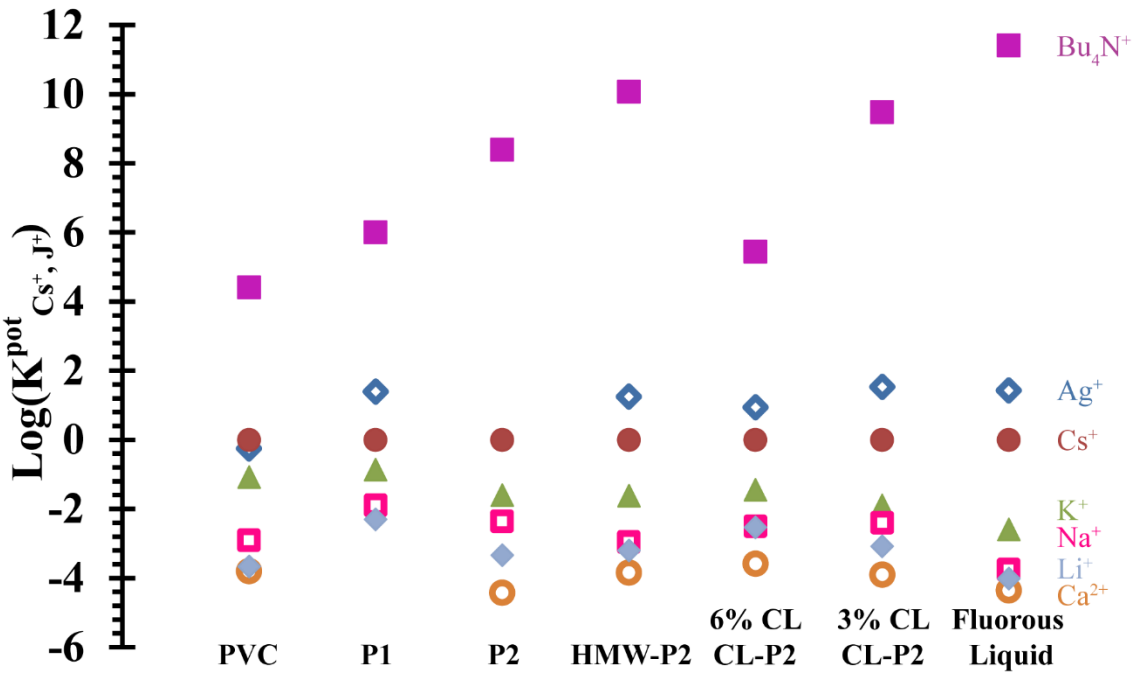

Figure 3.4: Selectivity comparison between ion-exchanger electrodes left to right: PVC and o-NPOE,[68] **P1**, **P2**, **HMW-P2**, 6% cross-linker **CL-P2**, 3% cross-linker **CL-P2**, Fluorous liquid (perfluoroperhydrophenanthrene).[68]

3.3.3 Homopolymer ISEs with Ionophores

To test the ability of the semifluorinated homopolymers to be used in ISEs, several ionophores were used. Silver ISE membranes with **P1** as polymer matrix, 0.5 mmol/kg fluorophilic ionic sites, and 1.5 mmol/kg fluorophilic Ag^+ ionophore (**Ag-Rf$_{10}$**) (Figure 3.3) were fabricated, using the same concentrations that have been used with fluorous liquid membrane silver ISEs.[136] The response of the electrodes toward several ions was sub-Nernstian. The poor selectivity (Table 3.S1) of the electrodes is likely due to anionic impurities in the membrane.

To determine the amount of ionic site needed to overcome the suspected ionic impurities in **P1**, ion-exchanger electrodes with varying concentrations of the added ionic site were fabricated. The electrodes' response was Nernstian for all tested ions and selectivity coefficients were obtained, see Figure 3.5. The large decrease in selectivity between the electrodes with 4 and 7 mmol/kg indicates that impurities in the membrane likely occur at concentrations between 7 and 4 mmol/kg and that an ionic site concentration of at least 7 mmol/kg is needed to overcome this impurity.

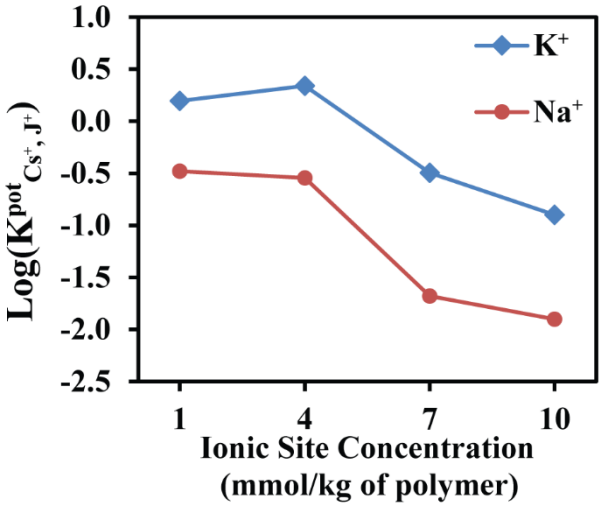

Figure 3.5: Ionic site variation for ion-exchanger membranes made from **P1**.

Silver ISE membranes with high concentrations of membrane components, 7 mmol/kg fluorophilic ionic site and 21 mmol/kg fluorophilic Ag^+ ionophore (**Ag-Rf$_{10}$**), to overcome the impurities, were fabricated. It has been previously shown that a 1:3 ratio of ionic site to the **Ag-Rf$_8$** and **Ag-Rf$_{10}$** ionophores gives the best selectivity coefficients, suggesting that these ionophores form 2:1 complexes with Ag^+.[136] It was necessary to wash the electrode bodies, beaker, pipettes and reference electrode in 1 M HNO_3 for several

hours prior to their use to avoid silver ion contamination and to perform the silver measurements last to avoid trace silver ion concentrations from affecting the responses to interfering ions and therefore would yield inaccurate selectivity coefficients.[15] The responses of the electrodes toward all tested ions were Nernstian. The limit of detection was 1.6 ± 0.1 μM, with a linear range from 5.0 mM to 2.5 μM (see Figure 3.S10). The increased concentration of the ionic site and the ionophore significantly improved the selectivity of the electrodes, but the selectivities are still not as good as those of the fluorous liquid ISEs (see Table 3.3), which is consistent with the inferior selectivities of the ionophore-free ion-exchange membranes.

Table 3.3: Selectivity coefficients for Ag^+ ISE made with **P1**, **CL-P2**, **HMW-P2**, or fluorous liquid (perfluoroperhydrophenanthrene) with fluorophilic ionophores.

	Ag^+ Selectivity (SSM) Log($K^{POT}_{Ag+,J+}$)						
Ion J^+	**P1** **Ag-Rf$_{10}$**	**CL-P2** **Ag-Rf$_{10}$**	**HMW-P2** **Ag-Rf$_{10}$**	Fluorous liquid[136] **Ag-Rf$_{10}$**	**CL-P2** **Ag-Rf$_8$**	**HMW-P2** **Ag-Rf$_8$**	Fluorous liquid[136] **Ag-Rf$_8$**
Cs^+	-5.1 ± 0.5	-6.8± 0.6	-5.1 ± 0.1	-9.4	-4.9 ± 0.4	-5.5 ± 0.4	--
K^+	-5.8 ± 0.5	-4.1± 0.6	-6.1± 0.1	-11.6 ± 0.1	-6.6 ± 0.6	-6.7 ± 0.3	-9.5 ± 0.2
Na^+	-6.3 ± 0.8	-7.7± 0.7	-6.3± 0.1	-12.9 ± 0.1	-7.6 ± 0.8	-7.7 ± 0.4	-10.9 ± 0.2
Li^+	-6.1 ± 0.6	-5.9± 0.5	-6.4± 0.2	--	-7.7 ± 0.7	-8.4 ± 0.3	--
Ca^{2+}	-5.6 ± 0.5	-7.1 ± 0.8	-5.3± 0.1	-12.7	-8.4 ± 0.8	-8.6 ± 0.3	--

Silver ISEs using the **HMW-P2**, the fluorophilic ionic site (7 mmol/ kg of polymer), and the fluorophilic **Ag-Rf$_8$** and **Ag-Rf$_{10}$** silver ionophores (21 mmol/ kg of polymer) were also tested. Selectivity coefficients for these electrodes are shown in Table 3.3. Selectivity coefficients could not be determined for Cu^{2+} due to the unstable signal in the presence of this ion. These electrodes showed improvements over those electrodes

using the fluorophilic ionophores and **P1**. Also, surprisingly, the electrodes made with the **Ag-Rf$_8$** ionophore showed a higher selectivity than those made with the **Ag-Rf$_{10}$** ionophore, opposite of the trend observed in the past with the fluorous liquids. It has been previously been suggested that the increased selectivity seen by the **Ag-Rf$_{10}$** ionophore over the **Ag-Rf$_8$** ionophore may be due to the perfluorodecyl groups' contribution to host preorganization because very long straight-chain perfluoroalkyl groups tend to not be very soluble even in fluorous solvents.[136, 147] It may be that in the **HMW-P2** system, the longer perfluoroalkyl groups of the **Ag-Rf$_{10}$** ionophore actually have a detrimental effect on the selectivity because of the difference in solubility in **HMW-P2** compared to perfluoroperhydrophenanthrene. These selectivity coefficients were, however, still substantially less than those of the silver ISEs made with fluorous liquids and the same ionophores. For the electrodes made from **HMW-P2** with the **Ag-Rf$_{10}$** ionophores, the limit of detection was 11 nM, and the linear range was from 15 nM to 0.5 mM (see Figure 3.S10). Electrodes made with the **Ag-Rf$_8$** ionophore showed a slightly lower limit of detection of 6.1 nM, and had a linear response down to 15 nM (see Figure 3.S10).

As the semifluorinated homopolymer **P1** is not perfluorinated and is soluble in THF, it appeared possible for a wider range of ionophores to be used in ISEs fabricated with this polymer while still maintaining some of the benefits of fluorous liquid membrane ISEs systems (i.e., increased selectivity and improved resistance to biofouling). In an attempt to improve the selectivity, electrodes were made using the silver ionophore Cu(II)-I (see Figure 3.4), which has been used to great effect in PVC-based ISEs in the past.[148] ISEs were fabricated with 7 mmol/kg fluorophilic ionic site and 21 mmol/kg Cu(II)-I

ionophore. Selectivity coefficients for these electrodes were superior to those obtained using the fluorous silver ionophore in this polymer and close to that of the conventional PVC Cu(II)-I silver ISE for some ions (see Table 3.4). The electrodes' response to silver (see Figure 3.S10) was Nernstian and had a linear range from 1 mM to 1 μM and a limit of detection of 19 ± 1 nM, which is slightly better than for electrodes made with **P1** and the fluorophilic **Ag-Rf$_{10}$** ionophore. Due to the fluorophilic nature of the **HMW-P2**, electrodes with this polymer and the lipophilic silver ionophore (Cu(II)-I) were not produced. While the more fluorophilic **HMW-P2** polymer with the fluorophilic ionophores showed improved selectivity over similar electrodes made with **P1**, the **P1** electrodes with the lipophilic silver ionophore (Cu(II)-I) showed overall slightly better selectivity then those made with **HMW-P2** and the fluorophilic ionophore.

Table 3.4: Selectivity coefficients for ISEs with lipophilic ionophores

	Log($K^{POT}_{Ag+,J+}$)					Log($K^{POT}_{K+,J+}$)	
Ion, J	**P1** Cu(II)-I	**CL-P2** Cu(II)-I	Fluorous liquid[136] **Ag-Rf$_{10}$**	PVC[148] Cu(II)-I	Ion, J	**CL-P2** valinomycin	PVC[15] valinomycin
Cs^+	-7.4 ± 0.3	-6.7 ± 0.6	-9.4	--	Na^+	-4.1 ± 0.6	-4.5 ± 0.1
K^+	-7.5 ± 0.1	-8.2 ± 0.7	-11.6 ± 0.1	-7.7 ± 0.1	Ca^{2+}	-6.2 ± 0.7	-6.9 ± 0.1
Na^+	-7.7 ± 0.1	-8.3 ± 0.5	-12.9 ± 0.1	-11.5 ± 0.7	Mg^{2+}	-7.6 ± 0.8	-7.5 ± 0.1
Li^+	----	-8.6 ± 0.8	--	--			
Ca^{2+}	----	-9.7 ± 0.6	-12.7	-12.8 ± 0.1			
Cu^{2+}	-6.8 ± 0.4	----	-13 ± 0.1	-8.2 ± 0.2			

3.3.4 Semifluorinated Cross-Linked Polymers for ISE Membranes

While the homopolymers **P1** and **P2** both could be made into functional ISE membranes, they lacked the mechanical stability to be fashioned into self-supported membranes and, therefore, still required the Fluoropore support. By cross-linking the polymers, the mechanical stability of the polymer can be greatly increased. To achieve this, a cross-linked fluorous polymer, **CL-P2**, was obtained by UV-initiated free radical polymerization with **M2**, AIBN as an initiator, and divinylbenzene as a cross-linker (see Figure 3.1). UV initiation was used in place of thermal initiation so that the polymer could be easily cross-linked into the desired shape; highly cross-linked polymers are not usually soluble and it would not be possible to cast a membrane once polymerized. This process produced a polymer that could be cut into membranes suitable for use in ISEs without the need of an additional support (see Figure 3.S9). After the polymerization, the polymers were washed several times with THF, perfluorohexane, and HFE-7100 to remove any remaining initiator and other impurities.

To create ion-exchange electrodes, fluorophilic ionic site (7 mmol per kg of polymer) was dissolved in HFE-7100 and then the solution was used to swell the membrane, and the solvent was allowed to evaporate, leaving the ionic site inside of the cross-linked polymer. Swelling with perfluorohexane was unsuccessful due to precipitation of the ionic site while the solvent was evaporating due to the relatively low solubility of the ionic site in perfluorohexane. Attempts made to use THF to swell the polymer resulted in membranes that, when used for ion-exchange membranes, resulted in sub-Nernstian or no response for many cross-linker concentrations. This is likely due to low swelling with

this non-fluorous solvent, which does not allow for sufficient ionic site penetration into the polymers. Membranes were made with a variety of initiator and cross-linker combinations.

Table 3.5 summarizes the characteristics of ion-exchange electrodes made with these membranes when exposed to varying potassium ion concentrations. Only membranes made with 1 mol % initiator and either 3 or 6 mol % cross-linker had a low failure rate and exhibited consistent Nernstian slopes. Membranes made with lower cross-linker concentrations did not have the mechanical strength to be used in the Philips body electrodes. DSC measurements showed increasing glass transition temperatures with increasing cross-linker concentration (see Table 3.6), but none of the membranes had a T_g above room temperature. Therefore, all membranes that were robust enough to be used as self-supported membranes had sufficiently low glass transition temperatures to allow for the ion mobilities needed to function as ISE membranes. To further improve the durability of the **CL-P2** membrane, a porous Teflon filter membrane was cut to the size of the casting dish and placed in the casting dish before the polymerization reaction. This allowed the polymer to cross-link within the porous support, further increasing the durability of the electrode membrane.

The measured selectivity coefficients of the ion-exchanger electrodes made with the **CL-P2** polymers showed that those made with a higher extent of cross-linking had a narrower selectivity range due their lower fluorinated content (see Figure 3.4 and Table 3.2). The selectivity range of the ion-exchanger electrodes made with 1 mol % initiator and 3 mol % cross-linker (**CL-P2**) had a selectivity range of approximately 14 orders of magnitude, similar to that of the fluorous homopolymer **HMW-P2**. The limit of detection

for K^+ of these membranes was 4.6 μM and the typical linear range extended down to 0.02 mM, as shown in Figure 3.S11. The resistance of the electrodes made with 6% initiator **CL-P2** was 170 ± 20 MΩ, which was slightly higher than for those made with 3% initiator **CL-P2**, which had a resistance of 70 ± 30 MΩ. This could be explained by the lower glass transition temperature of the membranes made with 3% initiator allowing for higher ion mobility within those membranes (see Table 3.6).

Table 3.5: Success rate and response slope to K^+ of ion-exchange electrodes made with cross-linked semifluorinated polymer, **CL-P2**

	Initiator Concentration / mol %					
Cross-Link Concentration mol %	1.0%		0.5%		0.1%	
	Percent Responding	Slope mV	Percent Responding	Slope mV	Percent Responding	Slope mV
6.0%	100%	54 ± 4	0%	--	25%	45.5 ± 0.9
3.0%	100%	58 ± 2	50 %	31 ± 14	0%	--
1.0%	25 %	33 ± 11	0%	--	0%	--

Table 3.6: DSC measurements of **CL-P2** with 1 mol % initiator

mol % cross-linker	T_g / °C
1%	-37.5 ± 0.9
3%	8.3 ± 0.5
6%	19.1 ± 0.6

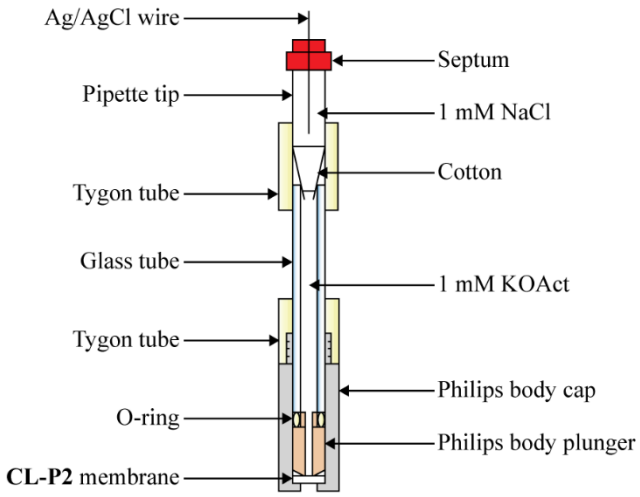

Figure 3.6: Schematic of Ag^+ ISE made with **CL-P2**.

Membranes for silver selective electrodes were made with **CL-P2** with 6 mol % cross-linker by swelling the **CL-P2** membranes with a HFE-7100 solution containing a fluorophilic ionophore (21 mmol per kg of polymer) and the fluorophilic ionic site (7 mmol per kg of polymer) and letting the solvent evaporate. These membranes were placed in custom made electrode bodies that utilized the same cap and plunger as the Philips body electrodes but allowed for the addition of a second solution compartment (see Figure 3.6). This setup prevented the silver ions contained in the inner filling solution, which was in direct contact with the Ag/AgCl reference electrode, from affecting the selectivity coefficient measurements as exposure to the target analyte can cause sub-Nernstian response slopes in the response slopes of interfering ions.[40] Moreover, it prevented chloride ions from enter the ISE membranes and causing precipitation of AgCl in the sensing membrane. These electrodes displayed selectivity coefficients for both the **Ag-Rf$_8$** and **Ag-Rf$_{10}$** ionophores that were similar to those observed with silver selective electrodes made

from **HMW-P2** (see Table 3.3). This shows that the small amount of cross-linker has minimal effect on the selectivity of the electrode, which is consistent with the results for the ion-exchange electrodes. The limit of detection for these electrodes were, however, worse than that those seen for electrodes made with the corresponding homopolymer, **HMW-P2**. The electrodes made from **CL-P2** with the **Ag-Rf$_8$** ionophore showed only a slight increase in the limit of detection to 35 nM, whereas those made with the **Ag-Rf$_{10}$** ionophores showed a dramatic increase to 2 μM (see Figure 3.S12). This trend is also showcased in the linear range of the electrodes, where electrodes made with **Ag-Rf$_{10}$** ionophore and the **CL-P2** showed a slight increase in the lower limit of their linear rage (100 nM) when compared to corresponding electrodes made from **HMW-P2** (15 nM). Like the ion-exchange electrodes made from **CL-P2**, the average E° for the silver selective ISEs varies dramatically between each electrode.

To test the ability to use traditional lipophilic ionophores in the cross-linked membranes, membranes were made using the Cu(II)-I ionophore to make silver selective electrodes and valinomycin to make a potassium selective electrode. Valinomycin and Cu(II)-I are not soluble in HFE-7100; however, a 2:1 mixture of HFE-7100 and THF was found to be a suitable solvent for the delivery of this ionophore into the **CL-P2** membranes.

Selectivity coefficients measured for the silver ISEs with the Cu(II)-I ionophore were superior to those obtained with the fluorophilic ionophores in **CL-P2** and **P2** as well as those obtained with the Cu(II)-I ionophore in **P1** (see Table 3.4). However, these are still inferior to those obtained with this ionophore in PVC.[148] Selectivity coefficients could not be determined for Cu^{2+} with the **CL-P2** membranes due to unstable signal in the

presence of this ion. The limit of detection of these silver ISEs was 13 ± 4 nM, with a linear range from 100 to 0.1 μM (see Figure 3.S12). Selectivity coefficients obtained for the potassium ISEs made with **CL-P2** and valinomycin were similar to those for potassium ISEs made from PVC and valinomycin (see Table 3.4).[15] These electrodes showed a limit of detection of 0.7 ± 0.5 μM and a linear range from down to 2.0 μM, see Figure 3.S12. These values are more than sufficient for most applications. For example, in human blood the typical range for potassium is 3.5 - 5.5 mM while sodium is 135 - 145 mM, and calcium and magnesium are only 1.03 - 1.23 and 0.49 - 0.59 mM, respectively.[149-152] The ability to use lipophilic ionophores, which are widely available, should allow for an expanded use of fluorous membrane ISEs. With the fluorous liquid, their application was limited due to the small selection of soluble ionophores.

3.3.5 High Temperature Testing

To test the ability of the **CL-P2** membranes to survive exposure to high temperatures, the K^+ selective **CL-P2** electrodes were heated in a solution of 1 mM KCl. The electrodes still showed a Nernstian response slope after being slowly heated to 90 °C over a period of 2 h and then cooled. The electrodes were then heated for an additional h to 90 °C. During this time, the electrodes suffered from a large drift, and upon cooling only 75% continued to respond to changes in the potassium concentration. While these electrodes still gave a Nernstian slope, their limit of detection was increased from 0.7 ± 0.5 μM to 6.0 ± 3.1 μM. After heating for 4 more hours to 90 °C no additional electrodes failed. All functioning electrodes gave a Nernstian response and showed no increase in the limit of detection after cooling. The electrodes were then placed in a boiling 1 mM KCl solution

for 3 h and still exhibited a near Nernstian (> 50 mV/decade) response slope after cooling, although there was a slight increase in the limit of detection to 8.1 μM. The electrodes were then placed in the boiling solution for an additional 13.5 h for a total of 17.5 h under boiling conditions, cooling and calibrating periodically (see Figure 3.7 and Table 3.S2). The electrodes showed Nernstian response slopes and no change in the limit of detection until 12.5 h of boiling, at which point 25% had sub-Nernstian slopes. The number of electrodes exhibiting Nernstian response slopes continued to drop until after 17.5 h, when none gave Nernstian response slopes. Further heating resulted in damage to several of the Philips bodies, so the experiment was halted. These tests subjected the electrodes to harsh thermal conditions as well as increased internal pressure on the membrane. It seems that except for some early failures, the membranes are very durable to elevated temperatures, and that the failure rate of such electrodes could be reduced by utilizing more thorough quality control. As these membranes can function after being heated to 100 °C for several hours they should be suitable for all but the highest temperature aqueous solution applications.

Potassium selective electrodes made with plasticized PVC membranes were also made to enable a comparison of the heat stability of PVC membranes to that of cross-linked membranes (see Figure 3.7 and Table 3.S2). Looking in the literature, it seemed that plasticized PVC membranes have only rarely been reported to be used in applications at temperatures exceeding 50 °C.[43, 44] It was therefore hypothesized that the PVC electrodes would fail quickly at high temperatures because they lack the additional durability provided by cross-linking. The PVC electrodes were exposed to the same harsh conditions as the cross-linked fluorous polymer electrodes. Surprisingly, the PVC electrodes performed

much better than expected, surviving when heated to 90 °C and still showing a Nernstian response slope upon cooling. They did, however, show large amounts of noise and drift while measuring at elevated temperatures. The electrodes showed a Nernstian response slope at room temperature after being heated at 90 °C for 5 h. Two-thirds of the PVC membranes showed a sub-Nernstian response to K^+ at room temperature after being placed in the boiling 1 mM KCl solution for 3 h. After 2 additional hours, for a total of 5 h in the boiling solution, all of the electrodes suffered from an erratic response with large drift when tested in room temperature solutions of KCl. These results show that while the PVC electrodes are inferior to the cross-linked membranes, they are also suitable for some high temperature aqueous applications and are therefore likely being underutilized.

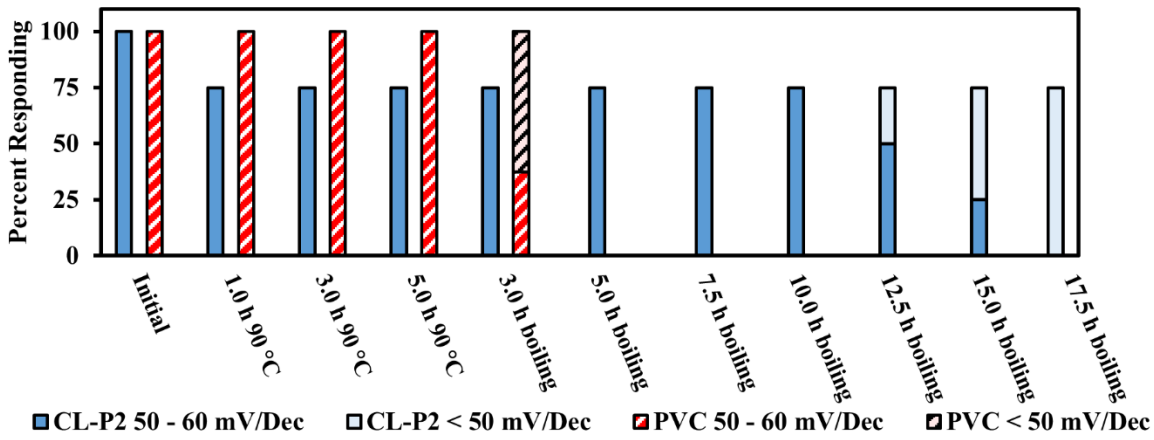

Figure 3.7: Percent of PVC or **CL-P2** polymer K^+ ISEs responding at 23 °C after heating at 90 °C or in a boiling solution.

3.4 Conclusions

Several semifluorinated polymers have been synthesized and utilized as ISE membranes with fluorophilic ionic sites and both fluorophilic and lipophilic ionophores. Ion-exchange electrodes made with **P1** did not show such a broad selectivity range as previously observed with fluorous liquid membrane ion-exchange electrodes, while those made with **P2** showed much broader selectivity ranges than those made with **P1**, approaching the selectivity range of electrodes made with fluorous liquids. ISEs utilizing both of these polymers and a fluorophilic ionophore were highly selective, however they showed less selectivity then their fluorous liquid counterparts. These polymers do, on the other hand, allow for the use of a broader range of ionophores, as several lipophilic ionophores have been used to fabricate ISEs with these polymers. Additionally, a self-supported semifluorinated polymer membrane ISE was created by cross-linking a fluorinated oligoether monomer, to form **CL-P2**. Highly selective ISEs have been fabricated with this material using both fluorophilic and lipophilic ionophores. The selectivity coefficients of the potassium electrodes made from the **CL-P2** using valinomycin approach that of the best PVC based potassium electrodes utilizing this ionophore. This membrane showed excellent resistance to high temperatures, functioning after being heated to 90 °C, and many still functioned after exposure to boiling 1.0 mM KCl_{aq} for 10 hours. Due to their fluorophilicity and lack of plasticizer, it is suspected that ISEs made with these materials should be resistant to biofouling. We hope to test this property in the near future. Due to the ability to control the polymerization, these polymers would also be ideal for addition of covalently attached ionic sites and ionophores, which

would further improve the resistance to biofouling and improve the lifetime of such sensors.

3.5 Supporting Information

3.5.1 Attempted Synthesis of Monomer 3 Fluorous Oligoether (M3)

Attempts to synthesize **M3** were similar to that of **M2**. This synthesis used the fluorous alcohol 1H,1H-Perfluoro(2,5,8-trimethyl-3,6,9-trioxadodecan)-1-ol as starting material. The reaction was attempted in the following solvents: dichloromethane, HFE-7100, perfluorohexane, and trichloro-trifluoro-ethane, as well as the mixtures of 1:1, 1:2, 2:1, 5:1, and 1:5 of dichloromethane and the fluorinated solvents. Attempts were also made by extending the reaction time to 2 d. However, none of the reactions produced the desired product.

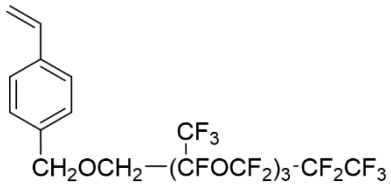

M3

Figure 3.S1: Structure of semifluorinated monomer, **M3**.

3.5.2 Homopolymer Electrode Body Diagram

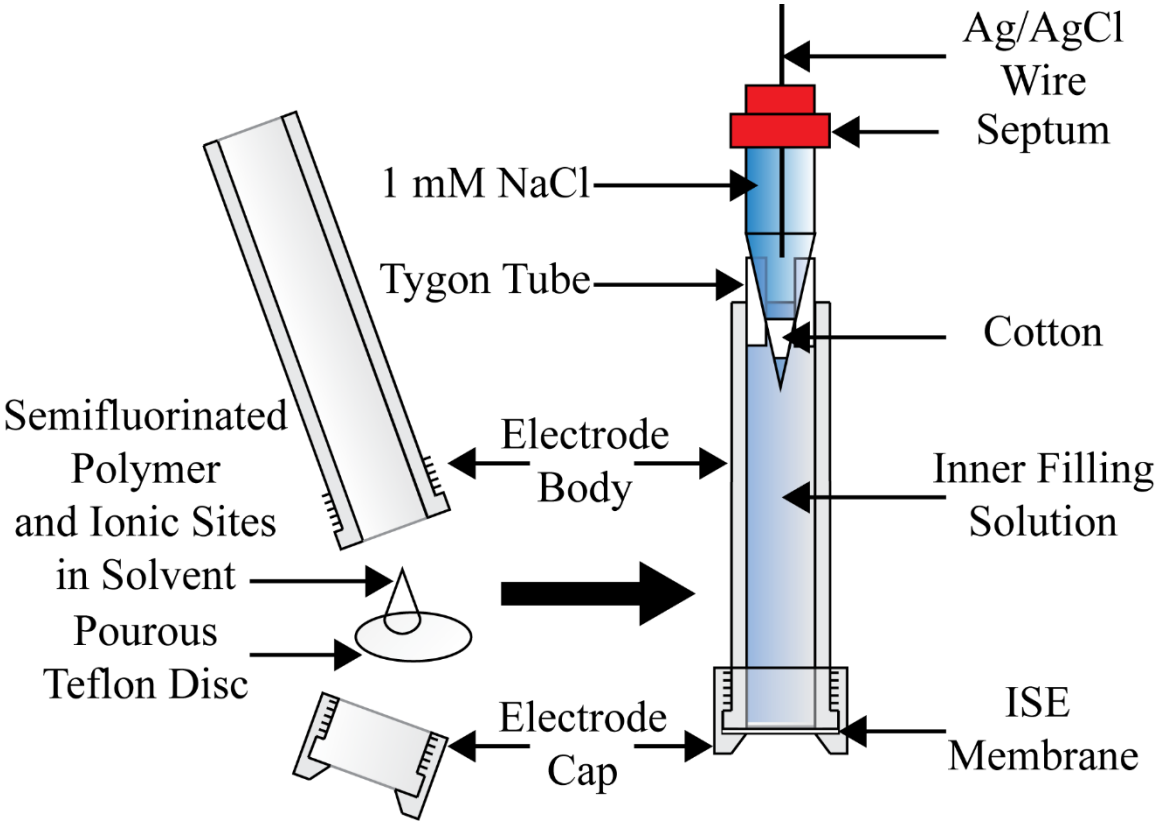

Figure 3.S2: electrode fabrication for ion-exchange electrodes made with fluorous polymers.

3.5.3 NMR, MALDI and DSC Spectra

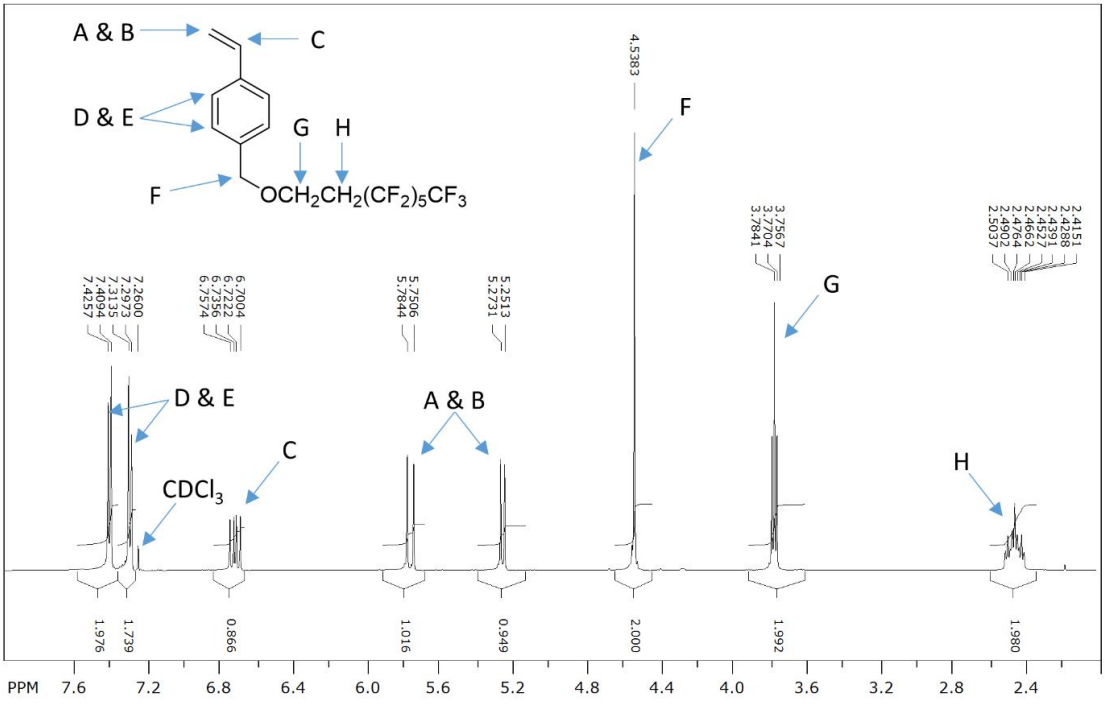

Figure 3.S3: ^{1}H-NMR of the semifluorinated **M1** (1*H*,1*H*,2*H*,2*H*-perfluorooctan-1-yl)styrene in $CDCl_3$.

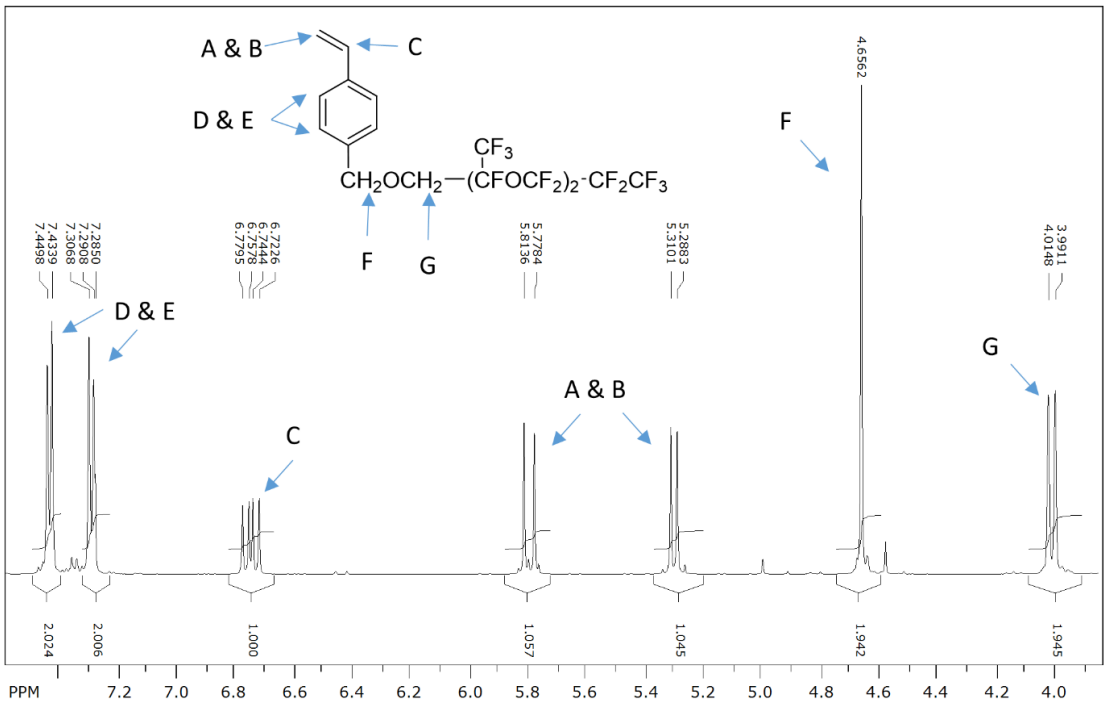

Figure 3.S4: ^{1}H NMR spectra of synthesized fluorinated oligoether monomer, **M2**.

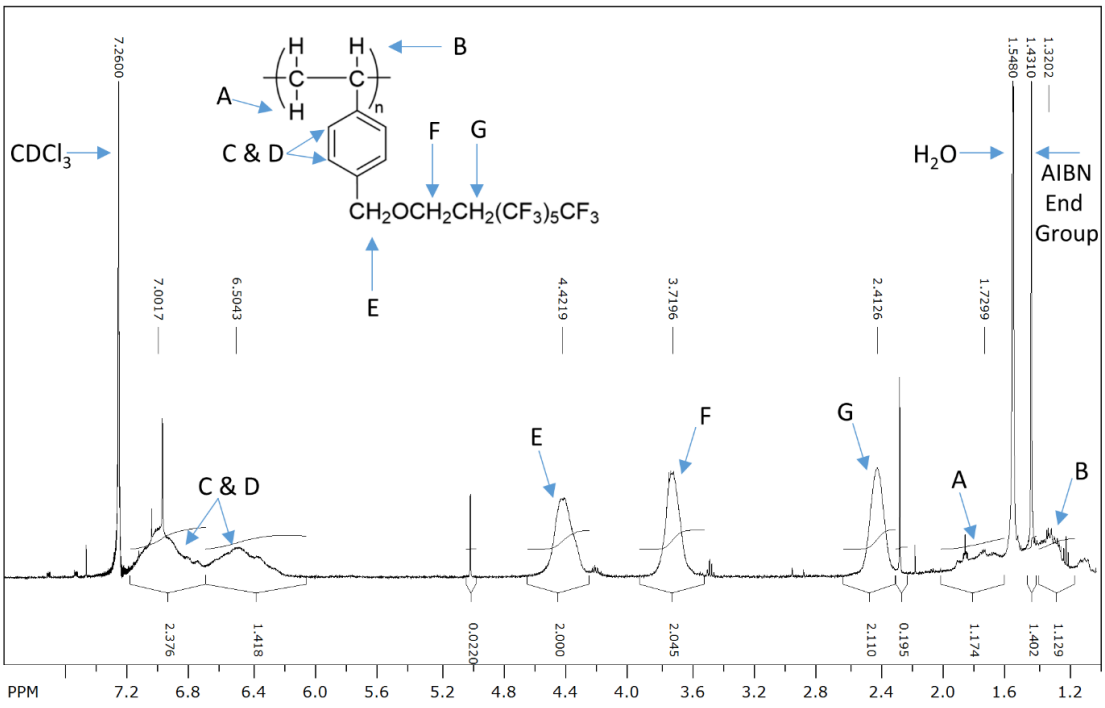

Figure 3.S5: ^{1}H-NMR spectra of semifluorinated polymer, **P1** in $CDCl_3$ prepared with 20% mol percent AIBN. The broad peaks are indicative of a polymerized molecule, where each repeat unit is in a slightly different chemical environment.

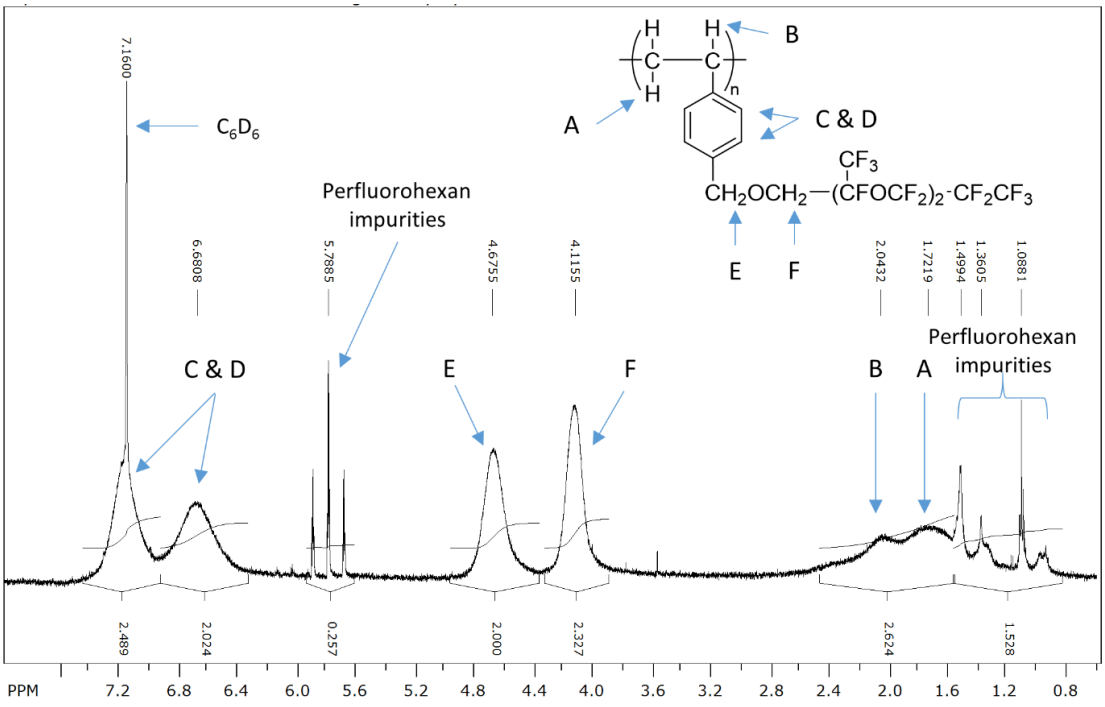

Figure 3.S6: ^{1}H-NMR spectra of **HMW-P2** in perfluorohexane with a C_6D_6 capillary for reference. Several of the peaks in this spectra are due to impurities in the perfluorohexane, as evident from the ^{1}H-NMR spectrum of perfluorohexane only. The broad peaks are indicative of a polymerized molecule, where each repeat unit is in a slightly different chemical environment.

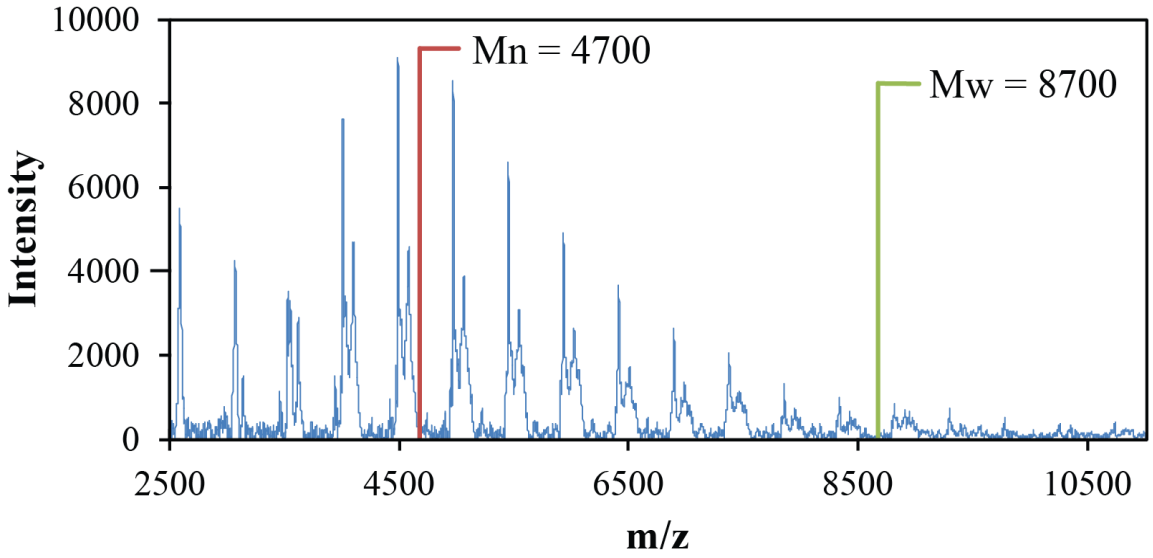

Figure 3.S7: MALDI mass spectrum of **P1** prepared with 20 mol % initiator; dithranol as matrix.

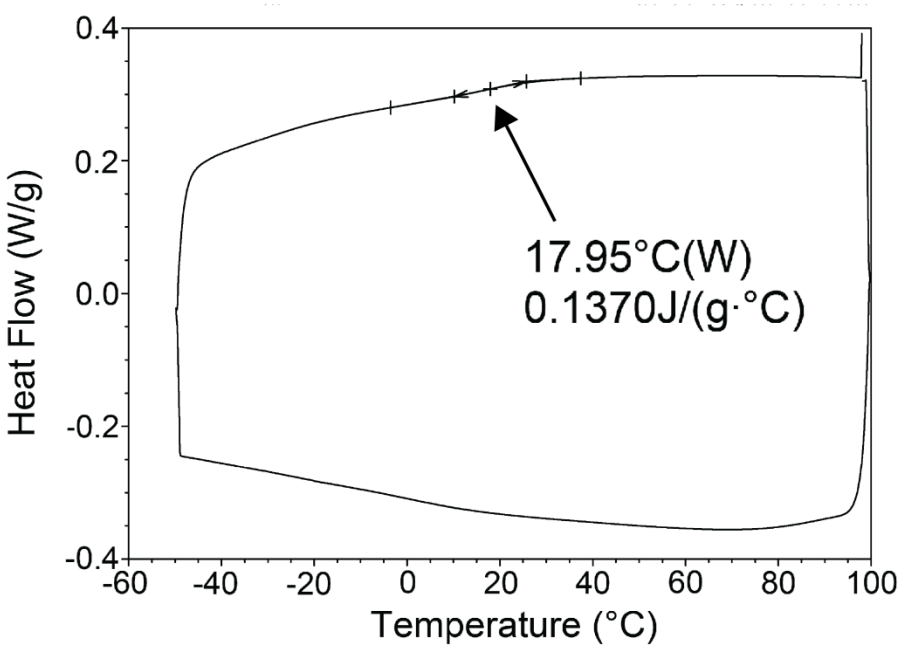

Figure 3.S8: DSC of **P1** made with 20 mol % initiator.

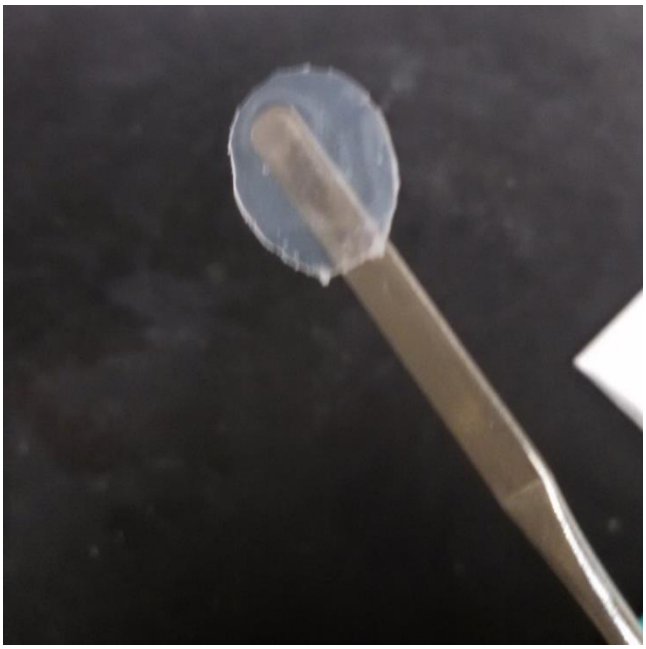

Figure 3.S9: Cross-linked semifluorinated polymer.

3.5.4 ISE Response Curves

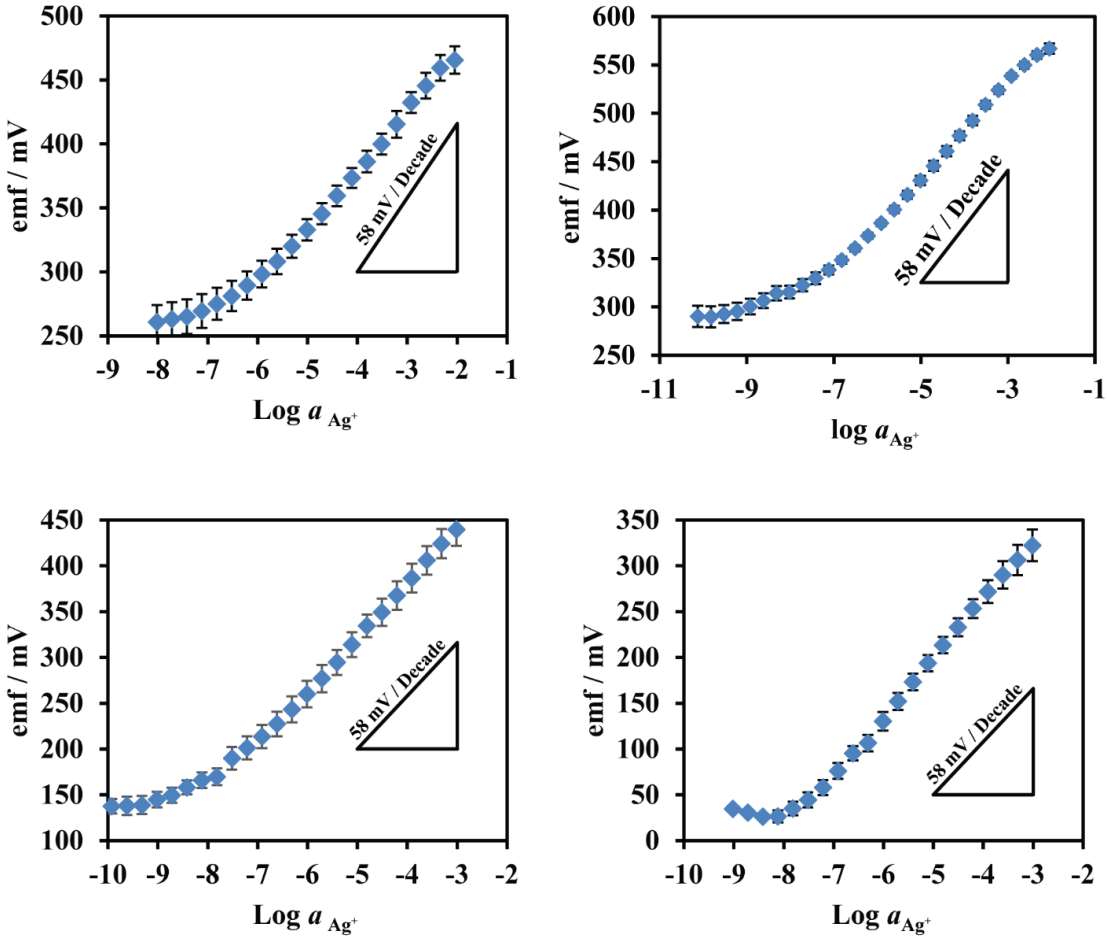

Figure 3.S10: Average response to Ag^+ of several Ag^+ ISEs made with **P1** membranes and **Ag-Rf$_{10}$** ionophore (top left); **P1** membranes and Cu(II)-I ionophore (top right); **HMW-P2** membranes and **Ag-Rf$_8$** ionophore (bottom left); and **HMW-P2** membranes and **Ag-Rf$_{10}$** ionophore (bottom right)

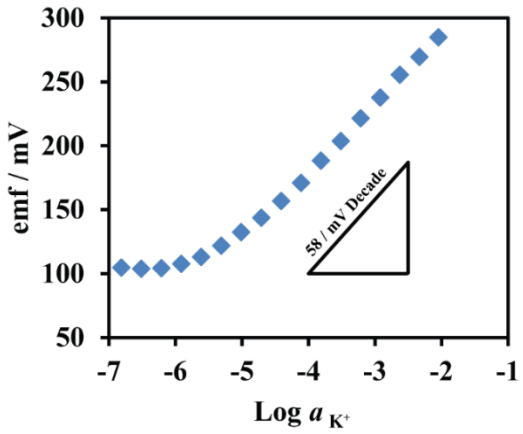

Figure 3.S11: Response to K^+ of an ion-exchange membrane made with a **CL-P2** membrane.

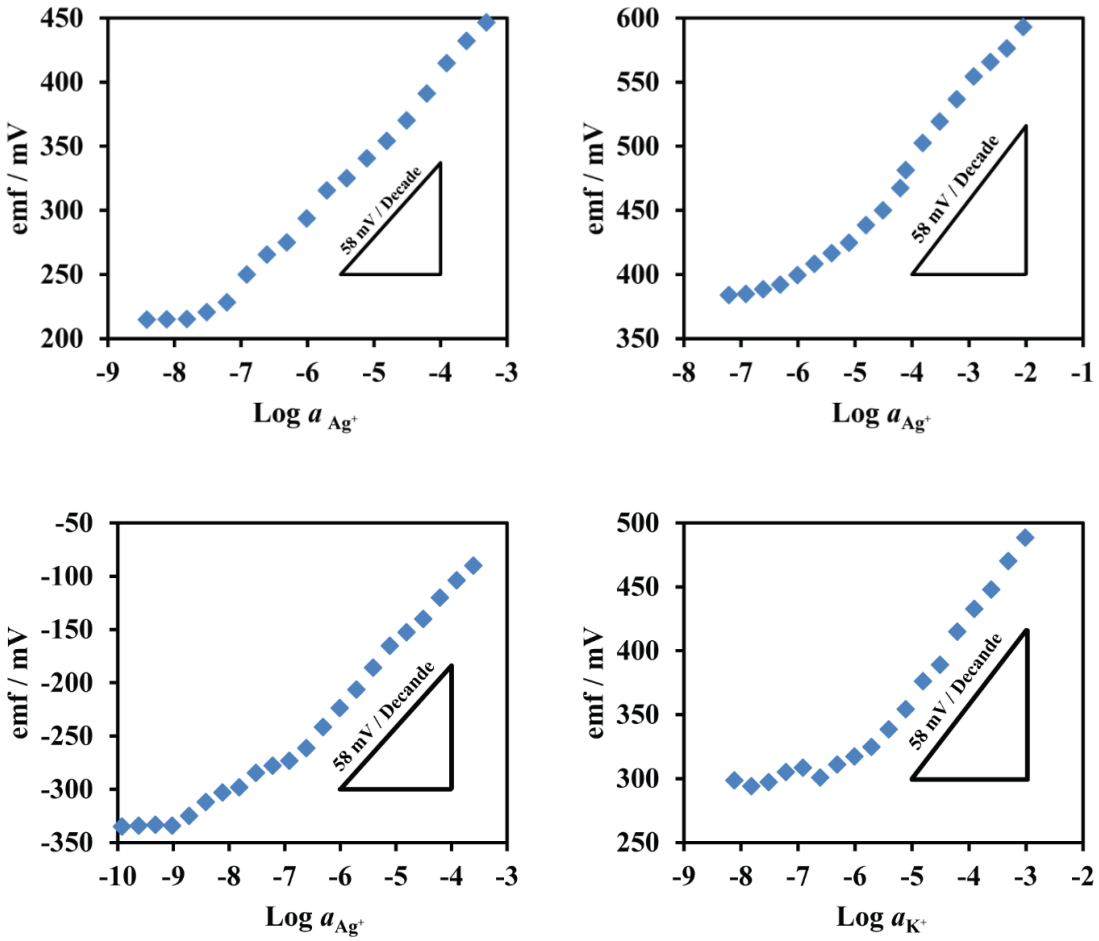

Figure 3.S12: Responses to Ag^+ of Ag^+ ISEs made with **CL-P2**, fluorophilic ionic site and with (top left) **Ag-Rf$_8$** ionophore, (top right) **Ag-Rf$_{10}$** ionophore, and (bottom left) Cu(II)-I ionophore. Responses to K^+ of K^+ ISE made with **CL-P2** and valinomycin (bottom right). The E° vales of electrodes made from **CL-P2** varied greatly between different electrodes; therefore, examples of typical responses for each type of electrode are shown.

3.5.5 Selectivity and Thermal Response Data

Table 3.S1: Selectivity coefficients of several Ag^+ electrodes made with **P1.**

	Selectivity (SSM) $Log(K^{POT}_{Ag+,J+})$		
Ion, J	**P1** 1.5 mmol/kg **Ag-Rf$_{10}$**	**P1** 21 mmol/kg **Ag-Rf$_{10}$**	Fluorous liquid **Ag-Rf$_{10}$**
Cs^+	-1.10 ± 0.7	-5.1 ± 0.5	-9.4
K^+	-1.66 ± 0.4	-5.8 ± 0.5	-11.6 ± 0.1
Na^+	-1.29 ± 0.4	-6.3 ± 0.8	-12.9 ± 0.1
Li^+	-1.24 ± 0.6	-6.1 ± 0.6	--
Cu^{2+}	------	-5.6 ± 0.5	-13.0 ± 0.1

Table 3.S2: Response of PVC based and semifluorinated cross-linked polymer based electrodes to K^+ at 23 °C after heating to 90 ºC for different time periods or exposure to boiling solutions for different time periods, showing the percent of tested ISEs that responded with slopes between 50 and 60 mV/decade, less than 50 mV/decade and those with no response (N.R.)

		90 °C								
Heating time (h)		1			3			5		
Response slope (mV /decade)		N.R.	< 50	50-60	N.R.	< 50	50-60	N.R.	< 50	50-60
PCV	% response	0	0	100	0	0	100	0	0	100
	Average slope (mV / decade)	-	-	54.1	-	-	53.4	-	-	52.9
Cross-linked	% response	25	0	75	25	0	75	25	0	75
	Average slope (mV / decade)	-	-	59.0	-	-	56.0	-	-	56.4

		Boiling solution								
Heating time (h)		3			5			7.5-10		
Response slope (mV /decade)		N.R.	< 50	50-60	N.R.	< 50	50-60	N.R.	< 50	50-60
PCV	% response	0	66.6	33.3	100	0	0	100	0	
	Average slope (mV / decade)	-	17.5	51.4	-	-	-	-	-	-
Cross-linked	% response	25	0	75	25	0	75	25	0	75
	Average slope (mV / decade)	-	-	53.4	-	-	53.0	-	-	55.7

		Boiling solution								
Heating time (h)		12.5			15			17.5		
Response slope (mV /decade)		N.R.	< 50	50-60	N.R.	< 50	50-60	N.R.	< 50	50-60
PCV	% response	100	0	0	100	0	0	100	0	
Cross-linked	% response	25	25	50	25	50	25	25	75	0
	Average slope (mV / decade)	-	20.0	52.8	-	18.9	50.2	-	22.9	-

4 CHAPTER FOUR:

Donnan Failure of Ion-Selective Electrodes with Hydrophilic High-Capacity Ion-Exchanger Membranes

Reprinted in part with permission from:

Ogawara, S; Carey, J. L., III; Zou, X; and Bühlmann, P., Donnan Failure of Ion-Selective Electrodes with Hydrophilic High-Capacity Ion-Exchanger Membranes, *ACS Sensors*, **2015**, Just Accepted Manuscript, DOI: 10.1021/acssensors.5b00128.

Available on web at http://pubs.acs.org/doi/abs/10.1021/acssensors.5b00128

This work was a joint effort by this author, Shogo Ogawara, Xu U. Zou who performed many of the Potentiometric measurments.

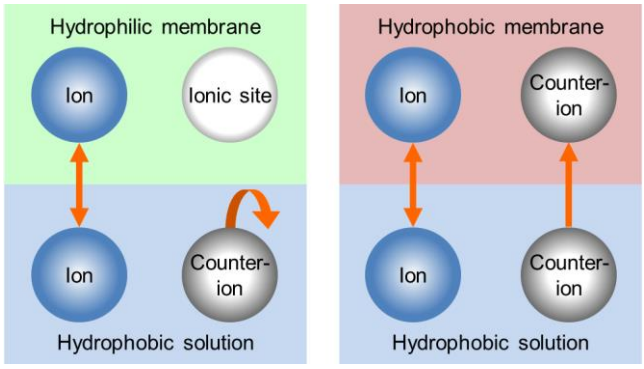

Hydrophilic ion-exchanger membranes with a high ion-exchange capacity find not only numerous applications in ion separations but have also interesting properties when used as sensing membranes of ion-selective electrodes (ISEs). As pointed out in the literature, the hydrophilic nature of these membranes may reduce biofouling of ISE sensing membranes as caused by electrically neutral, hydrophobic interferents. This work shows that hydrophilic high-capacity ion exchanger membranes are more resistant to Donnan failure (i.e., the limitation of the upper detection limit by co-ion transfer into the sensing membrane) than both hydrophobic ionophore-doped and hydrophobic ionophore-free ion-exchanger membranes. Nernstian responses of hydrophilic anion-exchanger membranes were found for anions as large as 2.0 nm, in spite of the crosslinked nature of the anion exchanger that was used. This shows that the high resistance of hydrophilic anion-exchangers to Donnan failure caused by cations such as tetrabutylammonium is not the result of size exclusion. For typical ions, the hydrophilicity of the anion exchanger does not play a decisive factor either. Instead, the excellent resistance to Donnan failure exhibited by hydrophilic ion exchange membranes is primarily caused by the high activity of exchangeable ions in the ion exchanger phase, which disfavors partitioning of ions of opposite charge (along with target ions) from samples into these sensing membranes. The absence of Donnan failure caused by hydrophobic co-ions may be of substantial benefit for measurements in biological samples.

4.1 Introduction

The majority of measurements with ion-selective electrodes (ISEs)[1, 4, 153-156] are performed in their linear (Nernstian) response range. Deviations of the emf response from linearity at the lower or upper detection limit are usually accompanied by other problems too, such as increased response times and lower selectivities. The deviation from linearity at the upper detection limit, which occurs when samples contain hydrophobic co-ions, is known as Donnan failure.[28, 51, 52, 157-161] The resistance of ISEs to Donnan failure is important, especially when ISEs are used in samples that contain organic hydrophobic co-ions, as it is often the case for samples of biological origin.

Different approaches have been described in the literature to reduce interferences from electrically charged and neutral, lipophilic interferents. Fluorous ISE membranes[8, 68, 73, 75] were introduced because fluorous phases are both hydrophobic and lipophobic, and exhibit particularly high selectivities, in part because of the poor solvation of interferents by the fluorous membrane matrix.[69-71] More recently, it was pointed out that ISEs with hydrophilic, polymeric ion-exchanger membranes suffer less from interferences by lipophilic ions of the same charge sign as the analyte than ISEs with conventional hydrophobic (i.e., lipophilic) sensing membranes.[94] It was explained that the transfer of hydrophilic ions from an aqueous sample into a water-swelled hydrophilic ion-exchanger membrane does not require the dehydratization of these ions and, therefore, does not result in a selectivity for lipophilic over hydrophilic ions.[94] The same can also be said about potentiometric sensors based on water-filled nanopores.[158, 162] which have ionic sites and ionophores covalently attached to the nanopore walls.

From a fundamental point of view, Donnan failure is a well-understood phenomenon that can be interpreted in two complementary and equally valid ways. On the one hand, one may focus on the ion with a charge sign opposite to the analyte ion, typically referred to as the co-ion. In this view, the failure of co-ion exclusion from the sensing membrane, i.e., Donnan failure, is favored by any chemical interaction that lowers the chemical potential of the co-ion in the sensing membrane, such as solvation and ion pair formation, and it is disfavored by the electrical potential difference across the sample/membrane interface. Using this explanation, the extent of Donnan failure can be discussed quantitatively on the basis of the electrochemical potential of the co-ion, which includes both thermodynamic and electrostatic components.[52] The latter are directly correlated to the surface charge density,[157, 158] which has to reach a minimum value to permit permselectivity, e.g., of a nanopore,[158, 163, 164] or result in the failure of a liquid junction based on a nanoporous glass plug.[121]

Alternatively, Donnan failure may be discussed in terms of partitioning of salts consisting of the analyte ion along with a co-ion between the aqueous sample and the sensing membrane. As long as the concentration of such salts in the sample is low, a Nernstian response to the target ion is observed, and the concentration of the co-ion in the sensing membrane is very low in comparison to the analyte ion. Donnan failure is reached when the transfer of the salt consisting of the analyte ion and a co-ion into the sensing has reached a level that the ratio of these two ions in the sensing membrane approaches their ratio in the salt[52, 165] (and, concomitantly, the analyte ion concentration in the sensing

membrane starts to exceed substantially the ion exchanger capacity of the sensing membrane).

While Donnan failure as a phenomenon is well understood, a comparison of the extent of Donnan failure of different types of ISE membranes has not been reported. We were interested in such a comparison, in particular in view of the promise of hydrophilic high-capacity ion-exchanger (HHCIE) membranes for measurements in biological samples, but also because of our recent interest in using ISEs with HHCIE membranes to monitor nanoparticle syntheses.[166] For a better understanding of the advantages of ISEs with HHCIE membranes, we compare here the Donnan failure characteristics of a typical commercial HHCIE membrane with those of ionophore-free[167] and ionophore-doped hydrophobic ISE membranes. The widely used plasticized poly(vinylchloride) (PVC) was chosen in this work as the membrane matrix for the hydrophobic ISE membranes, which is why the ion-exchanger and ionophore-free membranes are referred to in the following as PVC/IE and PVC/ionophore membranes, respectively. The high hydrophilicity of the HHCIE membranes used in this work is highlighted by the fact that they take up 11.5 wt % water at T = 25 ℃, which is two orders of magnitude more than the water content of 0.1 wt % reported for plasticized PVC membranes.[168] Undoubtedly, the this high hydrophilicity is to a large extent the result of the high ion exchange capacity of the HHCIE membranes, which in this study exceeded the ion exchange capacity of the ionophore-free ion exchanger membranes with a plasticized PVC matrix by a factor of 16. We also tested whether size exclusion has an effect on the performance of ISEs with the HHCIE membranes.

4.2 Experimental Section

4.2.1 Materials

All tetraalkylammonium salts were of >98%, purity and were used as received. Sample solutions were prepared using deionized and charcoal-treated water (0.18 MΩ cm specific resistance) obtained with a Milli-Q PLUS reagent grade water system (Millipore, Bedford, MA, USA). High molecular weight poly(vinyl chloride) (PVC), 2-nitrophenyl octyl ether (*o*-NPOE), tridodecylmethylammonium chloride (TDDMACl), and potassium tetrakis(4-chlorophenyl)borate (KTpClPB) were purchased from Fluka (Buchs, Switzerland), 5,10,15,20-tetraphenyl-21*H*,23*H*-porphine manganese(III) chloride (Mn(III)TPPCl, Figure 4.1) from Sigma Aldrich (St. Louis, MO, USA), and disodium 4-hydroxy-3-^{10}-1-naphthalenesulfonate (carmoisine, >95% purity; see Figure 4.2) from Pfaltz & Bauer (W. Chester, PA, USA).

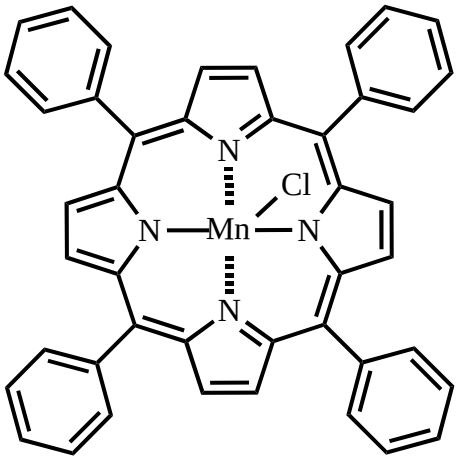

Figure 4.1: Structure formula of the ionophore Mn(III)TPPCl.

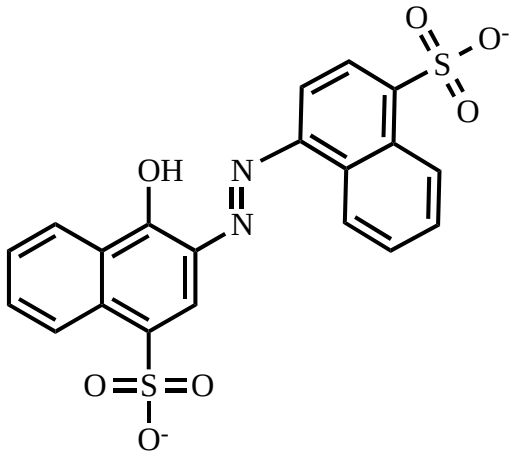

Figure 4.2: Structure formula of carmoisine; shown here as the dianion, which is the dominant species in mildly acidic solutions and up to pH 8.6 (see Experimental Section).

4.2.2 Ion-selective membranes

The anion exchange membranes sold by FuMA-Tech GmbH, Bietigheim-Bissingen, Germany) as "FAB anion exchange membranes"[169] (a PEEK reinforced anion exchanger resin, 0.13 mm thick, sold in a form loaded with bromide as counter ion, ion exchange capacity >1.3 mol/g for a monovalent anion, electrical resistance <1 Ω cm^2, 11.5 wt % uptake in H_2O at T = 25 ℃) are referred to in the following as HHCIE membranes. While the manufacturer does not comment on the chemical structure of the ionic sites of these membranes, they are reported as being extremely acid resistant, which led us to suspect that the ionic sites are trimethylammonium groups, as they are commonly used in many commercial anion exchange membranes. To confirm this, we exposed FAB membranes for 3 days at 60 ºC to a 2 M KOH_{aq} solution, and then extracted this solution with $CDCl_3$. ^{1}H-NMR spectra of the organic phase indeed showed a peak consistent with trimethylamine at 2.23 ppm. Moreover, upon addition of a few drops of trifluoroactic acid, this peak

disappeared and a new peak appeared at 2.87 ppm, consistent with the protonated form of trimethylamine. We conclude that FAB anion exchange membranes indeed contain trimethylammonium groups.

To fabricate the sensors, fresh HHCIE membranes were sandwiched between two note cards, and a hole punch was used to cut out 13 mm diameter disks. PVC/IE membranes were prepared by dissolving the membrane components (66 mg PVC as polymer matrix, 132 mg *o*-NPOE as plasticizer, 8.4×10^{-2} mmol/g TDDMACl to provide cationic sites) in tetrahydrofuran,[1, 31] pouring of the resulting solution into a Petri dish (31 mm i.d.), and allowing the solvent to evaporate at room temperature overnight.[170] The resulting membranes had a thickness of approximately 100 μm. PVC/ionophore membranes were prepared the same way from a tetrahydrofuran solution of 66 mg PVC, 132 mg *o*-NPOE, 8.6×10^{-3} mmol/g Mn(III)TPPCl as ionophore, and 3.0×10^{-3} mmol/g KTpClPB as cationic sites (molar ratio of cationic sites to ionophore, 0.35:1.00).[171-173]

4.2.3 Ion-selective electrodes

HHCIE membranes were mounted into custom-machined electrode bodies made from poly(chlorotrifluoroethylene).[68] A screw cap with an 8.3 mm diameter hole in the middle was screwed onto bodies holding the membranes, mechanically sealing the membrane perimeter while leaving its center exposed. PVC/IE and PVC/ionophore membranes were then cut and glued with tetrahydrofuran onto the end of a Tygon tube (4.8 mm i.d., 7.9 mm o.d.). An inner filling solution was added into the electrode body (1 mmol L^{-1} of NaCl for Cl^- measurements; 1 mmol L^{-1} of KCl and carmoisine for the carmoisine measurements) along with an AgCl-coated Ag wire as internal reference electrode. An electrochemical cell

was obtained by immersion of the thus fabricated measuring electrode and a double-junction type external reference electrode (DX200, Mettler Toledo, Switzerland; saturated KCl as inner solution, and 1 mol L^{-1} LiOAc as bridge electrolyte) into sample solutions. Prior to measurements, all electrodes were conditioned for 20 h in a solution identical with the inner filling solution. In the activity range of Nernstian responses to chloride, it took the electrodes only seconds to reach a stable emf, suggesting that response times were limited by how quickly samples were exchanged. As expected, response times were longer (up to a minute) in the region of Donnan failure, where significant ion exchange between the aqueous samples and the electrode membrane occurred. Response times to carmoisine were ≈30 s, which may be related to the larger size of this ion[174] (see also Results and Discussion).

EMF Suite 1.03 software (Fluorous Innovations, Arden Hills, MN, USA) was used to control an EMF 16 potentiometer (Lawson Labs, Malvern, PA, USA). The entire procedure was measured for each electrode at least in duplicate. Ion activities were calculated according to the extended Debye−Hückel approximation.[163] Liquid junction potentials at the reference electrode were calculated using the Henderson approximation,[143] except for the carmoisine responses, where no correction was attempted due the lack of appropriate parameters.

4.2.4 Carmoisine measurements

The two sulfonic acid groups of carmoisine are strongly acidic. Their pK_a values were predicted to be -3.2 and -1.1.[175] The pK_a of the phenolic group of carmoisine (pK_{a3}) was determined by titration of a carmoisine solution with 0.1 M NaOH after degassing of all

solutions for 1 h with argon. Fitting with Mathematica 8 (Wolfram Research, Champaign, IL, USA) using the Henderson-Hasselbalch equilibrium[176] gave the pK_{a3} of carmoisine as 8.6. This value is close to the pK_{a2} of the similar compound *p*-hydroxybenzenesulfonic acid, which was reported as 8.8.[177] This shows that in mildly acidic solutions and up to pH 8.6 carmoisine occurs predominantly as a dianion.

For the potentiometric carmoisine calibration curves, aliquots of a concentrated carmoisine solution were added to a solution initially containing 1.0×10^{-7} mol L^{-1} carmoisine. In the range of carmoisine concentrations from 1.0×10^{-7} to 1.0×10^{-2} mol L^{-1}, the independently measured pH of the carmoisine solutions was between 6.5 and 8.0, confirming that the majority of carmoisine in these solutions was in the dianion form.

4.3 Results and Discussion

Donnan failure was assessed in this work by measurements of chloride as the target ion, using the tetrabutylammonium and tetrahexylammonium cations as hydrophobic model co-ions in the aqueous sample phase. These hydrophobic co-ions were chosen because they both prefer organic over aqueous phases (see ref. [178] and the discussion below), because they do not interact specifically with any of the ISE membrane components used in this study, and because their symmetric nature minimizes ion pair interactions. Measurements of the chloride response of ISEs with HHCIE, PVC/IE, and PVC/ionophore membranes were performed both at constant concentrations of a hydrophobic co-ion and by varying the concentrations of tetrabutylammonium and tetrahexylammonium chloride. In the experiments with a constant co-ion concentration,

tetraalkylammonium dihydrogenphosphate solutions of pH 8 were used to give a constant background concentration of a tetraalkylammonium ion because the highly hydrophilic phosphate shows only very small interference with the chloride responses of the PVC/IE and PVC/ionophore ISEs.

4.3.1 emf Responses to chloride at constant tetrabutylammonium concentrations

We evaluated the emf responses of all three types of ISEs using samples with different concentrations of the tetrabutylammonium cation. Responses to chloride were measured by adding to a tetrabutylammonium phosphate solution (adjusted to pH = 8.0 with NaOH) aliquots of a concentrated solution of NaCl (in a tetrabutylammonium phosphate solution, pH 8.0, of the same concentration) while monitoring the emf. This kept the tetrabutylammonium concentration constant while continuously increasing the chloride concentration. Figure 4.3 shows the resulting chloride responses.

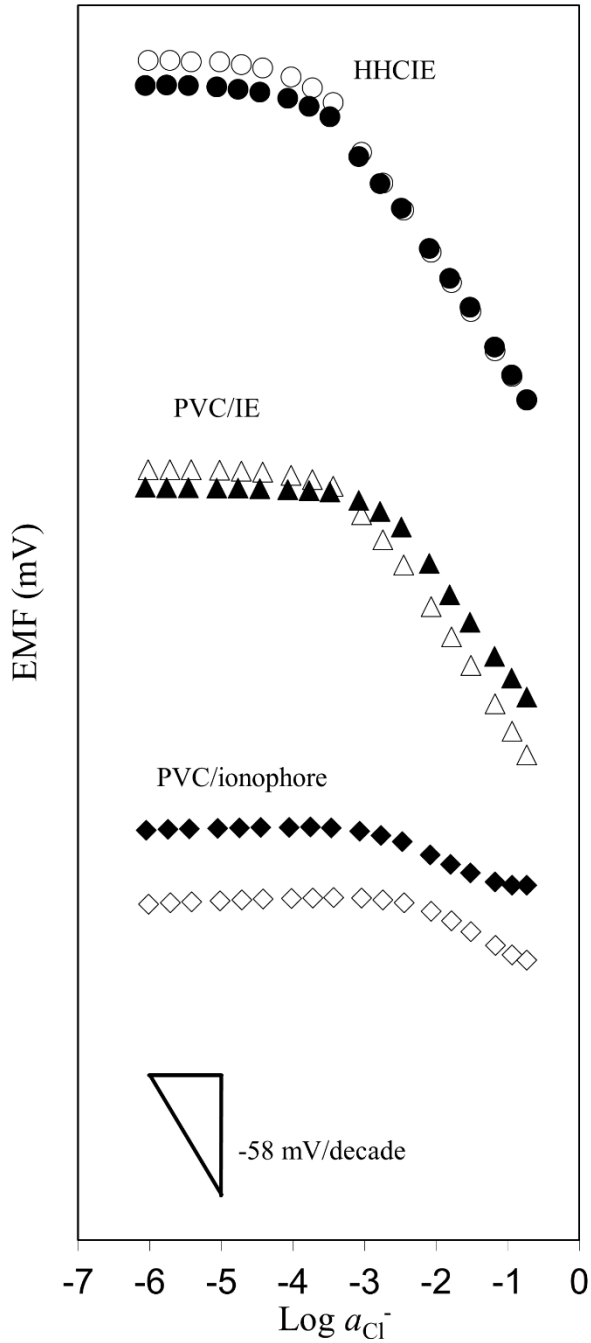

Figure 4.3: emf responses of ISEs with HHCIE or PVC/IE membranes to NaCl in a background of (○, △) 1.0 mM or (●, ▲) 10.0 mM tetrabutylammonium phosphate (pH 8). emf responses of ISEs with a PVC/ionophore membrane to NaCl in a background of (◇) 0.5 mM or (◆) 5.0 mM tetrabutylammonium phosphate (pH 8).

Despite a background concentration of the tetrabutylammonium cation as high as 10 mM, the HHCIE membranes showed a Nernstian response to chloride. The chloride response of the PVC/IE ISEs exhibited a slightly reduced response slope at the highest tetrabutylammonium concentration (10 mM), but a Nernstian response at lower concentrations of this hydrophobic co-ion. It may appear surprising that the energetically very favorable transfer of tetrabutylammonium from water into a hydrophobic phase does not result in a more pronounced extent of Donnan failure of the hydrophobic ion exchanger membrane. However, the explanation for this finding is straightforward, and can be found in the Gibbs free energies of ion partitioning between water and an organic phase. Importantly, it requires that both the analyte anion and the co-ion be considered. While indeed the transfer of tetrabutylammonium from water into both 1,2-dichloroethane and nitrobenzene has been reported to be very favorable (–21.8 and –24.0 kJ/mole, respectively),[178] partitioning of chloride from water into an organic solvent of low polarity is more unfavorable and overcompensates for the cation hydrophobicity (free energies of partitioning are +46.4 and +29.7 kJ/mole for 1,2-dichloroethane and nitrobenzene, respectively).[178] Since Donnan failure is the result of the net transfer of the cation and anion from the aqueous phase into the sensing phase, an increase in the vulnerability to Donnan failure when switching from a hydrophilic to a hydrophobic ion exchanger phase is only expected if the sum of the partitioning energies of the cation and anion is negative, which based on partition energies reported in the literature does not appear to be the case for tetrabutylammonium chloride.

It follows that the slightly higher resistance to Donnan failure of HHCIE membranes as compared to PVC/IE membranes is largely the result of the higher ion exchanger capacity of the former type of membranes. This can be readily understood by considering the salt partitioning equilibrium between the sample and the sensing phase, as described by the partition coefficient:

$$K_{R^+Cl^-} = (a_{R^+,mem}\, a_{Cl^-,mem}) / (a_{R^+,aq}\, a_{Cl^-,aq}) \quad (4.1)$$

where R^+ represents the tetrabutylammonium ion, and mem and aq refer to the sensing membrane and the aqueous sample, respectively. As expected in view of Le Châtelier's principle, a high activity of chloride in the sensing phase as a result of the high anion exchanging capacity of the HHCIE membrane helps to keep the tetrabutylammonium ion concentration in the sensing membrane low,[52] minimizing tetrabutylammonium chloride transfer into the chloride loaded ion exchanger.

Interestingly, ISEs with PVC/ionophore membranes suffered strongly from Donnan failure and gave hardly any emf response. This too can be readily understood by considering the free energies of partitioning of both chloride and the tetrabutylammonium cation from water into the sensing phase. In this case, the transfer of chloride into the plasticized PVC membrane is much more favorable since it is assisted by complexation of chloride to the ionophore. Formally, the same equilibrium constant K_{RCl} is valid as for the ionophore-free PVC/IE membrane, but the relevant $a_{Cl^-,mem}$ is not representative of all the chloride in the sensing membrane but only of the activity of the chloride ions that are not bound to the ionophore. Consequently, the much lower free chloride activity in the sensing membrane opposes Donnan failure to a much lesser extent.[52]

4.3.2 emf responses to tetraalkylammonium chlorides

In order to make conditions more favorable for Donnan failure, further experiments were performed by measuring responses of all three electrode types to tetrabutylammonium chloride up to high concentrations. Figure 4.4 shows the resulting emf responses, along with responses to NaCl for comparison. (Table 4.S1 of the Supporting Information lists the corresponding response slopes.) Again, the HHCIE membranes show nearly ideal responses not only to NaCl but also to tetrabutylammonium chloride. The PVC/IE membrane also performs fairly well, showing only a slightly **s**ub-Nernstian response in the high concentration range for tetrabutylammonium chloride. On the other hand, the emf response of the PVC/ionophore underwent massive Donnan failure at around log $a_{Cl^-} = -3$. Interestingly, the PVC/ionophore showed a response as expected theoretically for a mono*cation* from -2.4 to -0.7 mol L^{-1} tetrabutylammonium chloride. In view of earlier discussions of the Donnan failure of ionophore-based ISE,[52] this monocation response suggests that in this concentration range (i) all the ionophore in the ISE membrane is present in the form of chloride complexes, (ii) the tetrabutylammonium concentration in the membrane is high and equals the difference between the concentration of the total ionophore and tetrakis(4-chlorophenyl)borate, but (iii) the membrane concentration of chloride not bound to ionophore is still low. Consequently, the ISE exhibits the same response as it would be expected for membrane doped only with tetrabutylammonium tetrakis(4-chlorophenyl)borate.

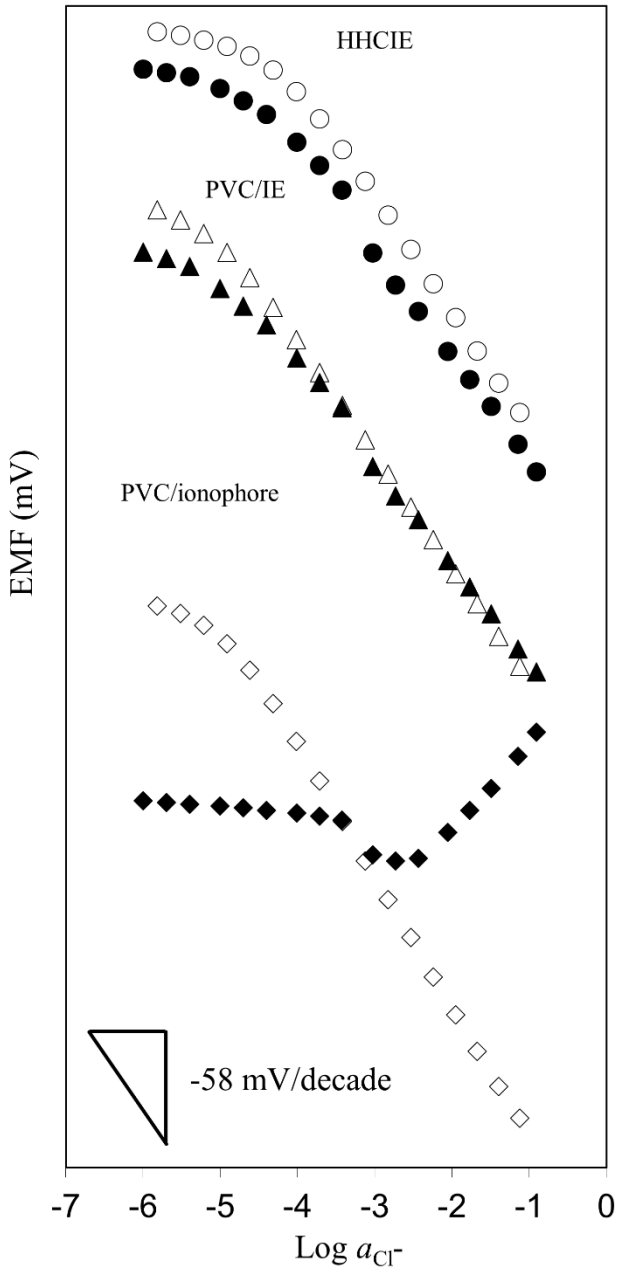

Figure 4.4: emf responses of ISEs with HHCIE, PVC/IE or PVC/ionophore membranes to NaCl (○, △, ◇) or tetrabutylammonium chloride (●, ▲, ◆). Measurements were performed either by dilution of a 0.1 mol L^{-1} NaCl solution with water or addition of concentrated aliquots of tetrabutylammonium chloride to 1.0×10^{-7} mol L^{-1} tetrabutylammonium chloride.

In an effort to make Donnan failure even more favorable and enforce a larger distinction between the performance of the HHCIE and PVC/IE membranes, emf responses to tetrahexylammonium chloride were measured as well (see Figure 4.5). Under these most extreme conditions, the HHCIE membranes still exhibited a large slope in response to chloride but the PVC/IE membranes showed massive Donnan failure. This confirms what is also evident from the chloride responses in the presence of tetrabutylammonium ion, i.e., that among all three membrane types the HHCIE membranes are most resistant to interference from hydrophobic co-ions.

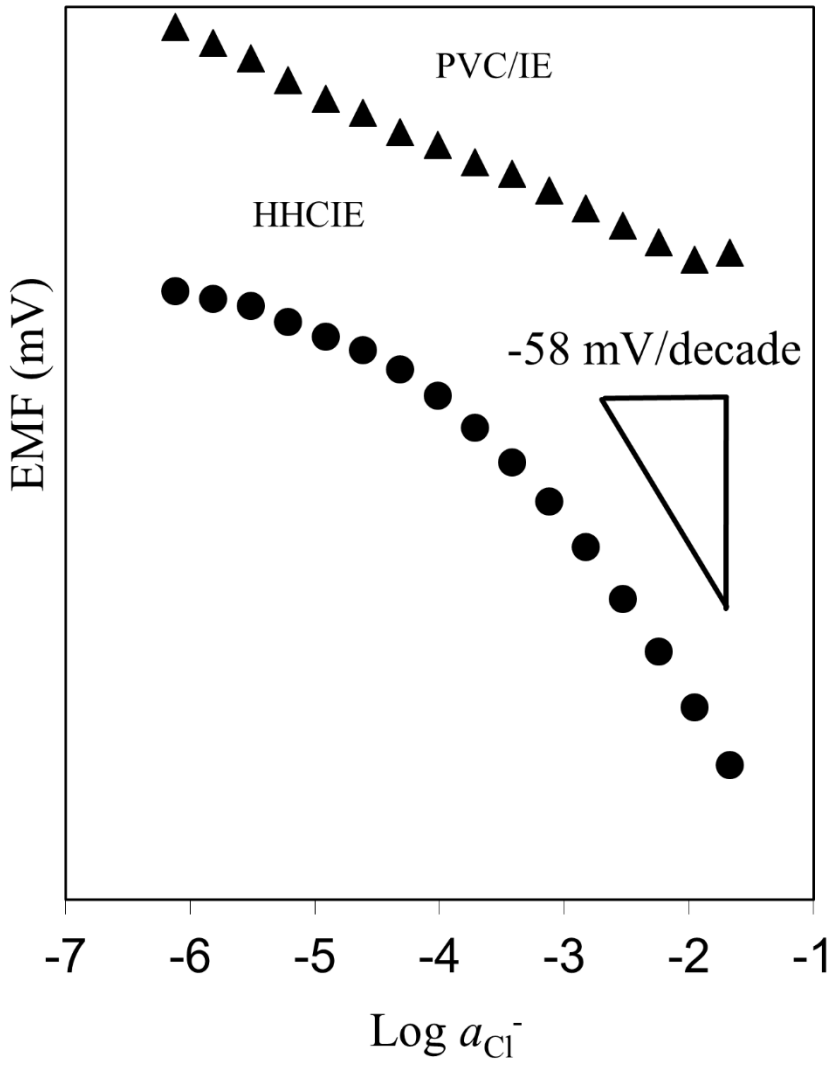

Figure 4.5: emf responses of HHCIE (●) and PVC/IE (▲) electrodes to chloride, as obtained by successive dilution of a 0.025 mol L^{-1} tetrahexylammonium chloride solution. The response slope for the HHCIE ISEs was -52.1 ± 0.5 mV in the range of Log a_{Cl^-} of -1.7 to -2.8.

Again, it is interesting to interpret this data in view of ion partitioning between aqueous samples and the sensing phases. The tetrahexylammonium ion is substantially more hydrophobic than the tetrabutylammonium ion (consider, e.g., the free energies of partition from water into 1,2-dichloroethane of –21.8 and –47.7 kJ/mole for the tetrabutylammonium and tetrahexylammonium ions, respectively).[178] However, the salt tetrahexylammonium chloride still does not exhibit a large preference for a water-immiscible organic phases of low polarity, which can be explained by the high hydrophilicity of chloride (consider, e.g., the free energy of partition from water into 1,2-dichloroethane +46.4 kJ/mole).[178] Importantly, tetraalkylammonium chlorides with a higher hydrophilicity than tetrahexylammonium chloride have only a very limited solubility in water [179] and, therefore, cannot reach concentrations high enough to lead to Donnan failure of ISEs with HHCIEs. This suggests that not only in the case of the tetrabutylammonium and tetrahexylammonium cations discussed here but indeed in the majority of cases of practical relevance, Donnan failure in potentiometric measurements of chloride with HHCIE membranes is absent primarily because of the high ion exchanger capacity and not because of the hydrophilic nature of these HHCIE membranes. Only in measurements of substantially less hydrophilic analyte ions would one expect that Donnan failure of more hydrophobic membranes, such as plasticized PVC membranes, occurs more readily as a result of the free energies of partitioning. Even for nitrate, the free energy of partition from water into 1,2-dichloroethane is with +46.4 kJ/mole still overcompensating the favorable free energy of partition of -34.7 kJ/mole of the tetrapentylammonium ion,[178] and only tetrahexylammonium nitrate prefers the 1,2-dichloroethane over the water phase.

4.3.3 Are there effects of size exclusion on Donnan failure characteristics?

The above discussion of Donnan failure is based on the assumption that salts partition between an aqueous phase and the hydrophobic sensing phase, as defined by Equation (1), with partition coefficients dominated by the free energy of ion solvation in the two phases. This assumption ignores the possible sieve action that polymeric, crosslinked ion exchangers may exhibit.[95] Indeed, studies performed with a view to ion separations showed that hydrophilic, high capacity, polymeric ion exchangers may exhibit an ion exchange capacity that is smaller for large than for small ions. This has been explained by a distribution of pore sizes within these ion exchangers, which makes some ion exchange sites inaccessible to large counter ions.[180, 181] For example, the anion exchanger De-Acidite E was reported to have an ion exchange capacity of 1.22 meq/g for the comparatively small sulfate but only 0.36 meq/g for the much larger carmoisine (see Fig. 2).[174] Consistent with the pore size explanation is that larger ions were found to exchange more slowly.[174] Moreover, increases in the degree of crosslinking in polymers prepared with as much as 16 mole % cross linker lowered the ion exchange capacity for larger ions.[95, 181] Reports in the ISE literature that suggest an effect of ion size exclusion on measured emf responses are few, though.[182, 183] It was suggested that asymmetric cellulose acetate membranes hindered the access of salicylate ions into carbonate-selective membranes because of their large ion size, resulting in slow responses to salicylate and high selectivities.[182] A similar explanation was also given for plasticized PVC membranes doped with an ionophore attached to a non-crosslinked poly(4-vinylpyridine-*co*-styrene) backbone.[183] In consideration of these findings, we wondered whether ion size effects could affect the

Donnan failure characteristics of HHCIE membranes. In particular, we wondered whether the high resistance of HHCIE membranes to Donnan failure might be affected by size exclusion of large co-ions.

Studying size exclusion effects of HHCIE membranes by use of a variety of large cations as co-ions did not seem promising, though, as it would not be clear whether the absence of Donnan failure was the result of size exclusion or of unfavorable phase transfer energies. Therefore, a more straightforward approach to assess the limits of size exclusion on ISEs with HHCIE membranes was the measurement of the emf responses to a large anion.

To test the possibility of size exclusion, we measured the response curves of HHCIE and conventional PVC membranes to the dianion carmoisine (see Figure 4.6). In its largest dimension, this organic dianion has a size of approximately 2.0 nm,[184] which makes it much bigger than the tetrabutylammonium (0.6 nm) and tetrahexylammonium (0.8 nm) cations.[184, 185] Only the HHCIE membranes exhibited a Nernstian response (-27.3 ± 0.9 mV/decade), showing that size exclusion does not affect the ISE response of the HHCIE membranes. This result indicates that the absence of Donnan failure in chloride measurements when the much smaller tetrabutylammonium cation was used as counter ion is not a size exclusion effect. Instead, the high resistance of the HHCIE membranes to Donnan failure is the result of the extremely high chloride activity in the hydrophilic ion-exchanger, as concluded already above.

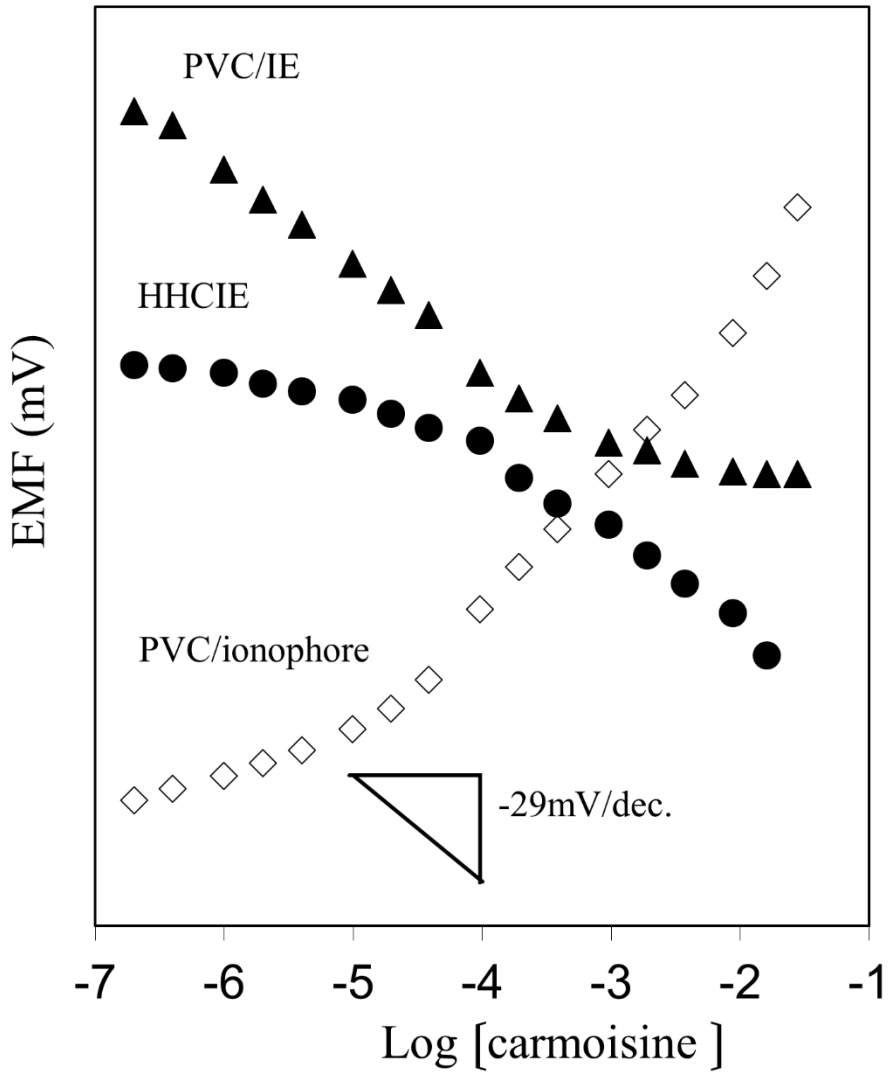

Figure 4.6: emf responses of HHCIE (●), PVC/IE (▲) and PVC/ionophore (◇) electrodes to the concentration of carmoisine.

In contrast the, hydrophobic PVC/IE membranes showed sub-Nernstian responses with a slope of -7.3 ± 0.1 mV/decade in the high concentration region of carmoisine, indicative of Donnan failure as a result of the very favorable transfer of carmoisine from water into the hydrophobic, plasticized PVC matrix. The ISEs with the PVC/ionophore

membranes performed even worse, exhibiting unexpectedly an emf response to *cations* (+42.6 ± 1.2 mV/decade), which is probably caused by a specific interaction between carmoisine and the ionophore.

4.4 Conclusions

Less interference by lipophilic ions of the same charge sign as the target ion was previously reported to be an advantage of ion-selective electrodes with hydrophilic high-capacity ion-exchanger membranes.[94] With this work, we show that hydrophilic high-capacity ion-exchanger membranes also exhibit a remarkably high resistance to Donnan failure, which is primarily a result of the high ion-exchanger capacity of these membranes. Only in potentiometric measurements of very hydrophobic ions do free energies of ion partitioning favor Donnan failure of hydrophobic ISE membranes more than in the case of hydrophilic ion-exchanger membranes. Doping of ISE membranes with ionophores improves the selectivity of sensing but favors Donnan failure, which is consistent with earlier findings. While the two complementary views of Donnan failure based either on the electrochemical potential or on salt partitioning are both correct in their own ways (as discussed in the introduction), it is apparent from this work that the partitioning model explains the effects of the measured ion and its co-ion on Donnan failure in a much more direct manner.

No effects of pore size were observed in the Donnan failure characteristics of the hydrophilic high-capacity ion-exchanger membranes used in this work. In view of reports of the slow salicylate potentiometric responses observed with asymmetric cellulose acetate

membranes[182] and membranes doped with an ionophore bound to a polymer,[183] it appears possible that moderately to highly crosslinked polymer matrixes could be used in combination with short measurement times (such as in a high throughput scenario) to minimize Donnan failure effects. However, such measures seem much more likely to be needed for (hydrophilic or hydrophobic) ionophore-doped ISE membranes than for high-capacity ion-exchanger membranes.

4.5 Supporting Information

In order to make conditions more favorable for Donnan failure, responses of all three electrode types to tetrabutylammonium chloride were measured up to high concentrations. Figure 4.4 in the main manuscript shows the resulting emf responses, along with responses to NaCl for comparison. Table 4.S1 lists the corresponding response slopes.

Table 4.S1: Potentiometric response slopes of HHCIE and conventional PVC membranes to Cl^-.

Membranes	Interfering ions	Slope (mV/decade)	Log a_{Cl^-}
HHCIE	Na^+	-60.1 ± 0.3	-2.8 ～ -1.1
	tetrabutylammonium	-59.1 ± 0.6	-3.7 ～ -2.0
		-53.6 ± 0.6	-2.0 ～ -0.9
PVC/IE	Na^+	-58.1 ± 0.6	-2.8 ～ -1.1
	tetrabutylammonium	-55.8 ± 0.6	-3.7 ～ -2.0
		-50.1 ± 2.0	-2.0 ～ -0.9
PVC/ionophore	Na^+	-65.2 ± 2.2	-2.8 ～ -1.1
	tetrabutylammonium	-12.4 ± 3.9	-3.7 ～ -2.0
		+44.7 ± 1.4	-2.0 ～ -0.9

5 CHAPTER FIVE:

Potentiometric *In Situ* Monitoring of Anions in the Synthesis of Copper and Silver Nanoparticles Using the Polyol Process

Adapted with permission form:

Carey III, Jesse. L.; Whitcomb, David R.; Chen, Suyue; Penn, R. Lee; Bühlmann, Philippe, Potentiometric In Situ Monitoring of Anions in the Synthesis of Copper and Silver Nanoparticles Using the Polyol Process, *ACS Nano*, **2015**, Just Accepted Manuscript November 18th 2015 DOI: 10.1021/acsnano.5b05170.

Available on web at: http://pubs.acs.org/doi/abs/10.1021/acsnano.5b05170

This work was a joint effort by this author and Suyue Chen who carried out the transmission electron microscopy (TEM) of the nanoparticles.

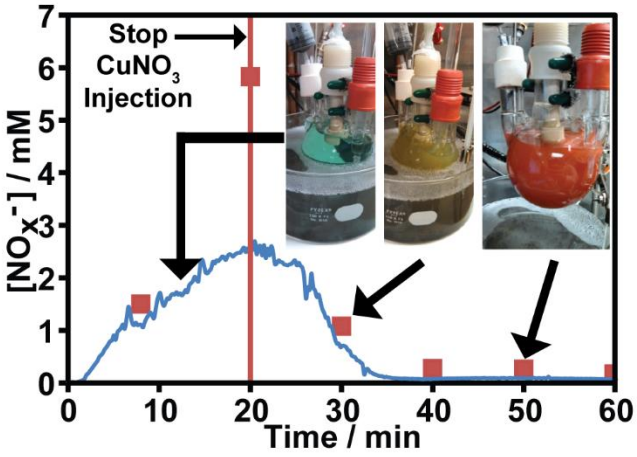

Potentiometric sensors, such as polymeric membrane, ion-selective electrodes (ISEs), have been used in the past to monitor a variety of chemical processes. However, the use of these sensors has traditionally been limited to aqueous solutions and moderate temperatures. Here we present an ISE with a high-capacity ion-exchange sensing membrane for measurements of nitrate and nitrite in the organic solvent propylene glycol at 150 ºC. It is capable of continuously measuring under these conditions for over 180 hours. We demonstrate the usefulness of this sensor by *in situ* monitoring of anion concentrations during the synthesis of copper and silver nanoparticles in propylene glycol using the polyol method. Ion chromatography and a colorimetric method were used to independently confirm anion concentrations measured *in situ*. In doing so, it was shown that in this reaction, the co-ion nitrate is reduced to nitrite.

5.1 Introduction

Silver nanoparticles have found use in a wide range of applications, such as in catalysis,[186, 187] electronics,[188, 189] electrochemical sensors,[189] surface-enhanced Raman spectroscopy (SERS),[190] optics,[189, 191] printable conducting inks,[192] antimicrobials,[193] and bioimaging.[194] Although less popular, copper nanoparticles are also the focus of growing interest, and uses are found in areas such as printable conducting inks, where the combination of similar conductivity but lower cost gives copper an advantage over silver nanoparticles.[195] These nanoparticles are often synthesized using the polyol process, which permits the control of the nanoparticle size and shape.[196-200] In these reactions, propylene glycol or ethylene glycol are used both as the solvent and the reagent to reduce the metal

ions.[198] The more viscous the solvent, the smaller and narrower the size distribution of the particles.[198] Importantly, these reactions are often performed at temperatures near 150 ºC because the reducing strength of these polyols increases with temperature, possibly as a result of the formation of aldehyde derivatives at high temperatures.[199, 201] The higher the temperature, the faster the reaction rate and the smaller the average particle size.[197] However, much about the mechanism of this reaction is still unknown, including the extent to which anions affect the size and shape of the nanoparticles.

Silver nitrate is commonly used in the synthesis of silver nanoparticles,[199] while copper nitrate has only been used a few times to synthesize copper nanoparticles.[197, 200] Nitrate may be reduced by aldehydes, which form in glycols at high temperatures.[202] In acidic environments, nitrate may also oxidize silver particles back into $AgNO_3$, with $NO_{(g)}$ as a byproduct.[202, 203] The effect of HNO_3 on silver nanoparticles is referred to as oxidative etching and can have dramatic effects on the shape and size distribution of nanoparticles.[204] The addition of NO_2 affects the shape of Pt/Pd nanoparticles, which has been hypothesized to result from interactions between NO_2 and the nanoparticle surface.[205]

For a better understanding of the parameters controlling nanoparticle synthesis, it is desirable to perform *in situ* monitoring of the chemical species that are formed or decomposed. *In situ* techniques that have been used for this purpose include UV-visible spectroscopy,[206] redox potential measurements,[207, 208] small-angle X-ray scattering (SAXS),[209] and dispersive X-ray absorption spectroscopy (DXAS),[210] but these techniques have only allowed for the observation of structural changes by nanoparticles during their synthesis. To expand the range of techniques available for *in situ* monitoring of the polyol

synthesis of nanoparticles, we explored the use of ion-selective electrodes (ISEs). The ability of ISEs to monitor ion activities *in situ*—without the inconvenience associated with sampling—is a major advantage, compared to methods of analysis that require the removal of aliquots from the reaction, such as colorimetric testing or ion chromatography. Sampling and sample workup can introduce artifacts, and *ex situ* techniques are often not able to distinguish between freely dissolved ions and ions that are either bound in the form of a complex or are adsorbed to the nanoparticle surface. *In situ* monitoring with potentiometric sensors has been demonstrated, e.g., in clinical chemistry,[211] in environmental studies,[212] or to assess the toxicological effects of silver nanoparticles on bacteria.[77] However, most of this work was performed in aqueous systems, with only few reports of measurements in water/alcohol mixtures (usually with less than 50% alcohol).[45, 47, 49, 213] The use of many ISEs in organic media is limited by leaching of the ionophore, ionic sites, and plasticizer out of the polymeric sensing membranes into the analyzed liquid. Also, little work has been performed at high temperatures, where plasticized polymeric sensing membranes have a reduced mechanical strength. Most plasticized polymer electrodes can only be used for work up to 50 °C, although the use of some plasticized polymer electrodes at slightly higher temperatures was reported.[43, 44] ISEs have previously been used to monitor the concentration of silver ions during the room temperature synthesis of silver nanoparticles in aqueous solutions by hydroquinone-induced precipitation of silver onto gold nanoparticle seeds. However, it appears unlikely that the sensors used for that work would be able to function in the harsh conditions of the polyol process since weakening of the

non-cross-linked polyacrylate membrane at high temperatures and leaching of membrane components into the hot organic solvent would be expected.[214]

We are demonstrating here the use of hydrophilic, high-capacity ion-exchange membranes (more commonly used in electrodialysis, fuel cells, and batteries)[93] as ISE sensing membranes that can function not only in aqueous samples but also in organic solvents and at high temperatures. Anion-exchange resins were first developed in the 1930s for ion-exchange separations,[215] and they have been used in organic solutions with relatively high dielectric constants.[95] ISEs with resin-based, ion-exchange membranes were used to measure ion concentrations in aqueous samples as early as the 1950s[98, 99] and also found applications for measurements in liquid ammonia and ethanol.[216] More recently, Bakker and co-workers showed that commercially available hydrophilic ion-exchange membranes can be used to prepare potentiometric ion sensors for the measurement of chloride in blood.[94]

Most modern high-capacity ion-exchange membranes consist of a highly cross-linked polymer to which ion exchange sites (often referred to as ionic sites) are covalently attached. Unlike many conventional ion-exchange ISE membranes, they do not contain a plasticizer.[95] Therefore, we expected that hydrophilic high-capacity ion-exchange membranes would suffer less from exposure to organic solvents. Moreover, the high level of crosslinking that is common in commercial high-capacity ion-exchange membranes and the absence of a plasticizer was expected to provide the membranes with sufficient mechanical strength even at high temperatures. Ion-exchange membranes with a high ion-exchange capacity are thought to contain nanometer-scale pores or channels with high

charge density,[93, 96] the size of which varies with the degree of crosslinking.[95] Ion transport through these membranes has been described as occurring through nanopores,[97, 217] which are filled with the solvent with which the membrane is in contact. In this regard, ISEs with high-capacity ion-exchange membranes resemble the recently developed sensors based on porous gold films with nanopores that are made to be permselective by charged species that are immobilized on the gold surface.[158, 162] Because the state of solvation of the exchangeable ions is very similar in these nanopores and within the sample solutions, high-capacity ion-exchange membranes without ionophores exhibit a very narrow range of selectivity,[94] quite in contrast to hydrophobic ion-exchange membranes with a low ion-exchange capacity and low dielectric constant.[68]

5.2 Results and Discussion

5.2.1 Effect of High Temperature Exposure on Subsequent ISE Performance at Room Temperature

Three types of hydrophilic, high-capacity ion-exchange membranes were used in this work, i.e., Fumasep FAB,[169] SELEMION AHO,[218] and AMI-7001S anion-exchange membranes.[219] While these three types of ion-exchange membranes differ somewhat in the way they are manufactured, they all have a thickness between 0.1 and 0.5 mm, show good permselectivity, and have a low electrical resistance (<40 Ω cm^{-2}). They were selected from among many commercially available anion-exchanger membranes because their manufacturers reported that they were suitable for use at higher temperatures. While only the manufacturers of the SELEMION AHO and AMI-7001S membranes specifically

identified the ion-exchanging groups as quaternary ammonium, the same is likely true for the Fumasep FAB membranes.

All anion-exchange membranes were first immersed into a 0.5 M sodium nitrate solution in propylene glycol for one day, followed by immersion into a 0.1 mM sodium nitrate solution in propylene glycol for at least three more days. This equilibration process, typically referred to as conditioning, replaces the anions originally present in the ion-exchange membrane with nitrate and permits some swelling of the ion exchanger with the solvent. Subsequent storage for up to three weeks in propylene glycol showed no degradation of the membranes' performance.

Electrodes with conditioned sensing membranes were then used to determine the nitrate response in propylene glycol at ambient temperatures before and after exposure to 150 ºC. Before any high-temperature exposure, the electrodes with all three types of membranes gave similar results, showing a decrease of the measured potential, emf, of approximately 50 mV per tenfold increase in the activity of nitrate. Next, the electrodes were placed in 0.1 mM sodium nitrate in propylene glycol, which was then heated to 150 ºC for five hours. Note that the boiling point of propylene glycol is 188 ºC, which is not only above the boiling point of water, but it is also well above the reaction temperature for the nanoparticle synthesis used in this work. After the electrodes were allowed to cool to ambient temperature, the nitrate response was measured again. Only the AHO membranes (made of polystyrene with quaternary ammonium ionic sites and cross-linked with divinylbenzene) exhibited consistent nitrate responses after the exposure to 150 ºC. In

contrast, the electrodes with the FAB and AMI membranes were prone to failure after heating, often failing to give any response to nitrate.

In an attempt to better understand the different behavior of the three types of ion-exchange membranes, they were characterized with differential scanning calorimetry (DSC; for DSC traces, see Supporting Information). Surprisingly, the AHO membranes exhibited, with a phase transition around 121 ºC, the largest response to temperature at ≤150 ºC. The shift of this transition from 125.6–130.5 ºC during the first segment to 114.9–127.5 ºC in subsequent heating segments, is likely due to annealing of the polymer.[21] Importantly, there was an almost perfect overlap of the DSCs of the second and third heating cycle, which shows that although the AHO membranes undergo a transition in every heating cycle, repeated heating does not degrade these membranes.

Since only the AHO membranes performed well in potentiometric measurements after exposure to 150 ºC, they were the only membranes further investigated. Therefore, let us briefly revisit the potentiometric response slope observed with the AHO membranes. Note that the Debye–Hückel limiting law was used to determine the activity of nitrate:[220]

$$\ln(\gamma_i) = -\frac{z_i^2 q^3 N_{\mathrm{A}}^{\frac{1}{2}}}{4\pi(\varepsilon_r \varepsilon_0 k_B T)^{\frac{3}{2}}}\sqrt{\frac{I}{2}} \tag{5.1}$$

where z_i is the charge of the ion species i, q is the elementary charge, N_{A} is Avogadro's number, ε_r is the relative permittivity (dielectric constant) of the solvent (32 at 20 ºC for propylene glycol), ε_o is the permittivity of free space, k_B is Boltzmann's constant, and I is the ionic strength of the solution. Using this formalism, the average response slopes for the AHO membranes before and after heating were calculated to be –50.8 ± 0.2 and –50.3 ±

0.3 mV/decade change in the activity of nitrate, respectively (Figure 5.1). These values are close to but somewhat lower than the theoretical response slope of –58.1 mV/decade for 20 ºC, as predicted by the Nernst equation:

$$emf = E^o + \frac{2.303RT}{z_i F}\log a_i \qquad (5.2)$$

where E^o is the calibration curve intercept, z_i is the charge of the measured ion, and R, T, and F are the gas constant, temperature, and Faraday's constant, respectively. This may be attributed to several factors. A more accurate assessment of the activity coefficients, for example, by using the extended Debye–Hückel equation, could possibly improve the slope. However, such calculations for solutions made from propylene glycol are not possible without considerable work outside of the scope of this project. Moreover, contributing to the slightly smaller than expected slope may be the liquid junction potential between the reference electrode and the sample solutions, which is expected to be small but may differ somewhat for the different points of the calibration curve.[121] Corrections of the measured emf for changes in the liquid junction potential[143, 221] were not attempted because ion mobilities in propylene glycol are also not known from the literature. Important for this work is the fact that the response slopes are reproducible, show an acceptable linear range, and are unaffected by heating for five hours in propylene glycol. This shows that the AHO membranes can successfully measure in propylene glycol and can survive being heated to 150 ºC. It should be noted that, after a concentration change, it takes approximately two minutes for the measured emf to stabilize. Because these electrodes respond much faster at higher temperatures (see below), it appears likely that this comparatively long response

time is explained predominantly by the high viscosity of propylene glycol at ambient temperature.

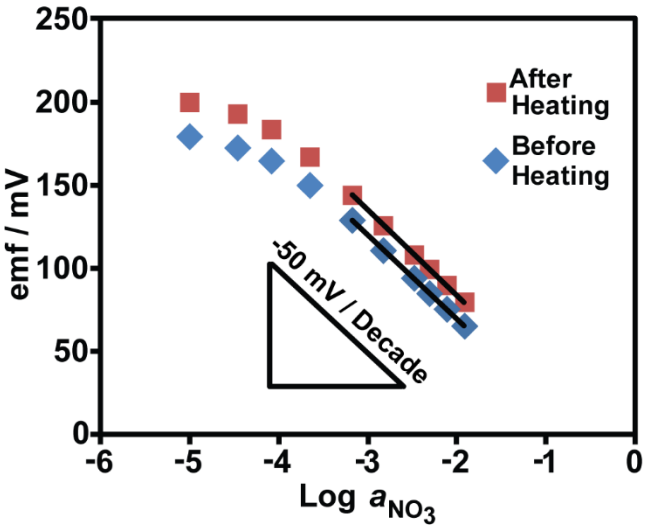

Figure 5.1: ISE with an AHO ion-exchange membrane: emf response to nitrate in propylene glycol at 22 ºC, before and after heating at 150 ºC for 5 h.

5.2.2 High Temperature Measurements

ISEs equipped with AHO sensing membranes were also used to directly measure the nitrate activity in propylene glycol at 150 ºC by stepwise addition of aliquots of $NaNO_3$ in propylene glycol (Figure 5.2). The average slope of the nitrate response at this temperature was -60 ± 1 mV/decade change in the concentration of nitrate. Activity coefficients for nitrate in propylene glycol were not calculated because that would require knowledge of the dielectric constant of propylene glycol at 150 ºC, which is not readily available. The limit of nitrate detection was determined to be 18 ± 6 µM, with a linear range from 0.1 mM to 10 mM. Within the linear response range, the emf response was very stable, with a drift of the measured emf of less than 0.1 mV/min. The response time in this range was with less than 10 s (see the Supporting Information) info much smaller than at

ambient temperature, which is likely due to the large decrease in the viscosity of propylene glycol at 150 ºC.[198]

To determine whether the electrochemical cell consisting of a reference electrode, the propylene glycol solution, and an ISE with an AHO membrane could function for several hours at 150 ºC, the whole cell was heated to 150 ºC, and a calibration curve for the nitrate response was measured. At this point, the solution was replaced with a propylene glycol solution containing 0.1 mM sodium nitrate, and the electrochemical cell was heated to 150 ºC for 5 h, after which the nitrate calibration curve was once again measured at 150 ºC (Figure 5.2). The comparison of the response curves before and after heating shows only a minor loss of the limit of detection (16 μM to 50 μM). Importantly, the linear range was unchanged, and the change in $E°$ was only 1.8 mV ± 2.7 mV. This demonstrates that the sensor can function for the duration of a typical nanoparticle synthesis with minimal performance changes over the course of the experiment.

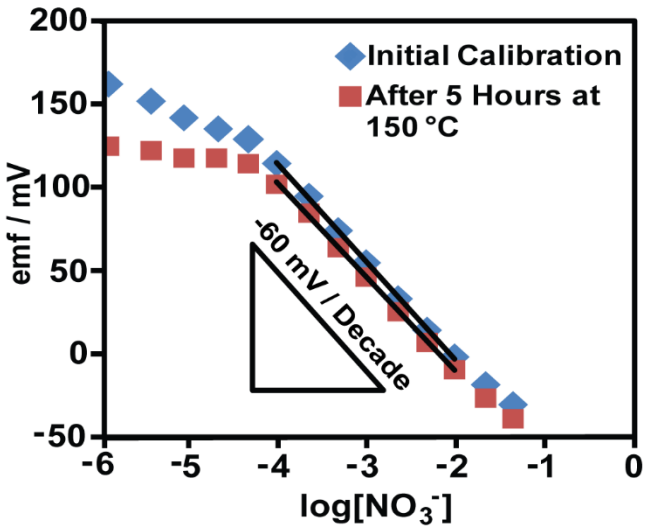

Figure 5.2: Nitrate response of an ISE with an AHO ion-exchange membrane at 150 ºC in propylene glycol: Initial response and response after 5 h at 150 ºC.

5.2.3 Lifetime

To determine the lifetime of the electrodes at high temperatures, the emf was monitored continuously for 180 h at 150 ºC in a stirred propylene glycol solution containing 1.0 mM sodium nitrate solution (Figure 5.3). The electrode showed only a small overall drift (0.0019 mV/min), with a standard deviation of 7.5 mV from the average value over the course of the entire experiment. The nitrate response before and after 180 h at 150 ºC also showed little change, as shown in Figure 5.4. This illustrates that the AHO membranes have good thermal stability and can function at high temperatures for long periods of time.

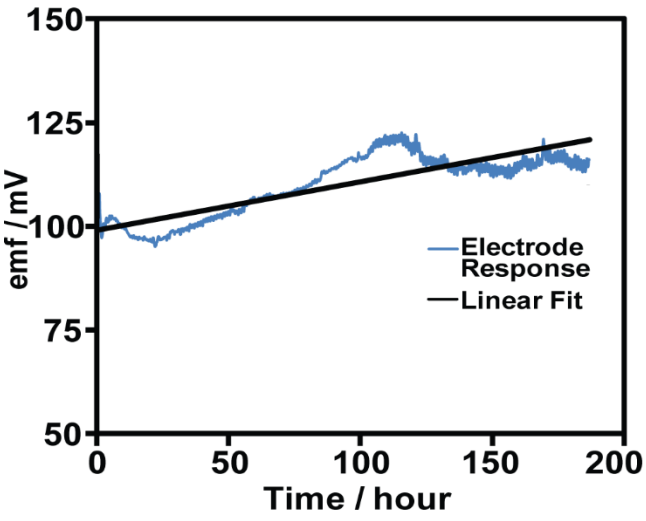

Figure 5.3: AHO membrane nitrate sensor response at 150 ºC for over 180 h.

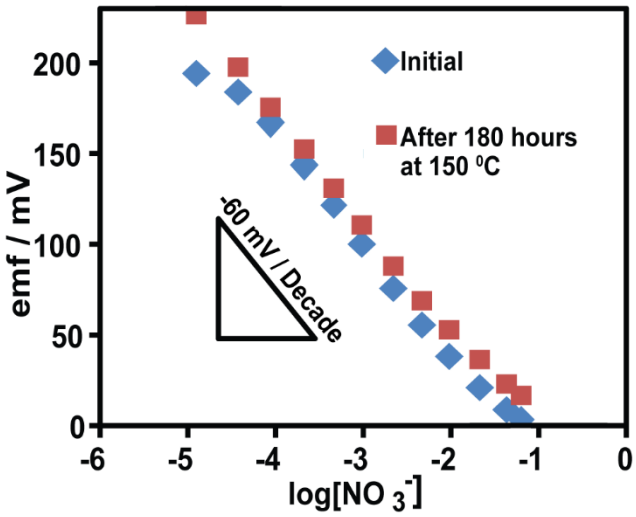

Figure 5.4: Response of AHO membrane nitrate sensor to nitrate in propylene glycol at 150 ºC: Initial response curve and response curve after 180 h of heating.

To test the effects of repeated heating and cooling, an electrochemical cell was set up using an ISE with an AHO ion-exchange membrane and a reference electrode in a 1.0

mM sodium nitrate solution in propylene glycol. The temperature was switched several times in 30 min intervals between room temperature (22 ºC) and 150 ºC. The sensors' average response for three cycles is shown in Figure 5.5. The average value of the emf at 150 ºC was highly reproducible, with a standard deviation of only 1.0 mV between heating cycles. There was a change in the emf at room temperature after the first heating cycle (approximately 10 mV), compared to the emf before heating. However, there was little to no change thereafter, with a standard deviation of 0.9 mV between measurements at room temperature after subsequent heat exposures, which is consistent with the results of the DSC. Moreover, the calibration curve for nitrate at 150 ºC after the cycling of the temperature showed little change compared to the response of the electrodes that had only been heated to 150 ºC once (Figure 5.6).

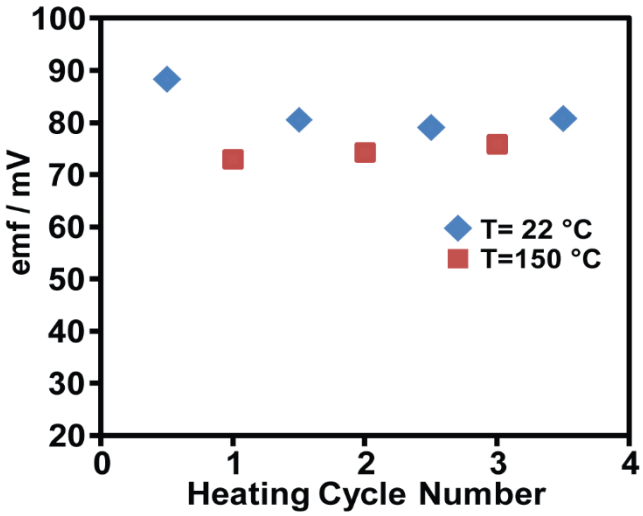

Figure 5.5: Average emf response of ISEs with an AHO ion-exchange membrane after multiple heating/cooling cycles between 22 ºC and 150 ºC.

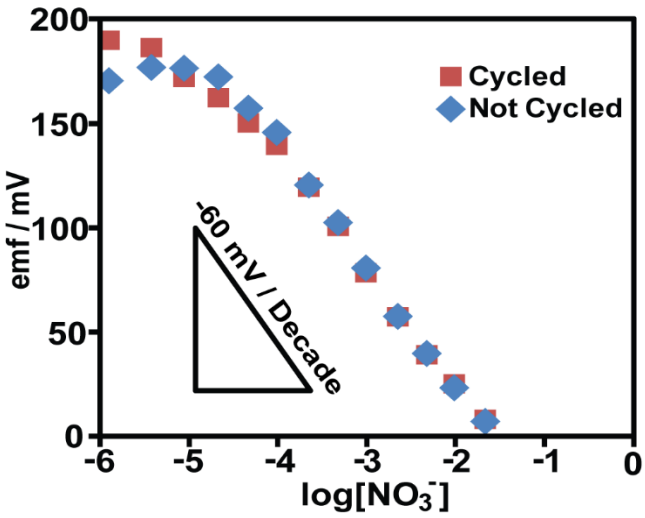

Figure 5.6: Calibration curve for nitrate ISEs with an AHO ion-exchange membrane at 150 ºC before and after temperature cycling.

5.2.4 Selectivities

Before determining the selectivity of ISEs equipped with an AHO ion-exchange membrane, the response of these electrodes to the anions of interest was measured in propylene glycol at 150 ºC. Both the fixed primary ion method and the separate solution methods were used to determine selectivity coefficients,[14] and they showed good agreement between one another (see Table 5.1; for response slopes values, see the Supporting Information), suggesting that these values are unbiased manifestations of the thermodynamic ion-exchange properties of the AHO ion-exchange membranes. The coefficients represent a much reduced selectivity, compared to classical solvent-polymeric ionophore-free ion-exchange membranes.[222] As expected, they are similar in range to those determined in aqueous solutions for other types of hydrophilic high-capacity ion-exchange membranes[94] and are comparable to analogous selectivity ranges for ion-exchange resins.[95]

The rather narrow range of selectivity coefficients suggests that these ISEs are best used when the concentration of the anion of interest is much higher than the concentration of other anions in solution and would not be useful in a system with a high concentration of background electrolyte. While this may appear to be a drawback, it is worthwhile to remember that, unlike in the case of classical solvent polymeric ionophore-free ion-exchange membranes, highly lipophilic ions at low to intermediate concentrations will not cause substantial interference.[94]

Table 5.1: Selectivity coefficients of the ISE for chloride and acetate, as measured with the separate solution method (SSM) and the fixed primary ion methods (FPIM) with respect to nitrate.

$\mathrm{Log}K^{\mathrm{pot}}_{\mathrm{NO_3^-},\mathrm{J}}$	SSM	FPIM
Cl^-	0.29 ± 0.05	0.17 ± 0.16
NO_2^-	–0.03 ± 0.03	0.02 ±0.06
OAc^-	–0.11 ± 0.07	–0.09 ± 0.24

5.2.5 Measurements During Nanoparticle Synthesis

Having confirmed the suitability of ISEs with AHO ion-exchange membranes for measurements at 150 ºC in propylene glycol, these electrodes were used for *in situ* measurements in the polyol synthesis of nanoparticles. First, an ISE was calibrated at 150 ºC by additions of $NaNO_3$ aliquots into a propylene glycol solution containing 1.11 g/L polyvinylpyrrolidone (PVP), which corresponds to 10 mM of the PVP monomer. The ISE

was then used to monitor the synthesis of copper nanoparticles, which was performed by using a modified literature procedure reported for the synthesis of Ag nanoparticles.[198, 202] The electrodes were placed in propylene glycol containing PVP, the solution was heated to 150 ºC, and then $Cu(NO_3)_2$ in propylene glycol was added at a rate of 1 mL/s. The potential of the electrochemical cell was monitored over the course of the whole reaction time, and aliquots were taken for *ex situ* analysis by ion chromatography and colorimetric analysis. During the course of the copper nanoparticle synthesis, the light-blue solution changed, initially, to a blue suspension, which later turned green and, finally, brown/red, consistent with earlier reports of copper nanoparticle synthesis.[200] The synthesis of silver nanoparticles was performed similarly by the addition of 110 mM $AgNO_3$ over 20 min and ending the reaction after 1 h. In this case, the initially colorless solution first turned yellow and then turned into a suspension, whose appearance was first yellow but changed later into yellowish gray, again, consistent with earlier observations.[199]

As shown in Figure 5.7, the ISEs were able to measure the concentration of anions throughout the course of both the copper and silver nanoparticle syntheses. As discussed below, this led us to discover the formation of NO_2^- in these reactions. Note that the calibration curve for $NaNO_3$ described above could be used without modification to determine the concentration of NO_X^- because the electrodes were found to respond nearly equally to NO_3^- and NO_2^- ($K^{pot}_{NO_3^-,NO_2^-} \approx 1$). Therefore, in the context of the nanoparticle syntheses, we will refer from hereon to potentiometric measurements of NO_x^-.

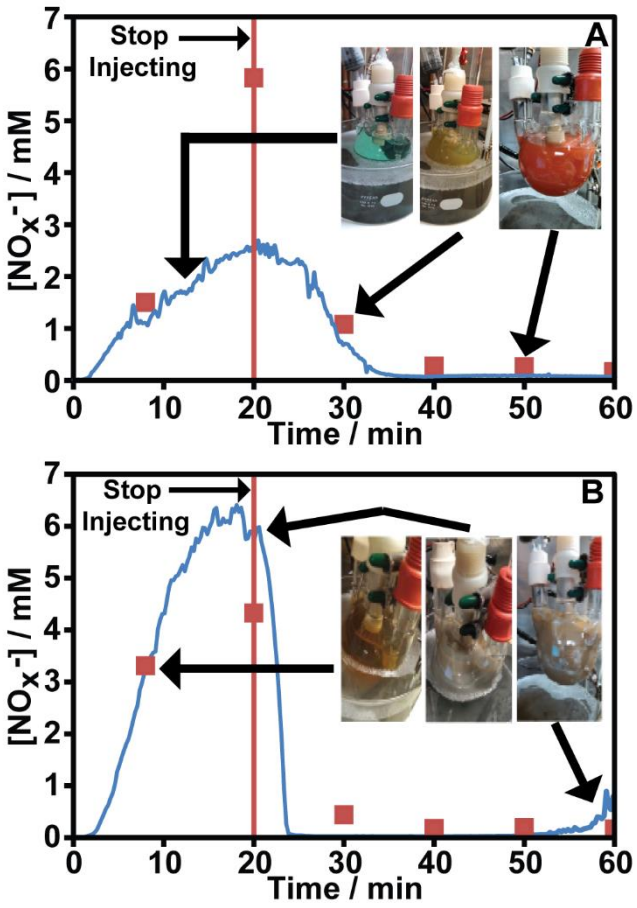

Figure 5.7: Concentration of NO_X^- as determined by potentiometry with ion-exchange membranes (blue line) and ion-exchange chromatography (red squares) during a typical (A) copper nanoparticle synthesis, and (B) silver nanoparticle synthesis (both at 150 ºC). Inserts: Photographs of reaction flask showing the colors of the suspensions as the reactions progressed.

In both reactions, the highest detected NO_X^- concentration was much lower than would be expected based on the amount of nitrate injected. While the concentration of NO_X^- at the end of the metal nitrate addition should have reached 10 mM in both the copper and the silver nanoparticle synthesis, the highest detected values were 2.5 ± 0.44 mM for

the copper reaction and 6.3 ± 0.33 mM for the silver reaction. Evidently, in both cases nitrate decomposition began quickly. The measured NO_X^- concentration increased gradually but slower than predicted from the addition rate. Also, soon after the injection was stopped, the NO_X^- concentrations began to fall. For the copper reaction, the NO_X^- concentration fell to 0.1 mM approximately 12 min after the injection was stopped and then continued to slowly decrease down to a minimum of 0.040 mM. Note that the blue-to-green change in color in the copper nanoparticle synthesis occurred between 30 and 40 min after the start of the reaction and the change from green to red occurred after 50 min. In the silver reaction, the drop in NO_X^- concentration is much steeper, reaching 0.1 mM in less than 4 min, followed by a further but slower decrease in NO_X^- concentration down to a value nearly two orders of magnitude lower than the maximum concentration. In the silver reaction, a yellow color appeared almost immediately and turned to a yellowish gray after about 15 min, when the NO_X^- concentration also leveled off. Between 10 and 25 min, gas bubbles could be seen vigorously forming in the reaction mixture.

We found that it is important to make sure that the electrode membrane does not become covered with bubbles, as this can affect the potential of the electrodes and cause errors in determining the ion concentration. To avoid this problem, the lip on the cap of the electrode was reduced in size, and the electrode was inserted into the reaction solution at an angle of approximately 45º with respect to the horizontal level of the solution to prevent bubbles from being trapped on the surface of the electrode membrane (see Supporting Information). For both reactions, the low concentration of detected anions at the end of the reaction suggests that the majority of NO_X^- ions were either bound to the surface of the

nanoparticles or were converted into decomposition products such as NO or NO_2 gas. However, the distinctive color of NO_2 gas was not observed in the gas leaving the reaction flask.

A comparison of the results of the colorimetric analysis, the ion chromatography, and the results obtained by using the potentiometric sensor is shown in Figure 5.8 and Table S2. Surprisingly, the colorimetric analysis and the ion chromatography showed that nitrite was formed during the reaction. We have not been able to find in the literature any mention of nitrite formation during this type of nanoparticle synthesis. In a control experiment, propylene glycol solutions with PVP and sodium nitrate, but no transition metal nitrate, were heated to 150 ºC. Colorimetric analysis and ion chromatography showed no evidence for the reduction of nitrate to nitrite. This demonstrates that the presence of copper or silver is necessary for the nitrate reduction to occur.

There are several possibilities on what is causing the reduction of nitrate. One possibility is that the NPs are being oxidized. Another possibility is that the NP surface catalyzes the reduction of nitrate by aldehydes that are formed in heated propylene glycol (reducing agents that also have been proposed to be relevant in the formation of nanoparticles).[201] Further study will be needed to clarify the mechanism of nitrate reduction.

In the copper reaction, the NO_X^- concentration determined by the potentiometric sensor varied substantially from that of the total concentration of nitrate and nitrite as determined by the colorimetric method and by ion chromatography. However, the trend of decreasing NO_X^- concentration over time after the stop of the $Cu(NO_3)_2$ injection is apparent in the data from all three methods of analysis. The differences between the data

from the *in situ* and the *ex situ* methods is likely explained by NO_X^- binding to the copper surface of the nanoparticles. Indeed, nitrate binding to Cu(100) has been reported in the literature, and density functional theory calculations suggest that this anion binds strongly (–249 kJ/mol) in a bidentate fashion (through two oxygen atoms) to the copper surface.[223] This is consistent with near quantitative binding, allowing for a high surface coverage. Indeed, binding of NO_3^- to Cu nanoparticles in systems containing 1-butyl-3-methylimidazolium nitrate has been shown using X-ray photoelectron spectroscopy.[224] While the potentiometric method measures only the NO_X^- anions that are freely dissolved but not those adsorbed to nanoparticles, the two *ex situ* techniques are based on a workup that displaced NO_X^- from the nanoparticle surface and measured the total NO_X^- in the reaction suspension. The ion chromatography, colorimetric, and potentiometric data for the silver reaction match much better, suggesting little binding of NO_X^- onto silver nanoparticles. Note that the *ex situ* methods also suffered from the error introduced by the time it takes one to remove and quench the sampled aliquot. In particular, the standard deviation for the NO_X^- concentration as determined with *ex situ* techniques is very large for sampling during the time range in which the NO_X^- concentration drops sharply in the silver reaction, which is right after injection has ceased (20 min). This showcases the advantages of *in situ* measurements to monitor polyol synthesis reactions.

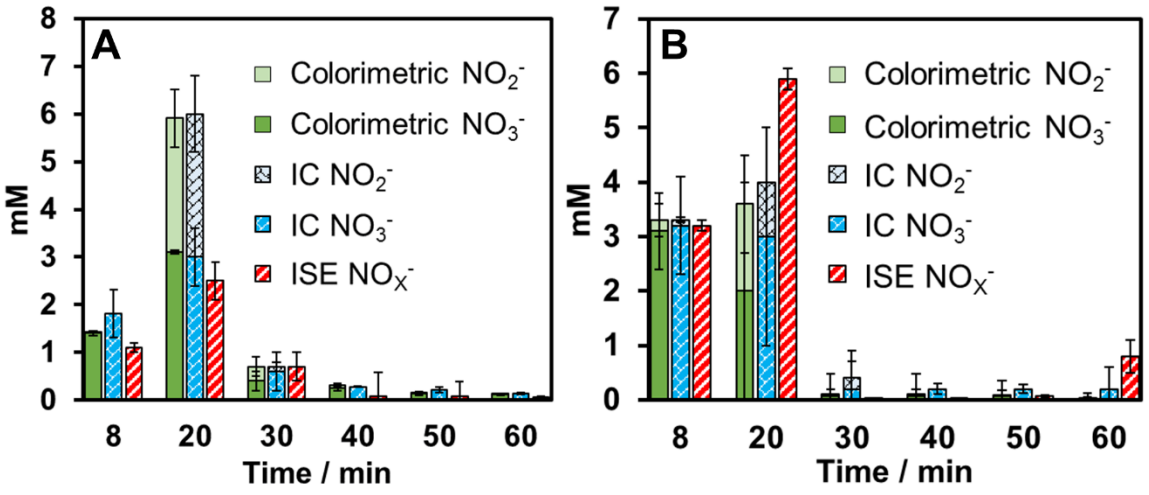

Figure 5.8: Comparison of average NO_X^- concentrations during three (A) copper and (B) silver nanoparticle syntheses, as determined by the electrochemical nitrate sensor, ion chromatography, and colorimetric analysis. Concentration values are cumulative.

UV-visible spectra were taken of the samples from both the copper and silver nanoparticle reactions, as shown in Figure 5.9. For the silver nanoparticle reaction, the maximum absorbance for each sample was at 422 nm. There is increased absorbance at wavelengths higher than 422 nm in samples from the second half of the reaction, which suggests that larger particles are forming and that the particle size is becoming more disperse. Transmission electron microscopy (TEM) of nanoparticles taken from the end of the reaction confirmed the average size of the particles to be 35 ± 14 nm (see Supporting Information for images). Small amounts of bars similar in width to that of the diameter nanoparticles were also observed. The obtained absorbance values match well for particles of this size, as seen in the literature.[225] Energy-dispersive X-ray spectroscopy (EDS) spectra confirmed the identity of the particles as silver.

For the copper nanoparticle reaction, the UV spectra suggest small particles <10 nm in diameter at early times (absorbance at approximately 400 nm).[224] Their small size provides a large surface area for binding of nitrate, which explains in part the differences seen in between the nitrate concentrations determined with ISEs and with ion chromatography. After 50 min, there is an increase in the concentration of larger particles, as evidenced by the appearance of absorbance at 596 nm.[200] TEM of nanoparticles taken from the end of the reaction confirmed the average size of the particles to be 360 ± 12 nm (see Supporting Information for images), small amounts of bars similar in width to that of the nanoparticles Were also observed. EDS spectra confirmed the identity of the particles as copper.

Reactions performed with and without immersion of the sensor and reference electrode into the reaction mixture showed very similar absorption spectra, with no significant changes in the absorbance maxima. This is not surprising as these electrodes do not contain metal surfaces, nor do they have sharp edges that would affect the nucleation of nanoparticles or permit leaching of any ions into the samples that are not already in the reaction solutions.

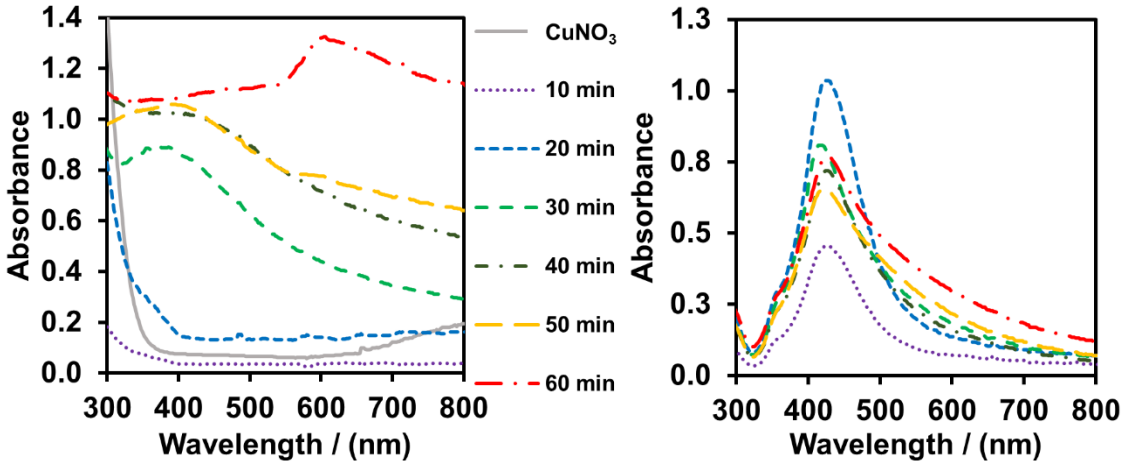

Figure 5.9:

Absorbance spectra of samples from the syntheses of copper (right) and silver nanoparticles (left).

5.3 Conclusion

The new potentiometric sensors with a hydrophilic high-capacity ion-exchange membrane can be used to measure *in situ* under the harsh conditions of propylene glycol at 150 ºC. Unlike many spectroscopic probes, the ISE can be applied in completely turbid solutions and, with proper design, it is also immune to error from the abundant bubbles that form in the synthesis of nanoparticles. The sensor has a long lifetime, as it is able to measure at 150 ºC for over 180 h and survives several heating and cooling cycles, showing its suitability as a useful tool for *in situ* monitoring in nanoparticle synthesis. We used this sensor successfully to monitor the co-ion concentration in the synthesis of two types of nanoparticles. In both of them, a change in the nitrate concentration of almost two orders of magnitude was observed. Using colorimetric and ion chromatography measurements,

we discovered that the reduction of nitrate to nitrite is an important process, and that NO_X^- species are bound to the copper nanoparticles. The changes in the concentration of nitrate during the nanoparticle synthesis raise the question whether the counter ions of the metal precursor may have an effect on how quickly nanoparticles grow. The potentiometric sensors introduced here have promise to help answer questions of this type. Sensing of this type is not limited to the detection of anions, as cation-exchange membranes similar to the anion-exchange membranes used in this work exist.[95] Hydrophilic high-capacity ion exchange membranes are also suitable for ions of various sizes and shapes.[226] This suggests that similar sensors could be used to monitor a variety of other ions under similar conditions.

5.4 Methods

5.4.1 Materials

Three types of ion-exchange membranes were used in this study: Fumasep FAB anion exchange membranes (a PEEK reinforced membrane, 0.13 mm thick, sold loaded with bromide as counter ion, with a capacity of >1.3 meq/g, electrical resistance <1 □ cm^2, and reported by the manufacturer to be functional at 80 ºC, although under substantial swelling with water; Fumatech, Bietigheim-Bissingen, Germany),[169] SELEMION AHO anion exchange membranes (a polystyrene with quaternary ammonium ionic sites and cross-linked with divinylbenzene, 0.30 mm thick, loaded with bromide, with an electrical resistance of 20 □ cm^2, and labeled by the manufacturer as suitable for use in hot water and in the presence of oxidants; AGC Engineering, Nakase, Japan),[218] and AMI-7001S

anion exchange membranes (a gel polystyrene with quaternary ammonium ionic sites and cross-linked with divinylbenzene, 0.45 mm thick, loaded with chloride, with an ion exchange capacity of 1.3 ± 0.1 meq/g, electrical resistance <40 □ cm^2, and the thermal stability was reported by the manufacturer to be 90 ºC; Membrane International, Ringwood, NJ, USA).[219] All ion exchangers were characterized by using differential scanning calorimetry on a TA Instruments Q1000 (New Castle, DE, USA). The temperature was cycled from –20 ºC to 200 ºC, several times, with a scan rate of 10 ºC/min. The AHO membrane was received in a solution and was rinsed with deionized water, blotted dry, and allowed to dry for 24 h under ambient conditions before DSC measurements. Experiments after drying these ion-exchange membranes under vacuum yielded nearly identical results. Propylene glycol (99%) was purchased from Sigma Aldrich (St. Louis, MO, USA), porous glass frits from Princeton Applied Research (Oak Ridge, TN, USA), and polyvinylpyrrolidone (sold as Kollidon 30, M_w = 44,000–54,000) from BASF (Ludwigshafen, Rheinland-Pfaltz, Germany).

5.4.2 Assembly of the Ion-Selective Electrodes

Ion-exchange membranes where cut into 15 mm diameter disks, conditioned in propylene glycol containing different concentrations of $NaNO_3$ (see above), and then mounted into custom-machined electrode bodies made from polyether ether ketone (PEEK) using a silicone O-ring and a screw-on PEEK cap, as previously described in the literature.[55, 73] See the Supporting Information for further details. All electrode components exposed to the sample solution were fabricated with rounded edges to reduce nanoparticle growth on the surface of the electrode. The electrode contained two inner liquid

compartments: (i) the outer filling solution (0.1 mM sodium nitrate solution in propylene glycol), which was in direct contact with the sensing membrane, and (ii) a 0.1 mM sodium chloride solution in propylene glycol (referred to as the inner filling solution), into which a AgCl-coated Ag wire was inserted as the reference half-cell. A compartment to contain the inner filling solution and allow for a liquid junction between the two filling solutions was prepared by securing a plastic micropipette tip packed at the narrow end with cotton and sealed at the top with a septum. The thus prepared inner reference electrode was mounted from the top into the PEEK body, using Tygon tubing and Parafilm.

5.4.3 Assembly of the Reference Electrode

A custom-made double-junction reference electrode was equipped with a porous glass frit (Princeton Applied Research, Oak Ridge, TN, USA) to separate the sample from the outer filling solution (propylene glycol saturated with KNO_3). A second porous glass frit separated the outer filling solution from the inner filling solution (propylene glycol saturated with KCl and AgCl). A AgCl-coated Ag wire was inserted into the latter as an internal reference element (see Supporting Information).

5.4.4 Potentiometric Measurements

All calibration curves and nanoparticle syntheses were performed in solutions contained in a round-bottom flask with three necks, which were all stoppered with a rubber septum. The reference electrode and the ISE were inserted into the propylene glycol solution through two septa. The third septum was used to insert a temperature probe in order to add reagents with a syringe, and in the case of nanoparticle syntheses, to flush with nitrogen. For measurements at 150 ºC, the reaction solution was heated with an oil bath on

a hot plate connected to the temperature probe. Sensor calibrations were performed by the addition of aliquots of a propylene glycol solution of the sodium salt of the anion of interest. Selectivity coefficients were determined using the fixed primary ion method[14] and the separate solutions method, both at 150 ºC. EMF Suite 1.03 software (Fluorous Innovations, Arden Hills, MN) was used with an EMF 16 potentiometer (Lawson Labs, Malvern, PA).

5.4.5 Copper and Silver Nanoparticle Synthesis

An ISE was placed into 200 mL of propylene glycol containing 0.122 g of PVP, and the solution was heated to 150 ºC. Then, 20 mL of 55 mM $Cu(NO_3)_2$ or 110 mM of $AgNO_3$ in propylene glycol was added at a rate of 1 mL/s. The potential of the electrochemical cell was monitored over the course of the whole reaction time, which was 60 min. Over this time, six aliquots were taken for *ex situ* analyses by ion chromatography and by colorimetric analysis.

5.4.6 *Ex Situ* Colorimetric Analysis of Nitrate and Nitrite

Samples for *ex situ* measurements of nitrate and nitrite concentrations in the silver nanoparticle synthesis solutions were collected periodically over the course of the reactions. All samples were diluted with water by a factor of five and frozen to quench any further reaction. For analysis, the samples were thawed and centrifuged. Colorimetric analysis at 520 nm was performed on the supernatant at the University of Minnesota Research analytical lab using a Lachet 8500 FIA spectrophotometer. The nitrite concentration was determined first, followed by reduction with cadmium to give the total nitrite and nitrate concentrations. The nitrate concentration was determined by difference.[227]

5.4.7 Ion Chromatography

Ion chromatography was performed with a Dionex Ion Pac AS11 column and a Dionex Anion Self-Regulating Suppressor ASRS-I with a suppression voltage of 300 mV, with 3 mM NaOH in a 1:4 propylene glycol/water mixture as the eluent.

5.4.8 UV-Vis Absorbance Spectroscopy

UV-Vis spectroscopy was performed using a Hewlett Packard 8452A diode array spectrophotometer.

5.4.9 Transmission Electron Microscopy (TEM) and energy-dispersive X-ray spectroscopy (EDS)

TEM images and EDS spectra were obtained on a FEI Tecnai T12 microscope with a voltage of 120 kV and equipped with a LaB6 electron source. Images were recorded using a Gatan MSC794 CCD camera. Samples were prepared on a copper TEM grid. Particle size measurements were performed using ImageJ (version 1.8.0), an open source program written by Wayne Rasband at the U.S. National Institutes of Health.[228] 1 mL of sample was added to 5 mL isopropanol and then centrifuged twice at 9000 rpm for 30 min. The nanoparticles were then washed with 5 mL of isopropanol twice, re-suspended in isopropanol and dropped onto a TEM grid (holey carbon, 200 mesh, copper grid; SPI, Inc.), the solvent was then allowed to evaporate. The average particle size was determined by measuring the diameter of particles from several images taken from different sections of the sample.

5.5 Supporting Information

5.5.1 Assembly of the Reference Electrode

A custom-made, double-junction reference electrode was prepared from a glass tube that had a 5 mm outer diameter, at the bottom, and widened, to 10 mm, top. A 5 mm diameter porous glass frit was attached to the bottom of this tube using Teflon heat-shrink tubing. The glass tube was then filled with outer filling solution (propylene glycol saturated with KNO_3). A second 5 mm tube, with no taper and a porous glass frit attached to its lower end, was inserted into the outer filling solution and filled with the inner filling solution (propylene glycol saturated with KCl). A AgCl-coated Ag wire was inserted into the latter as an internal reference element.

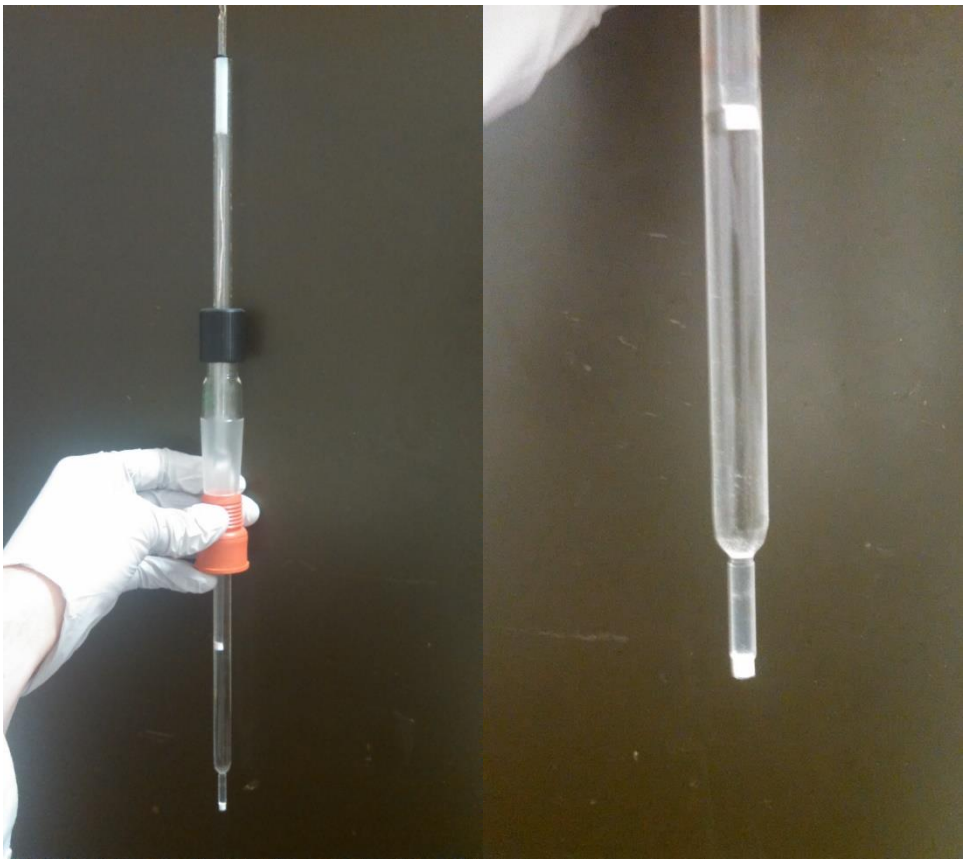

Figure 5.S1: Photographs of the reference electrode.

5.5.2 Design of the Ion-Selective Electrode

The dimensions of the ISE were as follows: shaft diameter, 10 mm; cap diameter, 13 mm; cap opening, 8 mm.

Figure 5.S2: Photographs of the ISE as seen from the side and from the bottom on the left and right, respectively.

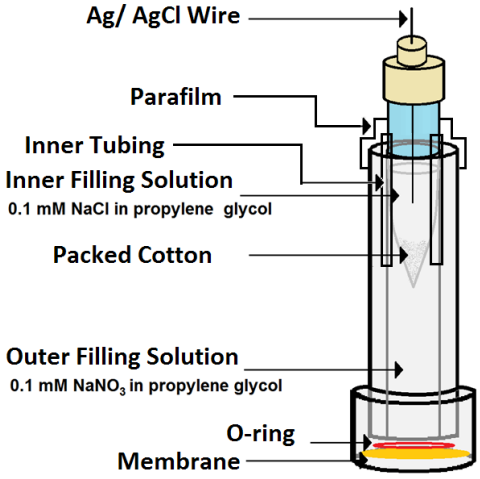

Figure 5.S3: ISE schematic.

We found that gas bubbles that were trapped on the surface of the electrode can cause large changes in the measured potential, which can be explained by a very large increase in the resistance of the electrochemical cell when bubbles are present. To illustrate this effect, we bubbled nitrogen gas through an aqueous solution with varying concentrations of the electrolyte. When one or several bubbles large enough to block most of the surface of the sensing membrane became trapped under the electrode, the potential increased significantly. When this bubble subsequently was removed, the potential quickly returned to the pre-bubble value (Figure 5.S4). Note that the data shown in Figure 5.S7 were taken with the screw cap of the electrode completely immersed into the sample solution. We note that the potential increase is even larger (>1 V) when the electrode cap is only partially submerged into the sample solution (i.e., when the area where the electrode screw cap and the main piece of the electrode body meet is not exposed to the sample). This suggests that there is stray impedance associated with minute volumes of sample solution trapped in between the screw cap and the main body of the ISE. This stray impedance does not interfere with the proper functioning of the electrode, but it affects the extent of the potential increase when bubbles completely block the sensing membrane of the ISE.

Two steps were taken to stop this effect from biasing the results of in situ measurements in the nanoparticle synthesis reactions in which bubbles form. First, the lip on the bottom of the electrode cap was reduced in size and cut to taper slightly outward (Figure 5.S5). Second, the electrode was held in the reaction vessel at approximately 45° from horizontal. This setup was tested by bubbling nitrogen gas through the cell from

underneath the electrode. No buildup of bubbles on the electrode surface was observed, and the measured emf was unaffected. Using this setup, we no longer observed potential changes due to the buildup of bubbles during nanoparticle synthesis reactions.

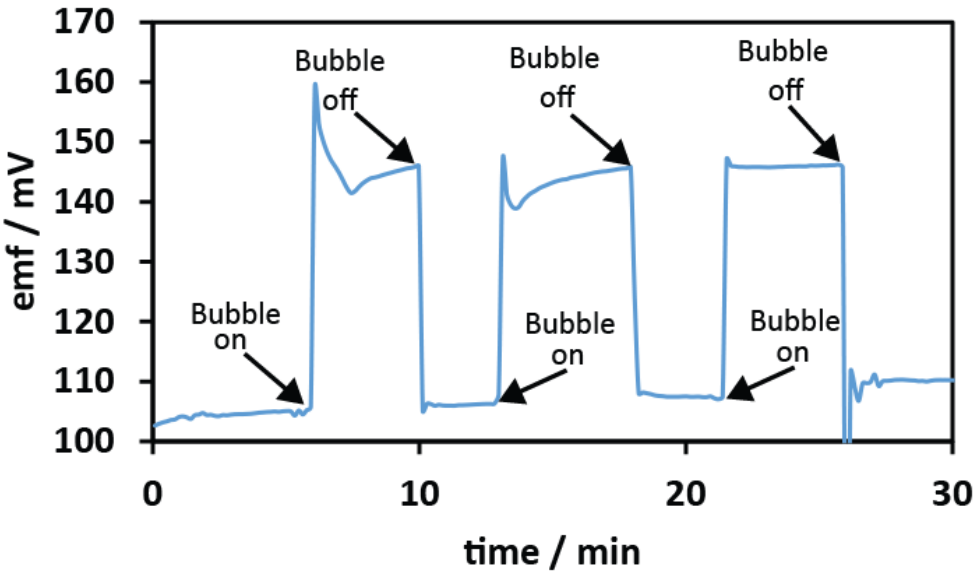

Figure 5.S4: Effect of bubbles on the AHO electrode potential in 5 mM $NaNO_{3\,(aq)}$.

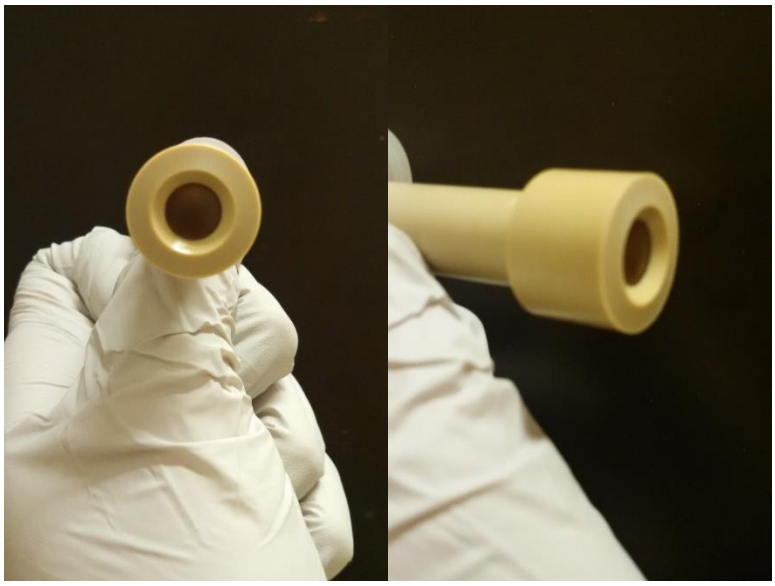

Figure 5.S5: Electrode screw cap modified to eliminate effect of gas bubbles on the measured potential.

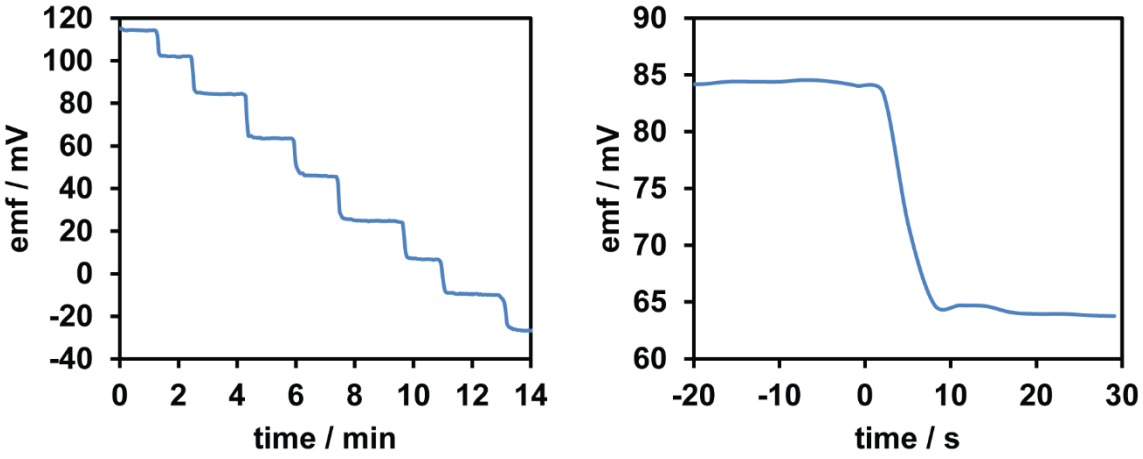

Figure 5.S6: AHO electrode response to changing nitrate condition in propylene glycol at 150 °C, Left: response after several additions of NO_3^- changing concentration from 0.046 mM to 21.273 mM Right: response when changing [NO_3^-] from 0.221mM to 0.471 mM at t = 0, response time of less than 10 s.

5.5.3 DSC Measurements

All ion exchangers were characterized using differential scanning calorimetry using a TA Instruments Q1000 (New Castle, DE, USA). The temperature was cycled from –20 ºC to 200 ºC, several times, with a scan rate of 10 ºC/min. The FAB and the AMI-7001S membranes were received dry, and no treatment prior to the DSC measurements was performed. The AHO membrane was received immersed in a solution and was rinsed with deionized water, blotted dry, and allowed to dry for 24 h before the DSC measurements were taken. See Figures 5.S6 through 5.S8 for plots of the temperature scans. The AHO membrane was subject to additional heating test in which it was heated to 150 ºC for multiple cycles with a heating rate of 1 ºC. The temperature was held at 150 ºC during each cycle for 5 m before continuing. The reproducibility between cycles is high excluding the first heating cycle. The differences between in the heat flow is likely due to the difference in the heating rate.

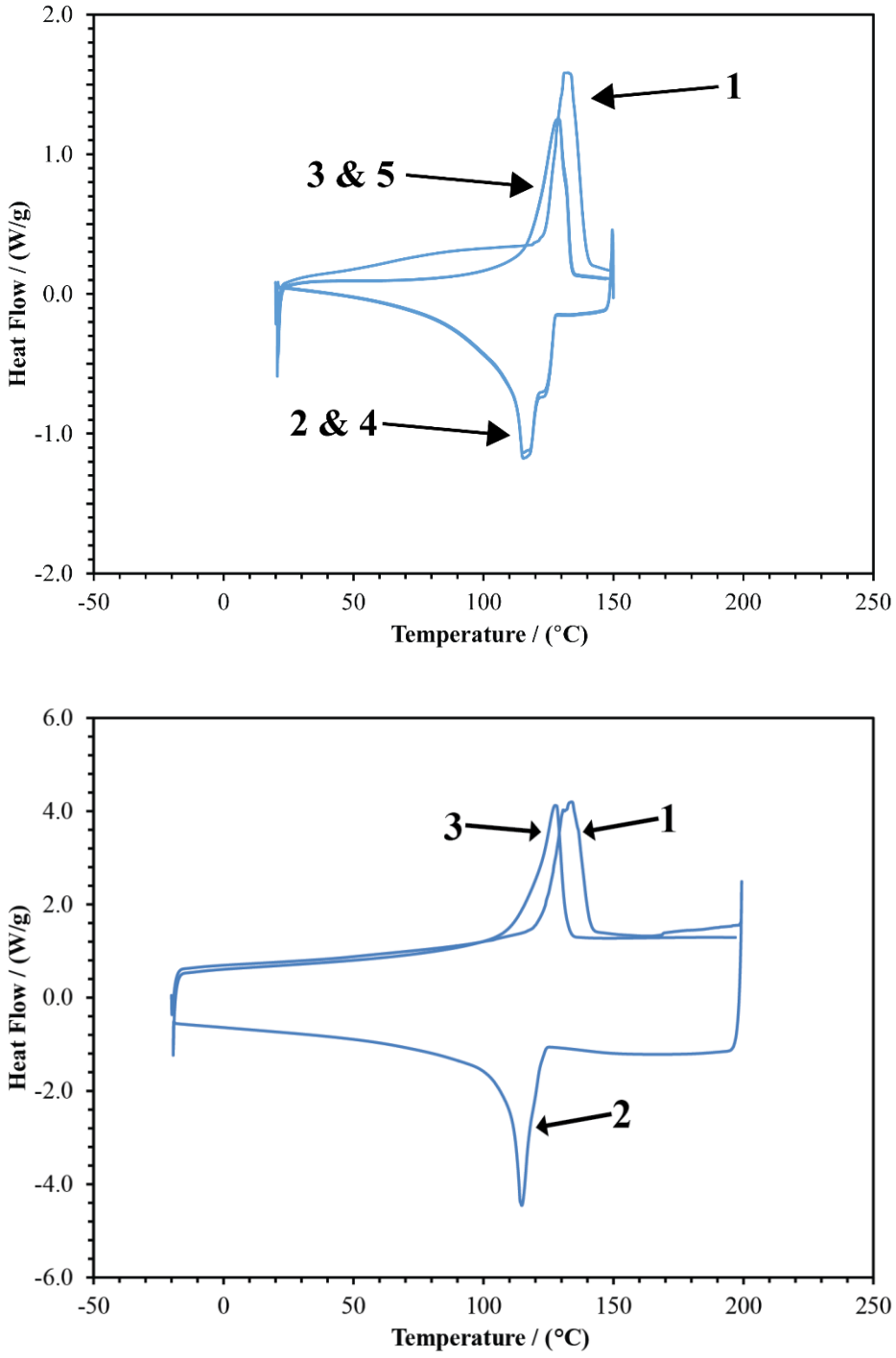

Figure 5.S7: Top: DSCs of AHO membranes with a scan rate of 1 ºC/min heated and held there for 5 min for each cycle. DSCs of AHO membranes with a scan rate of 10 ºC/min to 200 ºC. Odd numbers refer to the first and third segments of the DSC scan (from a low to

high temperature), and the even numbers refer to the second and fourth segments (from a high to low temperature).

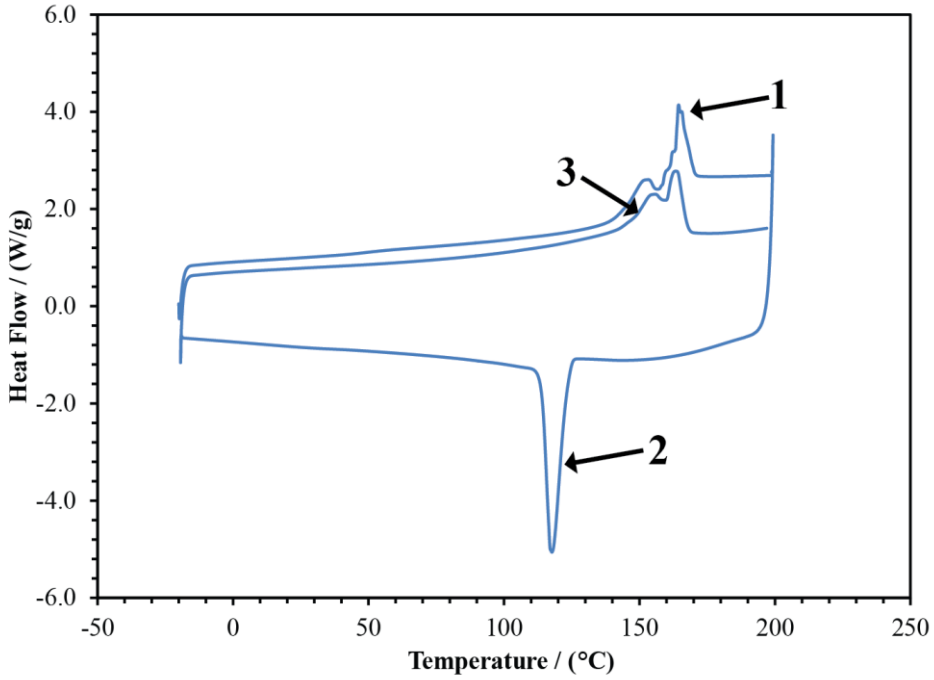

Figure 5.S8: The DSC of the AMI membrane with a scan rate of 10 ºC/min. Odd numbers refer to the first and third segments of the DSC scan (from –20 to 200 ºC), and the number 2 refers to the second segment (from 200 to –20 ºC).

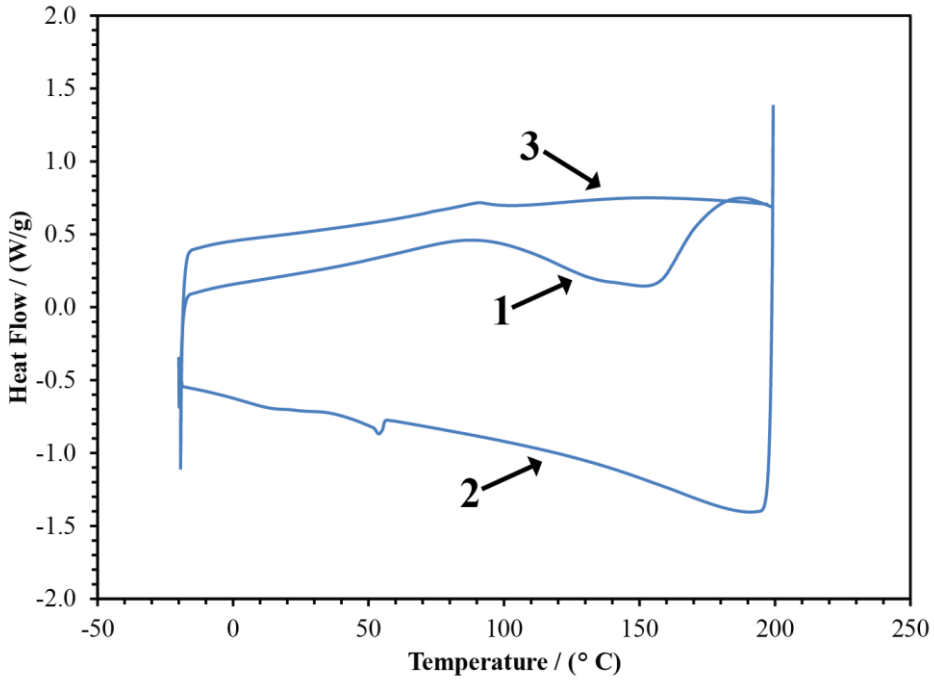

Figure 5.S9: DSC of a FAB membrane with a scan rate of 10 ºC/min. Odd numbers refer to the first and third segments of the DSC scan (from –20 to 200 ºC), and the number 2 refers to the second segment (from 200 to –20 ºC).

5.5.4 TEM Images

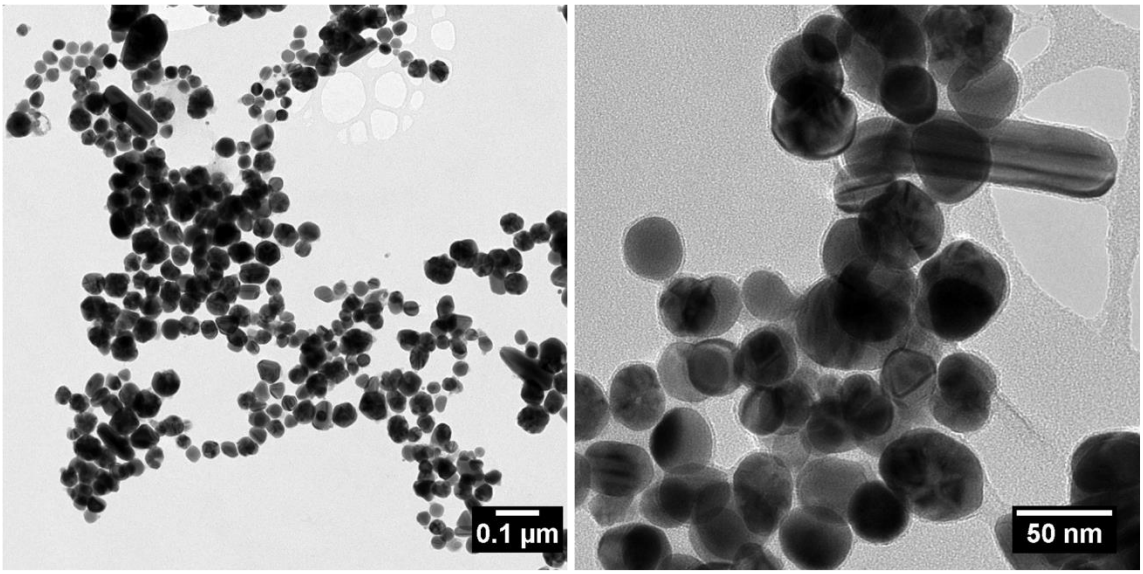

Figure 5.S10: TEM images of silver nanoparticles.

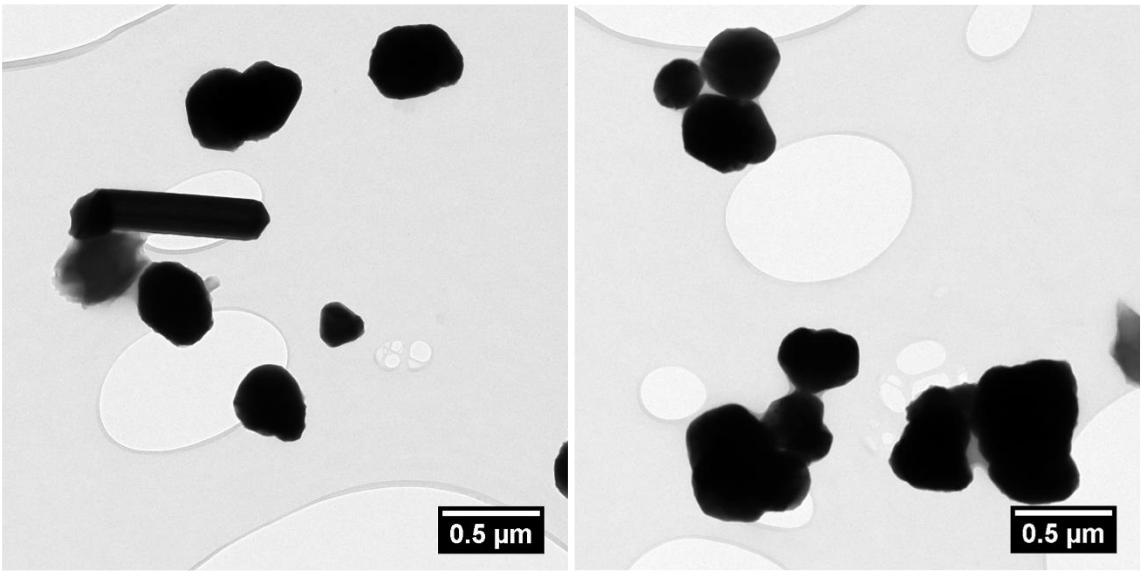

Figure 5.S11: TEM images of copper nanoparticles.

5.5.5 Response Slopes, Colorimetric and Ion Chromatography Data

Table 5.S1: Values of response slops for interfering ions used to determine selectivity coefficients with the separate solutions method.

Ion	Response slope
Cl^-	-65.3 ± 0.7
NO_2^-	-60.1 ± 0.1
OAc^-	–61.5± 1.5

Table 5.S2: Comparison of average nitrate concentrations during three copper and silver nanoparticle syntheses determined by the electrochemical nitrate sensor and colorimetric analysis.

Copper Nanoparticle Synthesis							
	Colorimetric			Ion Chromatography			Potentiometric
Time / (min)	$[NO_3^-]$ / (mM)	$[NO_2^-]$ / (mM)	Total $[NO_3^-]$ and $[NO_2^-]$/ (mM)	$[NO_3^-]$ / (mM)	$[NO_2^-]$ / (mM)	Total $[NO_3^-]$ and $[NO_2^-]$/ (mM)	Total $[NO_3^-]$ and $[NO_2^-]$/ (mM)
8	1.4 ± 0.4	0.03 ± 0.01	1.4 ± 0.4	1.82 ± 0.5	<0.04	1.8 ± 0.5	1.1 ± 0.3
20	3.1 ± 0.4	2.81 ± 0.6	6.0 ± 1.0	3.0 ± 0.6	3.0 ± 0.8	6 ± 1.4	2.5 ± 0.4
30	0.4 ± 0.2	0.3 ± 0.2	0.7 ± 0.4	0.6 ± 0.4	0.1 ± 0.1	0.7 ± 0.5	0.7 ± 0.3
40	0.26 ± 0.06	0.06 ± 0.03	0.32 ± 0.09	0.28 ± 0.01	<0.04	0.3 ± 0.1	0.08 ± 0.05
50	0.13 ± 0.04	0.01 ± 0.01	0.14 ± 0.05	0.22 ± 0.06	<0.04	0.22 ± 0.06	0.08 ± 0.03
60	0.12 ± 0.02	0.01 ± 0.01	0.14 ± 0.03	0.13 ± 0.02	<0.04	0.13 ± 0.02	0.06 ± 0.02

Silver Nanoparticle Synthesis							
	Colorimetric			Ion Chromatography			Potentiometric
Time / (min)	$[NO_3^-]$ / (mM)	$[NO_2^-]$ / (mM)	Total $[NO_3^-]$ and $[NO_2^-]$/ (mM)	$[NO_3^-]$ / (mM)	$[NO_2^-]$ / (mM)	Total $[NO_3^-]$ and $[NO_2^-]$/ (mM)	Total $[NO_3^-]$ and $[NO_2^-]$/ (mM)
8	3.1 ± 0.7	0.20 ± 0.03	3.29 ± 0.7	3.2 ± 0.9	0.11 ± 0.04	3.0 ± 1.0	3.2 ± 0.1
20	2.0 ± 2.0	1.6 ± 0.9	4.0 ± 3.0	3.0 ± 2.0	1.0 ± 1.0	4.0 ± 3.0	5.9 ± 0.2
30	0.07 ± 0.04	0.03 ± 0.01	0.10 ± 0.05	0.2 ± 0.5	0.20 ± 0.5	0.44 ± 0.10	0.03 ± 0.01
40	0.07 ± 0.04	0.03 ± 0.01	0.10 ± 0.05	0.2 ± 0.1	<0.04	0.17 ± 0.10	0.03 ± 0.01
50	0.06 ± 0.03	0.02 ± 0.01	0.08 ± 0.04	0.20 ± 0.08	<0.04	0.20 ± 0.08	0.06 ± 0.02
60	0.02 ± 0.01	0.02 ± 0.01	0.04 ± 0.02	0.2 ± 0.4	<0.04	0.17 ± 0.04	0.8 ± 0.3

6 CHAPTER SIX:

Current Pulse Based Reference Electrodes with Hydrophilic High Capacity Ion-Exchange (HHCEI) Membranes

This section details a proof of concept demonstration of a current pulse based reference electrode that utilize hydrophilic high capacity ion-exchange (HHCEI) membranes. Because HHCEI membranes have low electrical resistance, as well as a high resistance to interference from lipophilic ions and Donnan failure, they look to be promising membranes for these electrodes. Their low electrical resistance allows for higher magnitude current pulses to be used then is possible with previously developed current pulse reference electrodes with lipophilic membranes. This allows the reference electrode to produce a constant potential at higher sample solution concentrations. HHCEI membranes' resistance to interference from lipophilic ions and Donnan failure should allow for application in biological sample matrixes.

6.1 Introduction

Potentiometric measurements, like most electroanalytical measurements, require a reference electrode that is separated from the sample solution by a salt bridge.[1, 4, 222] However, these salt bridges can have several disadvantages. As these salt bridges often contain a free flow liquid junction, they can clog with sample components such as lipids and proteins, can contaminate samples of small volumes with the bridging electrolyte and can suffer from depletion of the bridging solution.[113, 114] Recently, reference electrodes that utilize an applied current pulse to lipophilic ion doped membranes have been developed.[126] The applied current pulse is used to control transmembrane ion fluxes, giving a potential that is independent of the sample solution. Current pulses have been used in the past to limit ion-fluxes to improve the limits of detection of ISEs.[127-129, 229] With these reference

electrodes, however, the current pulses are used to promote ion fluxes, and in effect worsen the detection limit, giving a constant potential. It has been previously shown that the response of this type of electrode can be predicted by:[126]

$$emf \approx E^{\circ\prime} + \frac{2.303\mathrm{R}T}{z\mathrm{F}}\log\left(c_{sample} + \frac{2it^{1/2}}{\mathrm{F}AD_{sample}{}^{1/2}\pi^{1/2}}\right) \tag{6.1}$$

where $E^{\circ\prime}$ is the standard potential including the activity coefficient of the sample solution, R is the gas constant, T is the temperature, F is Faradays constant, z is the charge of the ion released from the electrode, c_{sample} is the concentration of the ion in the sample solution, i is the amplitude of the current pulse, t is the length of the current pulse, A is the surface area of the membrane, and D_{sample} the diffusion coefficient of the ion released into the sample. When the concentration of released ions near the membrane surface, described by the term

$$\frac{2it^{1/2}}{\mathrm{F}AD_{sample}{}^{1/2}\pi^{1/2}} \tag{6.2}$$

is much larger than the concentration in the bulk sample, c_{sample}, the potential measured after the current pulse will be constant over that concentration range. Figure 6.1 shows a schematic of concentration gradients during pulse mode operation. These reference electrodes have been used in conjunction with polymeric ISE, releasing tetrabutylammonium ions, to measure Cl^- concentrations up to 50 mM.[126]

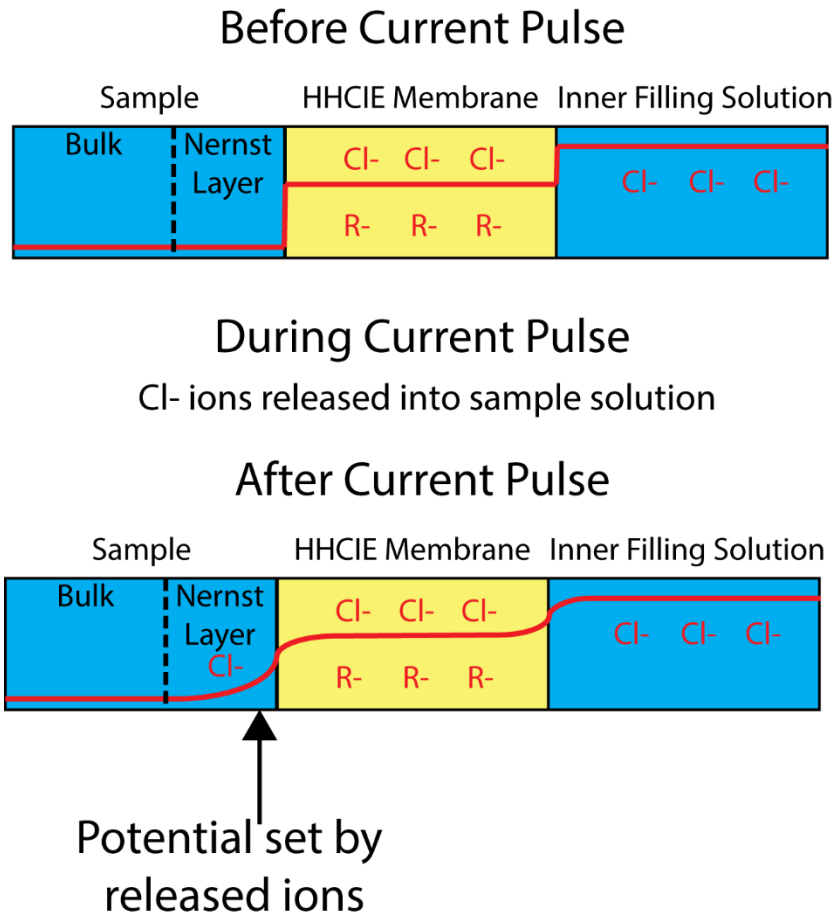

Figure 6.1: Schematic of concentration gradients during pulse mode operation of HHCIE membrane electrode with KCl inner filling solution.

Previously, plasticized PVC has been used as the membrane in current pulse reference electrodes. However, due to their relatively high resistance, typically hundreds of kΩ, and instrumental limitations on voltage magnitudes, the magnitude of the current pulse is limited. This in turn limits the rage of concentrations at which the electrode can provide a constant potential. Hydrophilic high capacity ion-exchange (HHCEI) membranes have much lower resistances, often only a few Ohms. This should allow for the use of

higher magnitude current pulses and, therefore, use of the reference electrodes over a larger range of concentrations.

Previous current pulse based electrodes based on lipophilic membranes released lipophilic ions, such as tetrabutylammonium. Because these membranes were lipophilic, they had a high selectivity toward lipophilic ions. This allowed for the lipophilic ion to determine the phase boundary potential even when there were other less lipophilic ions at high concentrations in the sample. However, this also means that the reference electrode is susceptible to interference from lipophilic ions in the sample and is susceptible to Donnan failure. HHCEI membranes have a very narrow selectivity range and therefore will not suffer from interference from lipophilic ions.[94] Additionally, as shown in Chapter 4, HHCEI are also extremely resistant to Donnan failure caused by lipophilic ions. However, due to their lack of selectivity, the concentration of released ions will need to be very high compared to the concentration of ions in the sample. This means that a large magnitude current pulse is necessary, further underlining the importance of low resistance and of optimization of the pulse duration and electrode geometry. Described below is a proof of concept of using a HHCEI membrane as a current pulse reference electrode.

6.2 Experimental

6.2.1 Materials

Fumasep FAB anion exchange membranes (a PEEK reinforced membrane, 0.13 mm thick, sold loaded with bromide as counter ion, with a capacity of >1.3 meq/g, electrical resistance <1 Ω/cm^2) were purchased from Fumatech, Bietigheim-Bissingen,

Germany. Platinum mesh (50 mm by 50 mm woven from 0.762 mm diameter wire) was purchased from Johnson Matthey Catalog Company, Ward Hill, MA. Deionized water (0.18 MΩ m specific resistance) purified with a Milli-Q PLUS reagent grade water system (Millipore, Bedford, MA) was used in all cases.

6.2.2 Electrode Assembly

The current pulse reference electrode body was made from half of a cylindrical plastic syringe holder with a 2.5 cm diameter opening cut in the cap to expose the FAB membrane the to the sample solution. The membrane was mounted into the electrode body and the electrode body was sealed using hot melt glue. An Ag/AgCl wire was inserted into the inner filling solution to serve as the inner reference electrode and was held in place by a rubber septum glued to the top of the electrode body. A platinum mesh was inserted into the inner filling solution to serve as an internal counter electrode and was held in place with a copper clamp glued to the top of the electrode body. An inner filling solution of concentrated KCl was used. See Figure 6.2 for a diagram of the current pulse reference electrode. Electrodes were conditioned in solutions of KCl of the same concentration as the inner filling solution for 24 h before use.

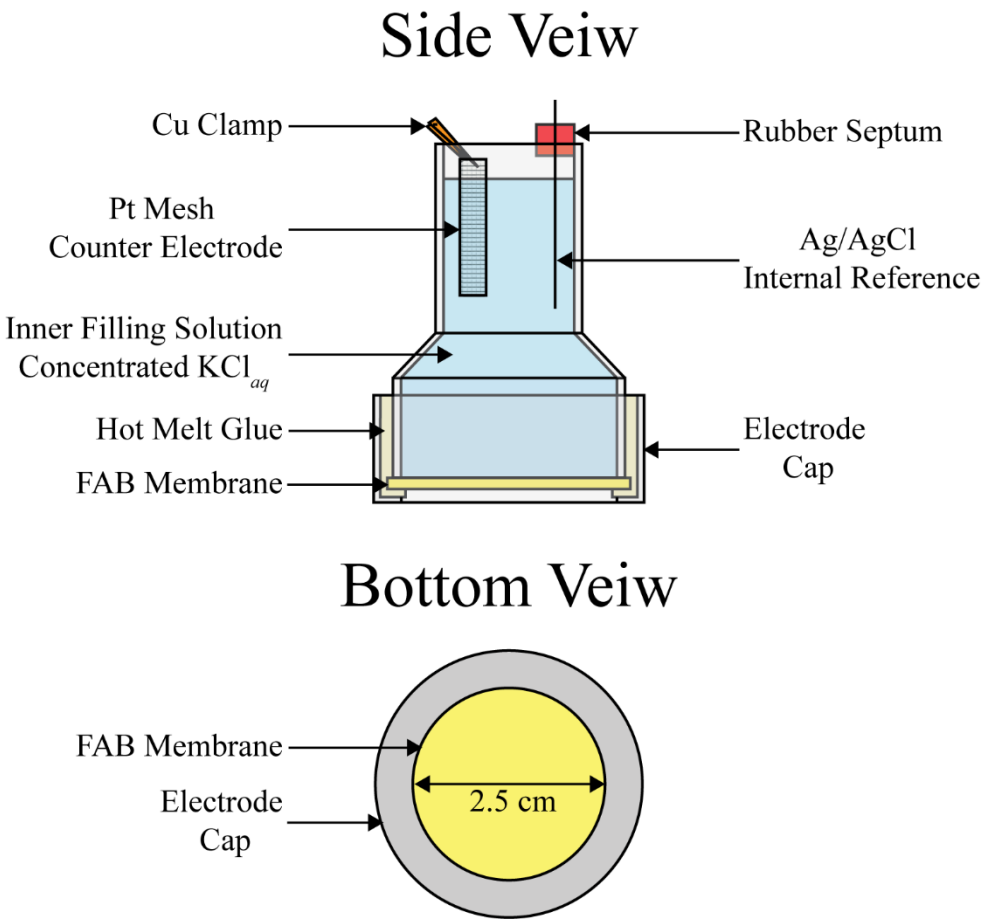

Figure 6.2. Diagram of the current pulse reference electrode made from a plastic syringe holder, with a FAB Anion exchange membrane, a Ag/AgCl internal reference electrode and a platinum internal counter electrode.

6.2.3 Electrochemical cell set up

A four electrode system was used for the current pulse experiments, as shown in Figure 6.3. For all measurements, the external reference electrode was a double-junction Ag/AgCl electrode (DX200, Mettler Toledo, OH) with a 1 M LiOAc bridge electrolyte and a 3 M KCl reference electrolyte. Platinum mesh was used as the external counter electrode; additionally, a 1.5 by 2 inch piece of platinum foil was added in an effort to increase the

surface area of the counter electrode to reduce the resistance of the cell. The FAB electrode containing the internal reference and counter electrodes was inserted into the sample solution.

EMF Suite 1.03 software (Fluorous Innovations, Arden Hills, MN) was used with an EMF 16 potentiometer (Lawson Labs, Malvern, PA) when determining the effects of the inner filling solution concentration.

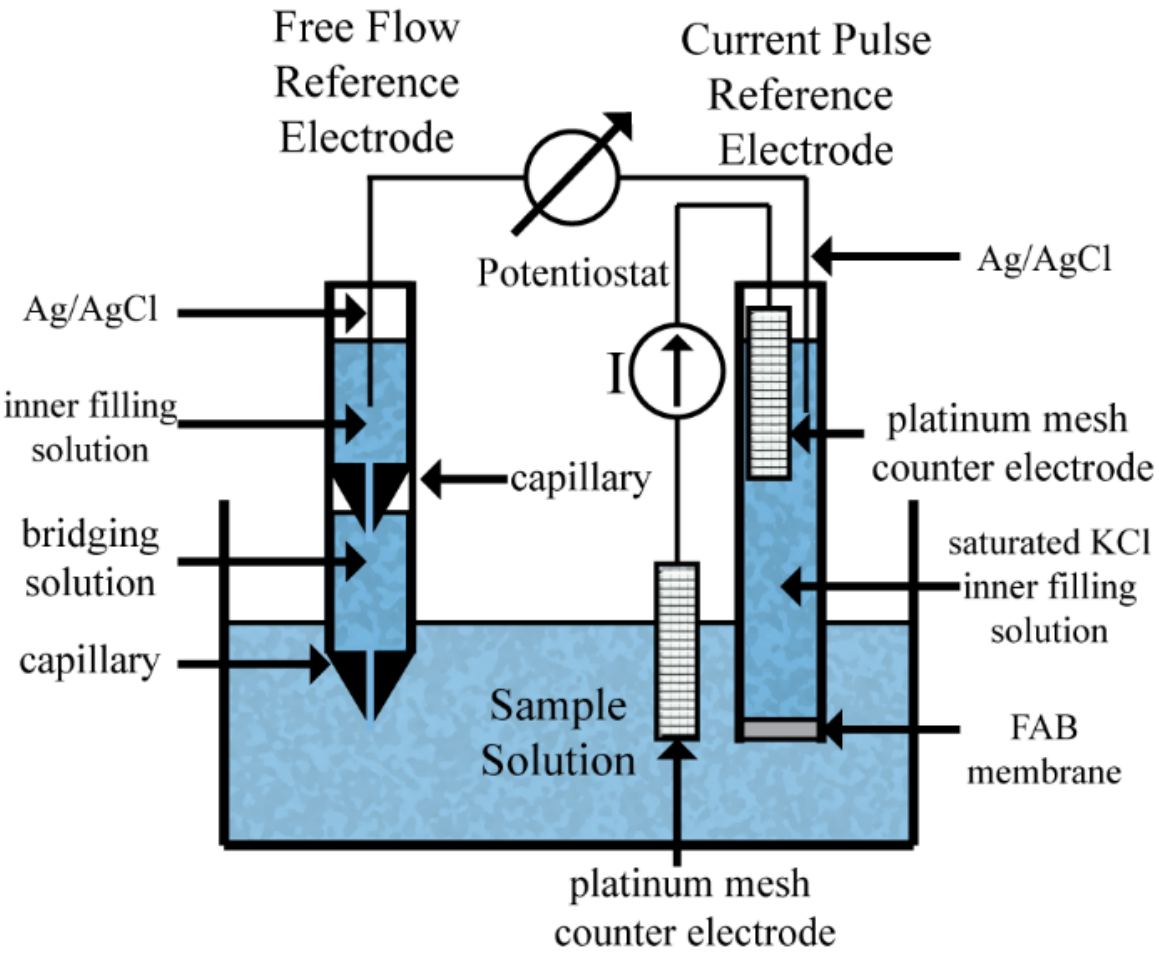

Figure 6.3: Setup of electrochemical cell for testing a current pulse reference electrode against a conventional free flow reference electrode.

6.2.4 Current Pulse Measurements

Current pulse measurements were performed on a Solartron SI 1287 electrochemical interface (Boston, MA). Current pulses were programmed with CorrWare software (Scribner Associates, Southern Pines, NC). Solutions were not stirred during the pulse or when taking the potentiometric measurements. A galvanostatic current pulse of 60 s was applied to the counter electrodes. The potential between the two reference electrodes

was measured 2 sec after the end of the pulse in order to achieve a reproducible potential, as, due to limitations of the instrument, the delay between the end of the pulse and the start of the potential measurement ranged from 1.2 to 1.7 seconds. The pH of the inner filling solution was also monitored after each current pulse by use of litmus paper.

6.2.5 Impedance Spectroscopy

Impedance spectroscopy was performed on a Solartron SI 1287 electrochemical interface (Boston, MA) using CorrWare software (Scribner Associates, Southern Pines, NC).

6.3 Results and Discussion

Using a high concentration inner filling solution is ideal for creating a reference electrode with a constant potential over a wide range of sample compositions. To test this, several potentiometric measurements were performed using various inner filling solution concentrations (0.1 M, 1 M and a saturated solution, ~3.7 M KCl). As expected, the electrodes made with the concentrated inner filling solution had a higher limit of detection then the other electrodes (132 μM for the saturated solution, compared to 32 μM for the 1 M solution or 25 μM for the 0.1 M solution, see Figure 6.4). As it is desirable for the reference electrode to have a constant potential over the largest concentration range as possible, this high detection limit is desirable. Therefore, the saturated inner filling solution was used for all of the pulse-based experiments. The high concentration of the inner filling solution also serves to lower the resistance of the cell. This low resistance is necessary

because at low sample concentrations the high resistance of the sample solution requires a higher voltage to produce the desired current, as evident from Ohm's law.

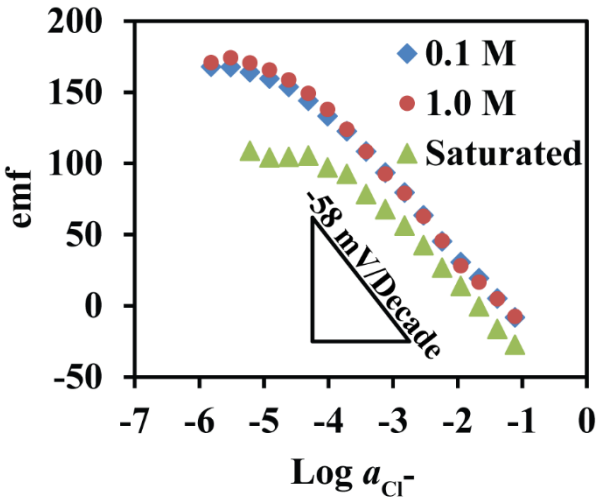

Figure 6.4: Potentiometric response slopes of FAB membrane electrodes with varying KCl inner filling solution concentrations (0.1 M, 1.0 M and saturated (~3.7 M) to varying KCl_{aq} concentrations.

Initial experiments with the current pulse electrode used a much smaller opening for the FAB membrane and coiled platinum wires. However, the voltage required to achieve the desired currents at low concentrations of sample solution was of greater magnitude than the maximum output of the instrumentation (-15 V). This, however, was not due to the resistance of the FAB membrane, which is low (<1 Ω/cm^2), but rather the large resistance due to the small surface area exposed to the sample. The resistance of the cell is determined by the following:

$$R = \frac{l}{A}\rho \tag{6.3}$$

where l is the distance between the electrodes, A is the area of the electrodes, and ρ is the specific electrical resistance of the solution. The resistance is large because of the small surface area of the platinum wire and the FAB membrane. By using a larger electrode body to increase the area of the FAB membrane, by replacing the platinum wire with platinum mesh, and shortening the distance between the electrodes, this resistance was reduced. Impendence measurements were performed at each concentration used in the current pulse experiments, both before and after the current pulses. The values obtained before and after the current pulse were within a standard deviation for each concentration. The resistance of the cell ranged from 3.3 kΩ when the sample solutions concentration was at 0.02 μM KCl to 2.1 Ω when the sample solutions concentration was 0.8 M KCl; see Figure 6.5.

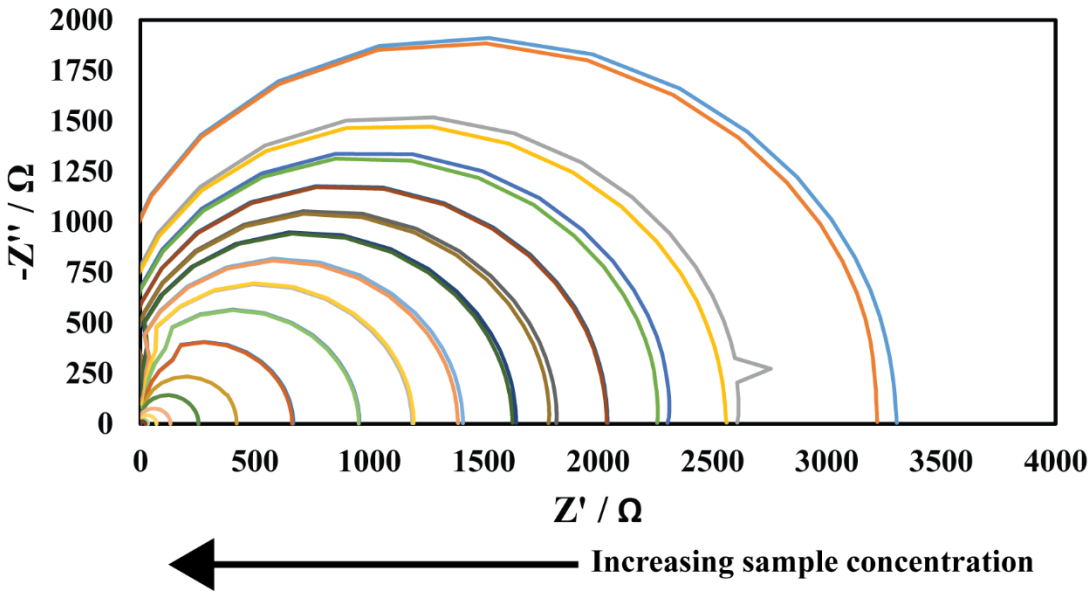

Figure 6.5: Nyquist plot of impedance spectra of the current pulse reference electrode cell with sample solution concentrations from 0.02 μM to 0.8 M.

This allows for a current pulse of a larger magnitude to be utilized in samples with low ionic strength. For example, in a 0.2 μM KCl solution, a 5 mA current can be produced using only 8.9 V, whereas with the previous setup a similar voltage could produce a 5mA current only in a 0.1 mM KCl solution. By using larger magnitude current pulses, the range at which the electrode can maintain a constant potential immediately following the pulse is increased; see Figure 6.6. At low currents (<800 μA) the limit of detection of the reference electrode is not significantly affected due to the already relatively high limit of detection of the electrode. By using -5 mA current pulses, the electrode can maintain a relatively constant potential across various in sample concentrations up to ~ 1 mM KCl. This represents an improvement of more than an order of magnitude compared to that of the previously developed current pulse reference electrode with a plasticized PVC.[126] However, there is a high standard deviation in the potential over the course of several trials, as shown by the error bars in Figure 6.6. The average response after the -5 mA current pulse can be fit well with Equation 6.1, see Figure 6.6. The pH of the inner filling solution of the FAB electrode monitored over the course of the experiment showed a change from pH 7 to 9 when the concentration of KCl in the sample solution was raised from 0.1 mM to 1 mM.

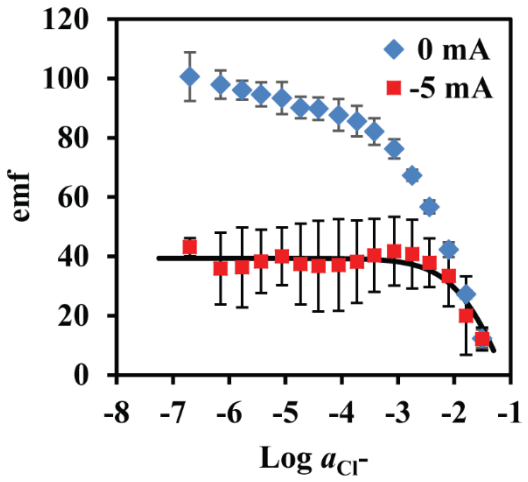

Figure 6.6: Average response of FAB membrane current pulse reference electrode over several trials before current pulse (0 mA) and after -5 mA current pulse (-5 mA), along w with a fit using Equation 6.1.

There are several ways that this system could be improved. The first is to design a setup which allows for the counter electrode in the sample to remain at a fixed distance from the FAB membrane and have a constant surface area exposed to the sample solution. This would likely help with the reproducibility of the experiments and allow for a more consistent potential. Another strategy would be to further increase the surface area of the electrodes in contact with the sample solution by increasing the size of the platinum mesh. This would allow for larger currents to be used without exceeding the voltage limitations of the instrumentation, thereby allowing for a constant potential at higher sample concentrations while maintaining the ability to use the electrode in systems with a low ionic strength. Alternatively, one may be able to simply increase the magnitude of the current without changing the counter electrode. This would allow for an increase in the upper range

of the constant potential, but sacrificing the ability to use the electrode in samples of low ionic strength, due to the high resistance of these solutions. However, based on Equation 6.1, using this electrode geometry, the current pulse would have to be raised to approximately -50 mA to obtain a constant potential up to 10 mM or over -150 mA to obtain a constant potential up to 100 mM (the concentration of chloride in blood);[230] see figure 6.7 top left. Decreasing the surface area of the electrode would allow for lower magnitude currents to be used to achieve higher concentrations, see Figure 6.7 top right. However, this would increase the resistance of the cell, as per Equation 6.3, requiring larger potentials to produce the desired current. Also, increasing the current pulse time should also reduce the magnitude of current needed, as shown by Figure 6.7 bottom left, although this will at some point be limited by diffusion away from the electrodes surface; due to the square root dependence on the pulse length, this effect is rather small. Therefore the most effective method of increasing the constant potential range would likely be to decrease the surface area of the FAB membrane and increase the magnitude of the current pulse; see Figure 6.7 bottom right, allowing for moderate changes to both variables to achieve constant potentials at high concentrations.

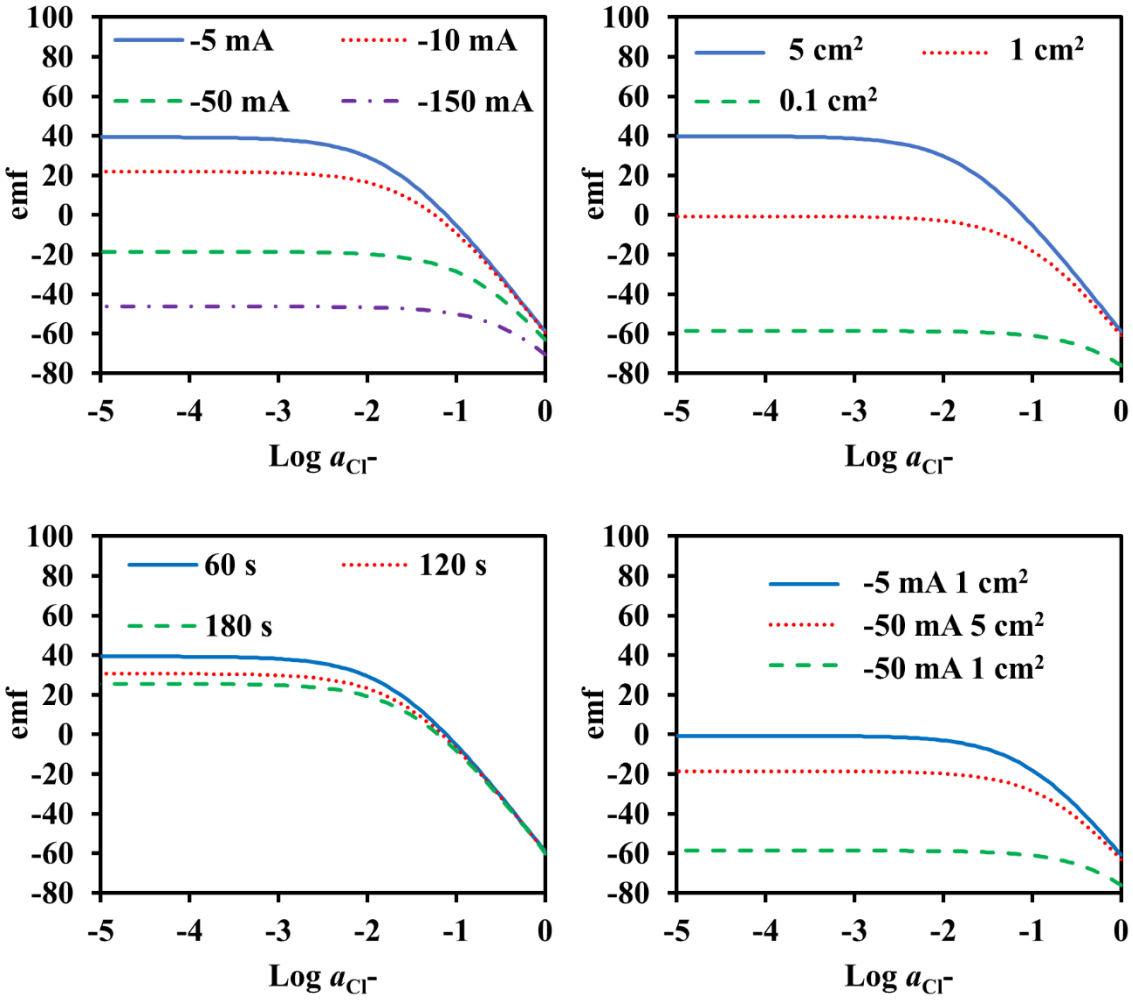

Figure 6.7: Theoretical response plots of current pulse reference electrode using Equation 6.1, with 60 s current pulse duration, 5 cm^2 electrode area and varying current pulse magnitude (top left); 60 s current pulse duration, varying electrode area, and -5 mA current pulse (top right); varying current pulse duration, 5 cm^2 electrode area and -5 mA current pulse (bottom left); and 60 s current pulse duration with varying electrode area and varying current pulse magnitude (bottom right).

6.4 Conclusion

The HHCEI membrane, FAB, has been shown to be a suitable membrane for use in a current pulse based reference electrode. Due to its low resistance, the membrane can be used with larger current pulses. This increases the upper limit of the background concentration of ions released into the sample at which a constant potential can be generated by one order of magnitude as compared to previous lipophilic current pulse based reference electrodes. This system is still limited by the resistance of the sample solution at low ionic strength. HHCEI membranes have other advantages over the lipophilic current pulse reference electrodes, such as their resistance to Donnan failure and their reduced inference from lipophilic ions. Further optimization of the electrode's features such as the magnitude and duration of the current pulse and the geometries of the electrode may be able to further extend the concentration range where the reference electrode is usable. Modifying the HHCEI membrane to make it selective for the released ion, perhaps by covalently attaching an ionophore, would allow for the HHCEI reference electrode to be used in systems with higher concentrations of ions other than the released ion, possibly with the use of a lower current.

7 CHAPTER SEVEN:

Conclusions

7.1 Results

The work in this thesis primarily focused on developing ion-selective electrodes that could function in harsh sample matrixes. A major part of this work focused on developing materials for use in ISEs to be used in the harsh sample matrixes as well as the testing and application of sensors made with these and other materials. Two general classes of membrane materials were the focus for much of this work, i. e., semifluorinated polymer membranes and hydrophilic high capacity ion-exchange (HHCEI) membranes. Fluorous ISE membranes have previously been shown to have high resistance to biofouling and increased selectivity compared to ISEs with more traditional lipophilic membranes, such as plasticized PVC, due to the low polarity and polarizability of fluorous compounds. However, much of this previous work was based on fluorous liquid membranes, which limited the lifetime and durability of the membranes, making ISE membranes based off of fluorous polymers desirable. Ion-exchanger electrodes made from HHCEI membranes have previously been shown to resist interference from lipophilic ions.

After an overview of ISEs and their current limitations in Chapter 1, Chapter 2 discussed attempts to modify lipophilic polymers into fluorophilic polymers by the addition of fluorinated side chains. While reactions that added lipophilic side chains were able to achieve high percent conversions, reactions to add the fluorinated side chains were less successful, with low percent conversions. Despite modifications to solvent composition, starting materials, reaction times, and the reaction temperature, the highest percent conversion rate achieved was 40%. These polymers would not be sufficiently

fluorophilic to produce ISEs with the desired resistance to biofouling or high selectivity exhibited by previously developed fluorous ISE membranes.

In Chapter 3 the synthesis and characterization of several semifluorinated polymers and their subsequent use in ion-exchange electrodes and ISEs was described. Ion-exchanger electrodes made from the most successful of these polymers, a polymerized styrene with a branched fluorous oligoether, had a broad selectivity range (~14 orders of magnitude) similar to that of ISEs previously made with fluorous liquids (~16 orders of magnitude). Cross-linked versions of this polymer were also made, which allowed for the creation of durable self-supported ISEs with similar selectivites. Although Ag^+ ISEs made with these polymers and fluorophilic ionophores were not as selective as the analogous fluorous liquid membrane ISEs, they are still suitable for many applications. Additionally, these electrodes can utilize commercially available lipophilic ionophores, such as valinomycin, allowing them to be used for a wider range of analytes. Potassium ISEs made from the cross-linked semifluorinated polymer with valinomycin showed comparable selectivity coefficients to that of electrodes made from plasticized PVC.

Chapter 4 focused on the study of HHCIE membranes resistance to Donnan failure. The response of HHCIE to chloride ions in the presence of the highly lipophilic teterabutylammonium ion was compared to that of lipophilic ion-exchanger electrodes and ISEs with ionophore-doped sensing membranes. The HHCIE membranes showed a higher resistance to Donnan failure than the lipophilic membranes; in fact, at the concentrations tested no Donnan failure was observed for the HHCIE membranes. This resistance was

shown to be due not to size exclusion of the large lipophilic ions but rather due to the very high ionic site concentration in the HHCIE membranes.

Chapter 5 focused on using HHCIE membranes for potentiometriclly measuring concentrations of NO_X^- species during the synthesis of copper and silver nanoparticles by the polyol process. Because these membranes are highly cross-linked, have covalently attached ionic sites, and are plasticizer-free, they were able to measure in the organic solvent and high temperatures necessary for these reactions, allowing for *in situ* measurements. The values obtained by the HHCIE ISEs were verified by colorimetric tests as well as by ion chromatography. These methods showed that some of the nitrate present in the reaction was reduced to nitrite, before leaving the system as NO_X gas.

A proof of concept for a current pulse reference electrode with a HHCIE membrane was presented in Chapter 6. The low resistance of the HHCIE membrane allowed for higher magnitude current pulses to be utilized than with previously developed current pulse reference electrodes based on plasticized PVC. The current pulse reference electrode HHCIE should allow for decreased interference from lipophilic ions as well as reduced Donnan failure. However, due to the low selectivity of these membranes, large currents are necessary to overcome the response due to changes in the sample concentration.

7.2 Future Work

While the work presented in this thesis presents several steps toward expanding the use of ISEs to harsh sample matrixes, there are several extensions of this work that would be highly beneficial. The semifluorinated polymer ISE's resistance to biofouling needs to

be thoroughly evaluated. Due to the fluorophilic nature of these polymers, they are expected to be resistant to this detrimental effect. The effect of both short-term and long-term exposure to biological media such as blood or urine on electrodes made with these polymers should be evaluated. To further combat the effects of biofouling and increase the lifetime, covalent attachment of ionic sites and ionophores to the polymer should be investigated. The membrane components could possibly be covalently attached to the polymer backbone during the polymerization of the polymers by adding ionic sites or ionophores with suitable reactive functional groups to the reaction mixture. Additional lipophilic ionophores can also be tested in these membranes, further expanding the range of ions that can be measured with sensors made from these polymers.

The HHCIE membrane ISE developed for measuring in nanoparticle synthesis could be used to further investigate the role that NO_X^- species play in nanoparticle synthesis. The sensor could be used to study a wide array of different nanoparticle reactions, with differences in reaction conditions or metal species. It could also be used to monitor anion concentrations when co-ions other than nitrate, such as acetate, are used in nanoparticle synthesis. The current pulse reference electrode with HHCIE membrane needs to be further optimized so that it can provide constant potentials in samples of higher ion concentrations.

References

1. Bakker, E.; Bühlmann, P.; Pretsch, E., Carrier-Based Ion-Selective Electrodes and Bulk Optodes. 1. General Characteristics. *Chem. Rev.* **1997,** *97*, 3083-3132.
2. Gunaratna, P. C.; Koch, W. F.; Paule, R. C.; Cormier, A. D.; D'Orazio, P.; Greenberg, N.; O'Connell, K. M.; Malenfant, A.; Okorodudu, A. O.; Miller, R., Frozen Human Serum Reference Material for Standardization of Sodium and Potassium Measurements in Serum or Plasma by Ion-Selective Electrode Analyzers. *Clin. Chem.* **1992,** *38*, 1459-1465.
3. D'Orazio, P., Abstract 152, Pittsburgh Conference. Chicago, IL, 1994.
4. Bühlmann, P.; Chen, L. D., Ion-Selective Electrodes With Ionophore-Doped Sensing Membranes. In *Supramolecular Chemistry: From Molecules to Nanomaterials*, Steed, A. W.; Ed, G. P., Eds. John Wiley & Sons, Ltd: New York, 2012; Vol. 5, pp 2539-2579.
5. Choi, K. K.; Fung, K. W., Determination of Nitrate and Nitrite in Meat Products by Using a Nitrate Ion-Selective Electrode. *Analyst* **1980,** *105*, 241-245.
6. Szigeti, Z.; Vigassy, T.; Bakker, E.; Pretsch, E., Approaches to Improving the Lower Detection Limit of Polymeric Membrane Ion-Selective Electrodes. *Electroanalysis* **2006,** *18*, 1254-1265.
7. Sokalski, T.; Ceresa, A.; Zwickl, T.; Pretsch, E., Large Improvement of the Lower Detection Limit of Ion-Selective Polymer Membrane Electrodes. *J. Am. Chem. Soc.* **1997,** *119*, 11347-11348.
8. Lai, C.-Z.; Joyer, M. M.; Fierke, M. A.; Petkovich, N. D.; Stein, A.; Bühlmann, P., Subnanomolar Detection Limit Application of Ion-Selective Electrodes with Three-Dimensionally Ordered Macroporous (3DOM) Carbon Solid Contacts. *J. Solid State Electrochem.* **2009,** *13*, 123-128.
9. Bakker, E.; Bühlmann, P.; Pretsch, E., Polymer Membrane Ion-Selective Electrodes–What are the Limits? *Electroanalysis* **1999,** *11*, 915-933.
10. Henderson, L. J., Blood as a Physicochemical System. *Biol. Chem.* **1921,** *46*, 411-419.
11. Bakker, E.; Nägele, M.; Schaller, U.; Pretsch, E., Applicability of the Phase Boundary Potential Model to the Mechanistic Understanding of Solvent Polymeric Membrane-Based Ion-Selective Electrodes. *Electroanal.* **1995,** *7*, 817-822.
12. Pungor, E., Working Mechanism of Ion-Selective Electrodes. *Pure. Appl. Chem.* **1992,** *64*.
13. Bühlmann, P.; Pretsch, E.; Bakker, E., Carrier-Based Ion-Selective Electrodes and Bulk Optodes. 2. Ionophores for Potentiometric and Optical Sensors. *Chem. Rev.* **1998,** *98*, 1593.
14. Bakker, E.; Pretsch, E.; Bühlmann, P., Selectivity of Potentiometric Ion Sensors. *Anal. Chem.* **2000,** *72*, 1127-1133.
15. Bakker, E., Determination of Improved Selectivity Coefficients of Polymer Membrane Ion-Selective Electrodes by Conditioning with a Discriminated Ion. *J. Electrochem. Soc.* **1996,** *143*, L83-L85

16. Qin, Y.; Peper, S.; Bakker, E., Plasticizer-Free Polymer Membrane Ion-Selective Electrodes Containing a Methacrylic Copolymer Matrix. *Electroanalysis* **2002,** *14*, 1375-1381.
17. Kazarjan, N. A.; Pungor, E., The Behaviour of Ion-Selective Silicone-Rubber Membrane Electrodes in Some Non-Aqueous Solvents. *Anal. Chim. Acta* **1970,** *51*, 213-220.
18. Lindfors, T.; Szücs, J.; Sundfors, F.; Gyurcsányi, R. E., Polyaniline Nanoparticle-Based Solid-Contact Silicone Rubber Ion-Selective Electrodes for Ultratrace Measurements. *Anal. Chem.* **2010,** *82*, 9425-9432.
19. Malinowska, E.; Niedziółka, J.; Meyerhoff, M. E., Potentiometric and Spectroscopic Characterization of Anion Selective Electrodes Based on Metal(III) Porphyrin Ionophores in Polyurethane Membranes. *Anal. Chim. Acta* **2001,** *432*, 67-78.
20. Fiedler, U.; Růžička, J., Selectrode—the Universal Ion-Selective Electrode : Part VII. A Valinomycin-Based Potassium Electrode With Nonporous Polymer Membrane and Solid-State Inner Reference System. *Anal. Chim. Acta* **1973,** *67*, 179-193.
21. Hiemenz, P. C.; Lodge, T. P., *Polymer Chemistry*. 2 ed.; CRC Press: Boca Raton, FL, 2007; p 585.
22. Karlsson, O. J.; Stubbs, J. M.; Karlsson, L. E.; Sundberg, D. C., Estimating Diffusion Coefficients for Small Molecules in Polymers and Polymer Solutions. *Polymer* **2001,** *42*, 4915-4923.
23. Anker, P.; Wieland, E.; Ammann, D.; Dohner, R. E.; Asper, R.; Simon, W., Neutral Carrier Based Ion-Selective Electrode For The Determination of Total Calcium in Blood Serum. *Anal. Chem.* **1981,** *53*, 1970-1974.
24. Shemyakin, M. M.; Ovchinnikov, Y. A.; Ivanov, V. T.; Antonov, V. K.; Vinogradova, E. I.; Shkrob, A. M.; Malenkov, G. G.; Evstratov, A. V.; Laine, I. A.; Melnik, E. I.; Ryabova, I. D., Cyclodepsipeptides as Chemical Tools for Studying Ionic Transport Through Membranes. *J. Membr. Biol.* **1969,** *1*, 402-430.
25. Malinowska, E.; Oklejas, V.; Hower, R. W.; Brown, R. B.; Meyerhoff, M. E., Enhanced Electrochemical Performance of Solid-State Ion Sensors Based on Silicone Rubber Membranes. *Sens. Actuators, B* **1996,** *33*, 161-167.
26. Bakker, E.; Xu, A.; Pretsch, E., Optimum Composition of Neutral Carrier Based pH Electrodes. *Anal. Chim. Acta* **1994,** *295*, 253-262.
27. Oesch, U.; Brzozka, Z.; Xu, A.; Rusterholz, B.; Suter, G.; Pham Hung, V.; Welti, D.; Ammann, D.; Pretsch, E.; Simon, W., Design of Neutral Hydrogen Ion Carriers for Solvent Polymeric Membrane Electrodes of Selected pH Range. *Anal. Chem.* **1986,** *58*, 2285-2289.
28. Bühlmann, P.; Yajima, S.; Tohda, K.; Umezawa, Y., EMF response of neutral-carrier based ion-sensitive field effect transistors with membranes free of ionic sites. *Electrochim. Acta* **1995,** *40*, 3021-3027.
29. Qin, Y.; Bakker, E., A Copolymerized Dodecacarborane Anion as Covalently Attached Cation Exchanger in Ion-Selective Sensors. *Anal. Chem.* **2003,** *75*, 6002-6010.

30. Buck, R. P.; Lindner, E., Recommendations for Nomenclature of Ion-Selective Electrodes. *Pure. App. Chem.* **1994,** *66*, 2527-2536.
31. Amemiya, S.; Bühlmann, P.; Pretsch, E.; Rusterholz, B.; Umezawa, Y., Cationic or Anionic Sites? Selectivity Optimization of Ion-Selective Electrodes Based on Charged Ionophores. *Anal. Chem.* **2000,** *72*, 1618-1631.
32. Püntener, M.; Vigassy, T.; Baier, E.; Ceresa, A.; Pretsch, E., Improving the Lower Detection Limit of Potentiometric Sensors by Covalently Binding the Ionophore to a Polymer Backbone. *Anal. Chim. Acta* **2004,** *503*, 187-194.
33. Bühlmann, P.; Hayakawa, M.; Ohshiro, T.; Amemiya, S.; Umezawa, Y., Influence of Natural, Electrically Neutral Lipids on the Potentiometric Responses of Cation-Selective Polymeric Membrane Electrodes. *Anal. Chem.* **2001,** *73*, 3199-3205.
34. Dinten, O.; Spichiger, U. E.; Chaniotakis, N.; Gehrig, P.; Rusterholz, B.; Morf, W. E.; Simon, W., Lifetime of Neutral-Carrier-Based Liquid Membranes in Aqueous Samples and Blood and the Lipophilicity of Membrane Components. *Anal. Chem.* **1991,** *63*, 596-603.
35. Upreti, P.; Metzger, L. E.; Bühlmann, P., Glass and Polymeric Membrane Electrodes for the Measurement of pH in Milk and Cheese. *Talanta* **2004,** *63*, 139-148.
36. Leung, A. Investigation in the Effects of Biological Interferents on Fluorous Membrane-based Ion Selective Electrodes. Masters Thesis, University of Minnesota, Minneapolis, MN, 2008.
37. Phillips, F.; Kaczor, K.; Gandhi, N.; Pendley, B. D.; Danish, R. K.; Neuman, M. R.; Toth, B.; Horvath, V.; Lindner, E., Measurement of Sodium Ion Concentration in Undiluted Urine With Cation-Selective Polymeric Membrane Electrodes After the Removal of Interfering Compounds. *Talanta* **2007,** *74*, 255-264.
38. Espadas-Torre, C.; Oklejas, V.; Mowery, K.; Meyerhoff, M. E., Thromboresistant Chemical Sensors Using Combined Nitric Oxide Release/Ion Sensing Polymeric Films. *J. Am. Chem. Soc.* **1997,** *119*, 2321-2322.
39. Frost, M. C.; Meyerhoff, M. E., Implantable Chemical Sensors for Real-Time Clinical Monitoring: Progress and Challenges. *Curr. Opin. Chem. Biol.* **2002,** *6*, 633-641.
40. Bakker, E., Determination of Unbiased Selectivity Coefficients of Neutral Carrier-Based Cation-Selective Electrodes. *Anal. Chem.* **1997,** *69*, 1061-1069.
41. Ebdon, L.; Ellis, A. T.; Corfield, G. C., Ion-Selective Polymeric-Membrane Electrodes with Immobilised Ion-Exchange Sites. Part II. Selectivity of and Application Studies on a Calcium Electrode. *Analyst* **1982,** *107*, 288-294.
42. Warner, J. L. Effect of Electrically Neutral Compounds on the Response of Fluorous Membrane-based Ion Selective Electrodes. University of Minnesota, Minneapolis, MN, 2006.
43. Durst, R. A.; Branscomb, L. M.; Stans, M. H. In *Ion-selective electrodes*, The Symposium on Ion-Selective Electrodes Sponsored by the Analytically Chemistry Division of the NBS Institute for Material Research, Gaithersburg, Maryland, Durst, R. A., Ed. National Bureau of Standards: Gaithersburg, Maryland, 1969; p 425.

44. Ibupoto, Z. H., Kimleang Khun and Magnus Willander, A Selective Iodide Ion Sensor Electrode Based on Functionalized ZnO Nanotubes. *Sensors* **2013,** *13*, 1984-1997.
45. Arvand, M.; Asadollahzadeh, S. A., Ion-Selective Electrode for Aluminum Determination in Pharmaceutical Substances, Tea Leaves and Water Samples. *Talanta* **2008,** *75*, 1046-1054.
46. Pungor, E.; Toth, K.; Klatsmanyi, P. G.; Izutsu, K., Applications of Ion-Selective Electrodes in Nonaqueous and Mixed Solvents. *Pure Appl. Chem.* **1983,** *55*, 2029-2065.
47. Kakabadse, G. J.; Al-Aziz, M.; Al-Yawer, N. F. N.; Kaklugin, P.; Karim, M. R. O.; Perry, R.; Tipping, A. E.; Wake, P., Recent Advances in Direct Potentiometry in Organic and Mixed Solvents. *Port. Electrochim. Acta* **1988,** *6*, 5-25.
48. Jain, A. K.; Gupta, V. K.; Singh, R. D.; Khurana, U.; Singh, L. P., Nickel(II)-Selective Sensors Based on Heterogeneous Membranes of Macrocyclic Compounds. *Sens. Actuators, B* **1997,** *40*, 15-20.
49. Hu, M.; Cui, R.; Li, S. n.; Jiang, Y.; Xia, S. P., Determination of Activity Coefficients for Cesium Chloride in Methanol−Water and Ethanol−Water Mixed Solvents by Electromotive Force Measurements at 298.15 K. *J. Chem. Eng. Data* **2007,** *52*, 357-362.
50. Nakamura, T., Development and Application of Ion-Selective Electrodes in Nonaqueous Solutions. *Analytical Sciences* **2009,** *25*, 33-40.
51. Buck, R. P.; Toth, K.; Graf, E.; Horvai, G.; Pungor, E., Donnan Exclusion Failure in Low Anion Site Density Membranes Containing Valinomycin. *J. Electroanal. Chem. Interfacial Electrochem.* **1987,** *223*, 51-66.
52. Bühlmann, P.; Amemiya, S.; Yajima, S.; Umezawa, Y., Co-Ion Interference for Ion-Selective Electrodes Based on Charged and Neutral Ionophores: A Comparison. *Anal. Chem.* **1998,** *70*, 4291-4303.
53. Brady, J. E.; Carr, P. W., Perfluorinated solvents as nonpolar test systems for generalized models of solvatochromic measures of solvent strength. *Anal. Chem.* **1982,** *54*, 1751-1757.
54. Horvath, I. T.; Rabai, J., Facile Catalyst Separation Without Water: Fluorous Biphase Hydroformylation of Olefins. *Science* **1994,** *266*, 72-75.
55. Boswell, P. G.; Anfang, A. C.; Bühlmann, P., Preparation of a Highly Fluorophilic Phosphonium Salt and its Use in a Fluorous Anion-Exchanger Membrane with High Selectivity for Perfluorinated Acids. *J. Fluorine Chem.* **2008,** *129*, 961-967.
56. van den Broeke, J.; Deelman, B.-J.; van Koten, G., Tetrakis{3,5-bis(perfluorohexyl)phenyl}borate: a Highly Fluorous Anion. *Tetrahedron Lett.* **2001,** *42*, 8085-8087.
57. Olson, E. J.; Boswell, P. G.; Givot, B. L.; Yao, L. J.; Bühlmann, P., Electrochemistry in Media of Exceptionally Low Polarity: Voltammetry with a Fluorous Solvent. *J. Electroanal. Chem.* **2010,** *639*, 154-160.
58. Auman, B. C.; Higley, D. P.; Scherer Jr, K. V.; McCord, E. F.; Shaw Jr, W. H., Synthesis of a New Fluoroalkylated Diamine, 5-[1H,1 H-2-bis(trifluoromethyl)-

Heptafluoropentyl]-1,3-Phenylenediamine, and Polyimides Prepared Therefrom. *Polymer* **1995,** *36*, 651-656.
59. Hopken, J.; Moller, M., Low-Surface-Energy Polystyrene. *Macromolecules* **1992,** *25*, 1461-1467.
60. Wang, J.; Mao, G.; Ober, C. K.; Kramer, E. J., Liquid Crystalline, Semifluorinated Side Group Block Copolymers with Stable Low Energy Surfaces: Synthesis, Liquid Crystalline Structure, and Critical Surface Tension. *Macromolecules* **1997,** *30*, 1906-1914.
61. Feiring, A. E.; Wonchoba, E. R., Synthesis of Soluble Fluorinated Vinyl Ether Copolymers by Ionic Addition of Fluoroolefins to Poly(vinyl alcohol). *Macromolecules* **1998,** *31*, 7103-7104.
62. Yamabe, M., A Challenge to Novel Fluoropolymers. *Makromol. Chem., Macromol. Symp.* **1992,** *64*, 11-18.
63. Koβmehl, G.; Fluthwedel, A.; Schäfer, H., Swellable Polymeric Networks With Star-Like Branching Points From Styrene, Acrylonitrile and Multifunctional Cyclosiloxanes. *Makromol. Chem.* **1992,** *193*, 2289-2301.
64. Marra, K. G.; Chapman, T. M.; Orban, J. M., Determination of Low Critical Surface Tensions of Novel Fluorinated Poly(amide urethane) Block Copolymers. 3. Siloxane-Containing Side Chains. *Macromolecules* **1996,** *29*, 7553-7558.
65. Miyamoto, M.; Yamanaka, H.; Aoi, K.; Sano, Y.; Saegusa, T., Preparation of Poly[(N-acetylimino)ethylene] Having (Perfluoroacylimino)ethyl End Group and Its Surface Activity. *Polym. J. (Tokyo, Jpn.)* **1995,** *27*, 461-468.
66. Ciardelli, F.; Aglietto, M.; Montagnini di Mirabello, L.; Passaglia, E.; Giancristoforo, S.; Castelvetro, V.; Ruggeri, G., New Fluorinated Acrylic Polymers for Improving Weatherability of Building Stone Materials. *Prog. Org. Coat.* **1997,** *32*, 43-50.
67. Ameduri, B.; Boutevin, B., *Well-Architectured Fluoropolymers: Synthesis, Properties and Applications*. 1 ed.; Elsevier: Oxford, UK, 2004.
68. Boswell, P. G.; Bühlmann, P., Fluorous Bulk Membranes for Potentiometric Sensors with Wide Selectivity Ranges: Observation of Exceptionally Strong Ion Pair Formation. *J. Am. Chem. Soc.* **2005,** *127*, 8958-8959.
69. Lai, C.-Z.; Fierke, M. A.; Costa, R. C. d.; Gladysz, J. A.; Stein, A.; Bühlmann, P., Highly Selective Detection of Silver in the Low ppt Range with Ion-Selective Electrodes Based on Ionophore-Doped Fluorous Membranes. *Anal. Chem.* **2010,** *82*, 7634-7640.
70. Chen, L. D.; Mandal, D.; Pozzi, G.; Gladysz, J. A.; Bühlmann, P., Potentiometric Sensors Based on Fluorous Membranes Doped with Highly Selective Ionophores for Carbonate. *J. Am. Chem. Soc.* **2011,** *133*, 20869-20877.
71. Boswell, P. G.; Szíjjártó, C.; Jurisch, M.; Gladysz, J. A.; Rábai, J.; Bühlmann, P., Fluorophilic Ionophores for Potentiometric pH Determinations with Fluorous Membranes of Exceptional Selectivity. *Anal. Chem.* **2008,** *80*, 2084-2090.
72. Chen, L. D.; Mandal, D.; Gladysz, J. A.; Buhlmann, P., Chemical Stability and Application of a Fluorophilic Tetraalkylphosphonium Salt in Fluorous Membrane Anion-Selective Electrodes. *New J. Chem.* **2010,** *34*, 1867-1874.

73. Chen, L. D.; Lai, C.-Z.; Granda, L. P.; Fierke, M. A.; Mandal, D.; Stein, A.; Gladysz, J. A.; Bühlmann, P., Fluorous Membrane Ion-Selective Electrodes for Perfluorinated Surfactants: Trace-Level Detection and in Situ Monitoring of Adsorption. *Anal. Chem.* **2013,** *85*, 7471-7477.
74. Boswell, P. G.; Lugert, E. C.; Rábai, J.; Amin, E. A.; Bühlmann, P., Coordinative Properties of Highly Fluorinated Solvents with Amino and Ether Groups. *J. Am. Chem. Soc.* **2005,** *127*, 16976-16984.
75. Lai, C.-Z.; Koseoglu, S. S.; Lugert, E. C.; Boswell, P. G.; Rábai, J.; Lodge, T. P.; Bühlmann, P., Fluorous Polymeric Membranes for Ionophore-Based Ion-Selective Potentiometry: How Inert Is Teflon AF? *J. Am. Chem. Soc.* **2009,** *131*, 1598-1606.
76. *Riess, J. G.*; *Le Blanc, M.*, Solubility and Transport Phenomena in Perfluorochemicals Relevant to Blood Substitution and Other Biomedical Applications. *Pure Appl. Chem.* **1982,** *54*, 2383-2406.
77. Maurer-Jones, M. A.; Mousavi, M. P. S.; Chen, L. D.; Bühlmann, P.; Haynes, C. L., Characterization of Silver Ion Dissolution From Silver Nanoparticles Using Fluorous-Phase Ion-Selective Electrodes and Assessment of Resultant Toxicity to Shewanella Oneidensis. *Chem. Sci.* **2013,** *4*, 2564-2572.
78. Mousavi, M. P. S.; Gunsolus, I. L.; Pérez De Jesús, C. E.; Lancaster, M.; Hussein, K.; Haynes, C. L.; Bühlmann, P., Dynamic Silver Speciation as Studied With Fluorous-Phase Ion-Selective Electrodes: Effect of Natural Organic Matter on the Toxicity and Speciation of Silver. *Sci. Total Environ.* **2015,** *537*, 453-461.
79. Latourte, L.; Blais, J.-C.; Tabet, J.-C.; Cole, R. B., Desorption Behavior and Distributions of Fluorinated Polymers in MALDI and Electrospray Ionization Mass Spectrometry. *Anal. Chem.* **1997,** *69*, 2742-2750.
80. Radhakrishnan, K.; Switek, K. A.; Hillmyer, M. A., Synthesis of Semifluorinated Block Copolymers by Atom Transfer Radical Polymerization. *J. Polym. Sci., Part A: Polym. Chem.* **2004,** *42*, 853-861.
81. Rindfleisch, F.; DiNoia, T. P.; McHugh, M. A., Solubility of Polymers and Copolymers in Supercritical CO2. *J. Phys. Chem.* **1996,** *100*, 15581-15587.
82. Just, U.; Much, H., Characterization of Polymers Using Supercritical Fluid Chromatography: Application of Adsorption Chromatography, Size Exclusion Chromatography and Adsorption Chromatography at Critical Conditions. *Int. J. Polym. Anal. Charact.* **1996,** *2*, 173-184.
83. Szwarc, M., "Living" Polymers. *Nature* **1956,** *178*, 1168-1169.
84. Hsieh, H. L.; Quirk, R. P., *Anionic polymerization: Principles and Practical Applications*. CRC Press: New york, 1996; Vol. 1.
85. Patten, T. E.; Xia, J.; Abernathy, T.; Matyjaszewski, K., Polymers with Very Low Polydispersities from Atom Transfer Radical Polymerization. *Science* **1996,** *272*, 866-868.
86. Angot, S.; Murthy, K. S.; Taton, D.; Gnanou, Y., Atom Transfer Radical Polymerization of Styrene Using a Novel Octafunctional Initiator: Synthesis of Well-Defined Polystyrene Stars. *Macromolecules* **1998,** *31*, 7218-7225.

87. Hirao, A.; Hayashi, M., Recent Advance in Syntheses and Applications of Well-Defined End-Functionalized Polymers by Means of Anionic Living Polymerization. *Acta Polym.* **1999,** *50*, 219-231.
88. Odian, G., *Principles of Polymerization*. 4 ed.; Wiley-Interscience: New York, 2004.
89. Shefer, A.; Gottlieb, M., Effect of Crosslinks on the Glass Transition Temperature of End-Linked Elastomers. *Macromolecules* **1992,** *25*, 4036-4042.
90. Ambrose, T. M.; Meyerhoff, M. E., Characterization of Photopolymerized Decyl Methacrylate as a Membrane Matrix for Ion-Selective Electrodes. *Electroanalysis* **1996,** *8*, 1095-1100.
91. Ambrose, T. M.; Meyerhoff, M. E., Photo-Cross-Linked Decyl Methacrylate Films for Electrochemical and Optical Polyion Probes. *Anal. Chem.* **1997,** *69*, 4092-4098.
92. Adams, B. A.; Holmes, E. L. Method of and Means For Effecting Anionic Exchanges in Solutions. 1939.
93. Li, N.; Guiver, M. D., Ion Transport by Nanochannels in Ion-Containing Aromatic Copolymers. *Macromolecules* **2014,** *47*, 2175-2198.
94. Grygolowicz-Pawlak, E.; Crespo, G. A.; Ghahraman Afshar, M.; Mistlberger, G.; Bakker, E., Potentiometric Sensors with Ion-Exchange Donnan Exclusion Membranes. *Anal. Chem.* **2013,** *85*, 6208-6212.
95. Helfferich, F., *Ion Exchange*. Unabridged Dover ed.; Dover: Mineola, N.Y., 1995.
96. Titvinidze, G.; Kreuer, K.-D.; Schuster, M.; de Araujo, C. C.; Melchior, J. P.; Meyer, W. H., Proton Conducting Phase-Separated Multiblock Copolymers with Sulfonated Poly(phenylene sulfone) Blocks for Electrochemical Applications: Preparation, Morphology, Hydration Behavior, and Transport. *Adv. Funct. Mater.* **2012,** *22*, 4456-4470.
97. Kong, X.; Schmidt-Rohr, K., Water–Polymer Interfacial Area in Nafion: Comparison with Structural Models. *Polymer* **2011,** *52*, 1971-1974.
98. Kressman, T. R. E., The Measurement of Ionic Activities in Solution With Electrodes Containing Ion-Exchange-Resin Membranes. *J. Appl. Chem.* **1954,** *4*, 123-131.
99. Wyllie, M. R. J.; Patnode, H. W., The The Development of Membranes Prepared from Artificial Cation-Exchange Materials with Particular Reference to the Determination of Sodium-Ion Activities. *J. Phys. Colloid Chem.* **1950,** *54*, 204-227.
100. Ghahraman Afshar, M.; Crespo, G. A.; Bakker, E., Counter Electrode Based on an Ion-Exchanger Donnan Exclusion Membrane for Bioelectroanalysis. *Biosens. Bioelectron.* **2014,** *61*, 64-69.
101. Crespo, G. A.; Ghahraman Afshar, M.; Bakker, E., Chronopotentiometry of Pure Electrolytes With Anion-Exchange Donnan Exclusion Membranes. *J. Electroanal. Chem.* **2014,** *731*, 100-106.
102. Shinwari, M. W.; Zhitomirsky, D.; Deen, I. A.; Selvaganapathy, P. R.; Deen, M. J.; Landheer, D., Microfabricated Reference Electrodes and their Biosensing Applications. *Sensors* **2010,** *10*, 1679.
103. Yu, P.; Dong, S., The Fabrication and Performance of an Ag/AgCl Reference Electrode in Human Serum. *Anal. Chim. Acta* **1996,** *330*, 167-174.
104. Bates, G. G.; Macaskill, J. B., Standard Potential of the Silver-Silver Chloride Electrode. *Pure Appl. Chem.* **1978,** *50*, 1701-1706.

105. Cobble, J. W., High-Temperature Aqueous Solutions. *Science* **1966,** *152*, 1479-1485.
106. Zhtaeva, G. V.; Shumilova, N. A., Silver. In *Standard Potentials in Aqueous Solution*, Bard, A. J.; Parsons, R.; Jordan, J., Eds. Marcel Dekker, Inc.: New York, 1985.
107. Smith, R. L.; Scott, D. C., An Integrated Sensor for Electrochemical Measurements. *IEEE Trans. Biomed. Eng.* **1986,** *BME-33*, 83-90.
108. Yee, S.; Jin, H.; Lam, L. K. C., Miniature Liquid Junction Reference Electrode With Micromachined Silicon Cavity. *Sens. Actuators* **1988,** *15*, 337-345.
109. van den Berg, A.; Grisel, A.; van den Vlekkert, H. H.; de Rooij, N. F., A Micro-Volume Open Liquid-Junction Reference Electrode for pH-ISFETs. *Sens. Actuators, B* **1990,** *1*, 425-432.
110. Huang, I. Y.; Huang, R.-S., Fabrication and Characterization of a New Planar Solid-State Reference Electrode for ISFET Sensors. *Thin Solid Films* **2002,** *406*, 255-261.
111. Liao, W.-Y.; Chou, T.-C., Fabrication of a Planar-Form Screen-Printed Solid Electrolyte Modified Ag/AgCl Reference Electrode for Application in a Potentiometric Biosensor. *Anal. Chem.* **2006,** *78*, 4219-4223.
112. Dohner, R. E.; Wegmann, D.; Morf, W. E.; Simon, W., Reference Electrode With Free-Flowing Free-Diffusion Liquid Junction. *Anal. Chem.* **1986,** *58*, 2585-2589.
113. Payne, R. B.; Buckley, B. M.; Rawson, K. M., Protein Interference with Ion-Selective Electrode Measurement Depends on Reference Electrode Composition and Design. *Ann. Clin. Biochem.* **1991,** *28*, 68-72.
114. D'Orazio, P.; Verghese, D., Hypertonic versus Isotonic Salt Bridges in Ion-Selective Electrode Based Clinical Analysers. *Ann. Clin. Biochem.* **1991,** *28*, 628-629.
115. Bosch, R. W.; Straetmans, S.; Dyck, S. V., Characterisation of Porous Ceramic Plugs for Use in Electrochemical Sensors. *J. Mater. Sci.* **2002,** *37*, 3973-3979.
116. Bott, A. W., Practical Problems in Voltammetry 3: Reference Electrodes for Voltammetry. *Curr. Sep.* **1995,** *14*, 64-68.
117. Carano, M.; Colonna, B.; Echegoyen, L.; Le Derf, F.; Levillain, E.; SallÉ, M., Aqueous Reference Electrodes are Unstable in Organic Media Containing Metal Ions: a Cautionary Note to the Supramolecular Chemistry Community. *Supramol. Chem.* **2003,** *15*, 83-85.
118. Rickert, P. G.; Antonio, M. R.; Firestone, M. A.; Kubatko, K.-A.; Szreder, T.; Wishart, J. F.; Dietz, M. L., Tetraalkylphosphonium Polyoxometalates: Electroactive, "Task-Specific" Ionic Liquids. *Dalton Trans.* **2007,** (5), 529-531.
119. Aşangil, D.; Hüdai Taşdemir, İ.; Kılıç, E., Adsorptive Stripping Voltammetric Methods for Determination of Aripiprazole. *J. Pharm. Anal.* **2012,** *2*, 193-199.
120. Do, K.; Kim, C.; Song, K.; Yun, S. J.; Lee, J. K.; Ko, J., Efficient Planar Organic Semiconductors Containing Fused Triphenylamine for Solution Processed Small Molecule Organic Solar Cells. *Sol. Energy Mater. Sol. Cells* **2013,** *115*, 52-57.
121. Mousavi, M. P. S.; Bühlmann, P., Reference Electrodes with Salt Bridges Contained in Nanoporous Glass: An Underappreciated Source of Error. *Anal. Chem.* **2013,** *85*, 8895-8901.
122. Newton, M. R.; Bohaty, A. K.; White, H. S.; Zharov, I., Chemically Modified Opals as Thin Permselective Nanoporous Membranes. *J. Am. Chem. Soc.* **2005,** *127*, 7268-7269.

123. Gyurcsányi, R. E., Chemically-Modified Nanopores for Sensing. *TrAC, Trends Anal. Chem.* **2008,** *27*, 627-639.
124. Behrens, S. H.; Grier, D. G., The Charge of Glass and Silica Surfaces. *J. Chem. Phys.* **2001,** *115*, 6716.
125. Li, P.; Zhang, F., The Electrochemistry of a Glass Surface and its Application to Bioactive Glass in Solution. *J. Non-Cryst. Solids* **1990,** *119*, 112-118.
126. Zou, X. U.; Bühlmann, P., Current Pulse Based Reference Electrodes Without Liquid Junctions. *Anal. Chem.* **2013,** *85*, 3817-3821.
127. Lindner, E.; Gyurcsányi, R. E.; Buck, R. P., Tailored Transport Through Ion-Selective Membranes for Improved Detection Limits and Selectivity Coefficients. *Electroanalysis* **1999,** *11*, 695-702.
128. Pretsch, E., The New Wave of Ion-Selective Electrodes. *Anal. chem.* **2002,** *74*, 420A-426A.
129. Morf, W. E.; Badertscher, M.; Zwickl, T.; de Rooij, N. F.; Pretsch, E., Effects of Controlled Current on the Response Behavior of Polymeric Membrane Ion-Selective Electrodes. *J. Electroanal. Chem.* **2002,** *526*, 19-28.
130. Dittmer, A., Investigation of Fluorous Phase Biofouling and Combinatorial Design of an Ammonium Ionophore. University of Minnesota: Written Preliminary Examination, 2011.
131. Ishihara, K.; Kogure, R.; Matsui, K., Polymerization Ability of Perfluoroalkyloxy Group-Substituted Styrene Derivatives and Their Surface Characteristics. *Kobunshi Ronbunshu* **1988,** *45*, 653-659.
132. Bouteiller, V.; Garnault, A. M.; Teyssié, D.; Boileau, S.; Möller, M., Synthesis, Thermal and Surface Characterization of Fluorinated Polystyrenes. *Polym. Int.* **1999,** *48*, 765-772.
133. Andruzzi, L.; Chiellini, E.; Galli, G.; Li, X.; Kang, S. H.; Ober, C. K., Engineering Low Surface Energy Polymers Through Molecular Design: Synthetic Routes to Fluorinated Polystyrene-Based Block Copolymers. *J. Mater. Chem.* **2002,** *12*, 1684-1692.
134. Lu, Z.; Zhou, X.; Hu, S.; Shu, X.; Tian, Y.; Zhu, J., Interfacial Assembly of Nanoparticles with Fluorous-Tagged Organic Molecules. *J. Phys. Chem. C* **2010,** *114*, 13546–13550.
135. *Handbook of Organic Synthesis: Fluorine-Containing Reagents*. Wiley: Chichester, England, 2007.
136. Lai, C.-Z.; Fierke, M. A.; Costa, R. C. d.; Gladysz, J. A.; Stein, A.; Bühlmann, P., Highly Selective Detection of Silver in the Low ppt Range with Ion-Selective Electrodes Based on Ionophore-Doped Fluorous Membranes. *Anal. Chem.* **2010,** *82* (18), 7634-7640.
137. Leung, A., Investigation in the Effects of Biological Interferents on Fluorous Membrane-based Ion Selective Electrodes. University of Minnesota: 2008.
138. Boswell, P. G.; Szíjjártó, C.; Jurisch, M.; Gladysz, J. A.; Rábai, J.; Bühlmann, P., Fluorophilic Ionophores for Potentiometric pH Determinations with Fluorous Membranes of Exceptional Selectivity. *Anal. Chem.* **2008,** *80* (6), 2084-2090.

139. Zhao, H.; Ismail, K.; Weber, S. G., How Fluorous Is Poly(2,2-bis(trifluoromethyl)-4,5-difluoro-1,3-dioxide-co-tetrafluoroethylene) (Teflon AF)? *J. Am. Chem. Soc.* **2004,** *126*, 13184-13185.
140. Lugert, E. C.; Lodge, T. P.; Bühlmann, P., Plasticization of Amorphous Perfluoropolymers. *J. Polym. Sci., Part B: Polym. Phys.* **2008,** *46*, 516-525.
141. da Costa, R. C.; Jurisch, M.; Gladysz, J. A., Synthesis of Fluorous Sulfur/Carbon/Sulfur Pincer Ligands and Palladium Complexes: New Catalyst Precursors for the Heck Reaction. *Inorg. Chim. Acta* **2008,** *361*, 3205-3214.
142. Mikhelson, K. N., *Ion-Selective Electrodes*. Springer: London, 2013.
143. Morf, W. E., *The Principles of Ion-selective Electrodes and of Membrane Transport*. Elsevier: New York, NY, 1981.
144. Meier, P. C., Two Parameter Debye-Huckel Approximation for the Evaluation of Mean Activity Coefficients 109 Electrolytes. *Anal. Chim. Acta* **1982,** *136*, 363–368.
145. Oesch, U.; Simon, W., Lifetime of Neutral Carrier Based Ion-Selective Liquid-Membrane Electrodes. *Anal. Chem.* **1980,** *52*, 692-700. DOI: 10.1021/ac50054a024.
146. Bassi, M.; Tonelli, C.; Di Meo, A., Glass Transition Behavior of a Microphase Segregated Polyurethane Based on PFPE and IPDI. A Calorimetric Study. *Macromolecules* **2003,** *36*, 8015-8023.
147. Gladysz, J. A.; Curran, D. P.; Horváth, I. T., *Handbook of Fluorous Chemistry*. Wiley & Sons New York, NY, 2005
148. Szigeti, Z.; Malona, A.; Vigassy, T.; Csokai, V.; Grün, A.; Wygladacz, K.; Ye, N.; Xuc, C.; Chebny, V. J.; Bitter, I.; Rathore, R.; Bakker, E.; Pretsch, E., Novel Potentiometric and Optical Silver Ion-Selective Sensors With Subnanomolar Detection Limits. *Anal. Chim. Acta* **2006,** *572*, 1-10.
149. Reynolds, R. M.; Padfield, P. L.; Seckl, J. R., Disorders of Sodium Balance. *Br. Med. J.* **2006,** *332*, 702-705.
150. Larsson, L.; Ohman, S., Serum Ionized Calcium and Corrected Total Calcium in Borderline Hyperparathyroidism. *Clin. Chem.* **1978,** *24*, 1962-1965.
151. Greenway, D. C.; Hindmarsh, J. T.; Wang, J.; Khodadeen, J. A.; Hébert, P. C., Reference Interval for Whole Blood Ionized Magnesium in a Healthy Population and the Stability of Ionized Magnesium Under Varied Laboratory Conditions. *Clin. Biochem.* **1996,** *29*, 515-520.
152. Lehnhardt, A.; Kemper, M., Pathogenesis, Diagnosis and Management of Hyperkalemia. *Pediatr. Nephrol. (Berlin)* **2011,** *26*, 377-384.
153. Bakker, E., Enhancing Ion-Selective Polymeric Membrane Electrodes by Instrumental Control. *TrAC, Trends Anal. Chem.* **2014,** *53*, 98-105.
154. Amemiya, S., *Potentiometric Ion-Selective Electrodes, in "Handbook of Electrochemistry"; Zoski, C. G., ed.;* . Elsevier: Amsterdam, 2007; p 261-294. DOI: 10.1016/b978-044451958-0.50020-3.
155. Bobacka, J.; Ivaska, A.; Lewenstam, A., Potentiometric Ion Sensors. *Chem. Rev.* **2008,** *108*, 329-351.
156. Bühlmann, P.; Pretsch, E.; Bakker, E., Carrier-Based Ion-Selective Electrodes and Bulk Optodes. 2. Ionophores for Potentiometric and Optical Sensors. *Chem. Rev.* **1998,** *98*, 1593-1688.

157. Yajima, S.; Tohda, K.; Bühlmann, P.; Umezawa, Y., Donnan Exclusion Failure of Neutral Ionophore-Based Ion-Selective Electrodes Studied by Optical Second-Harmonic Generation. *Anal. Chem.* **1997,** *69*, 1919-1924.
158. Makra, I.; Jágerszki, G.; Bitter, I.; Gyurcsányi, R. E., Nernst–Planck/Poisson Model for the Potential Response of Permselective Gold Nanopores. *Electrochim. Acta* **2012,** *73*, 70-77.
159. Lindner, E.; Umezawa, Y., Performance Evaluation Criteria for Preparation and Measurement of Macro- and Microfabricated Ion-Selective Electrodes (IUPAC Technical Report). *Pure Appl. Chem.* **2008,** *80*, 85-104.
160. Woźnica, E.; Wójcik, M. M.; Wojciechowski, M.; Mieczkowski, J.; Bulska, E.; Maksymiuk, K.; Michalska, A., Improving the Upper Detection Limit of Potentiometric Sensors. *Electroanalysis* **2015,** *27*, 720-726.
161. Kounaves, S. P.; Chaniotakis, N. A.; Chevrier, V. F.; Carrier, B. L.; Folds, K. E.; Hansen, V. M.; McElhoney, K. M.; O'Neil, G. D.; Weber, A. W., Identification of the perchlorate parent salts at the Phoenix Mars landing site and possible implications. *Icarus* **2014,** *232*, 226-231.
162. Jágerszki, G.; Takács, Á.; Bitter, I.; Gyurcsányi, R. E., Solid-State Ion Channels for Potentiometric Sensing. *Angew. Chem. Int. Ed.* **2011,** *50*, 1656-1659.
163. Wang, G.; Zhang, B.; Wayment, J. R.; Harris, J. M.; White, H. S., Electrostatic-Gated Transport in Chemically Modified Glass Nanopore Electrodes. *J. Am. Chem. Soc.* **2006,** *128*, 7679-7686.
164. Zhang, Y.; Zhang, B.; White, H. S., Electrochemistry of Nanopore Electrodes in Low Ionic Strength Solutions. *J. Phys. Chem. B* **2006,** *110*, 1768-1774.
165. Bakker, E.; Nägele, M.; Schaller, U.; Pretsch, E., Applicability of the Phase Boundary Potential Model to the Mechanistic Understanding of Solvent Polymeric Membrane-Based Ion-Selective Electrodes. *Electroanalysis* **1995,** *7*, 817-822.
166. Carey, J. L.; Whitcomb, D. R.; Chen, S.; Penn, R. L.; Bühlmann, P., Potentiometric in Situ Monitoring of Anions in the Synthesis of Copper and Silver Nanoparticles Using the Polyol Process. *ACS Nano* **2015**. DOI: 10.1021/acsnano.5b05170.
167. For a definition of ionophore-free ion-exchanger membranes, see ref. 5, p 1595.
168. He, N.; Lindfors, T., Determination of Water Uptake of Polymeric Ion-Selective Membranes with the Coulometric Karl Fischer and FT-IR-Attenuated Total Reflection Techniques. *Anal. Chem.* **2013,** *85*, 1006-1012.
169. Fumatech Technical Data Sheet - Fumasep FAB. http://www.fumatech.com/NR/rdonlyres/0351A53E-568D-4BB9-A0DA-A57848AA1B2D/0/fumasepFAB.pdf (accessed July 2, 2015).
170. Amemiya, S.; Bühlmann, P.; Tohda, K.; Umezawa, Y., Hydrogen bond based recognition of nucleotides by neutral-carrier ion-selective electrodes. *Anal. Chim. Acta* **1997,** *341*, 129-139.
171. Ammann, D.; Huser, M.; Kräutler, B.; Rusterholz, B.; Schulthess, P.; Lindemann, B.; Halder, E.; Simon, W., Anion Selectivity of Metalloporphyrins in Membranes. *Helv. Chim. Acta* **1986,** *69*, 849-854.

172. Chaniotakis, N. A.; Chasser, A. M.; Meyerhoff, M. E.; Groves, J. T., Influence of Porphyrin Structure on Anion Selectivities of Manganese(III) Porphyrin Based Membrane Electrodes. *Anal. Chem.* **1988,** *60*, 185-188.
173. Kondo, Y.; Bührer, T.; Frömter, E.; Simon, W., A New Double-Barrelled, Ionophore-Based Microelectrode For Chloride Ions. *Pflügers. Arch.* **1989,** *414*, 663-668.
174. Kressman, T. R. E., Ion Exchange Separations Based Upon Ionic Size. *J. Phys Chem.* **1952,** *56*, 118-123.
175. The Human Metabolome Database. http://www.hmdb.ca/metabolites/HMDB36795 (accessed September 23, 2015).
176. Henderson, L. J., Concerning the Relationship Between the Strength of Acids and their Capacity to Preserve Neutrality. *Am. J. Physiol.* **1908,** *21*, 173-79.
177. Tratnyek, P. G.; Hoigne, J., Kinetics of Reactions of Chlorine Dioxide (OClO) in Water. 2. Quantitative Structure–Activity Relationships for Phenolic Compounds. *Water Res.* **1994,** *28*, 57-66.
178. Girault, H. H. J.; Schiffrin, D. J., Electrochemistry of Liquid–Liquid Interfaces. In *Electroanalytical Chemistry*, Bard, A. J., Ed. Marcel Dekker: New York, 1989; Vol. 15, pp 1-141.
179. Nakayama, H.; Kuwata, H.; Yamamoto, N.; Akagi, Y.; Matsui, H., Solubilities and Dissolution States of a Series of Symmetrical Tetraalkylammonium Salts in Water. *Bull. Chem. Soc. Jpn.* **1989,** *62*, 985-992.
180. Richardson, R. W., Diffusion in Ion-Exchange Media. *Nature* **1949,** *164*, 916-17.
181. Gärtner, K.; Griessbach, R.; Anton, E., Porenstrukturuntersuchungen von Kunstharzaustauschern durch Austauschadsorption Grosser Organischer Farbstoffe. *Kolloid Z.* **1960,** *175*, 123-26.
182. Lee, K. S.; Shin, J. H.; Han, S. H.; Cha, G. S.; Shin, D. S.; Kim, H. D., Asymmetric Carbonate Ion-Selective Cellulose Acetate Membrane Electrodes With Reduced Salicylate Interference. *Anal. Chem.* **1993,** *65*, 3151-3155.
183. Oh, K.-C.; Kim, K.-A.; Paeng, I. R.; Baek, D.-j.; Paeng, K.-J., Anion-Selective Membrane Electrodes Based On Polymer-Supported Metalloporphyrins. *J. Electroanal. Chem.* **1999,** *468*, 98-103.
184. Griessbach, R., *Austauschadsorption in Theorie und Praxis*. Akademie-Verlag: Berlin, 1957.
185. Kim, H. S., Electrostatic Gibbs Free Energy and Solvation Number of Tetraalkylammonium Ions in Pyridine at 25 ºC Obtained Using Conductance of Corresponding Ion. *Bull. Korean Chem. Soc.* **1998,** *19*, 1347-50.
186. Pradhan, N.; Pal, A.; Pal, T., Silver Nanoparticle Catalyzed Reduction of Aromatic Nitro Compounds. *Colloids Surf. A* **2002,** *196*, 247-257.
187. Kamat, P. V., Photophysical, Photochemical and Photocatalytic Aspects of Metal Nanoparticles. *J. Phys. Chem. B* **2002,** *106*, 7729-7744.
188. Li, Y.; Wu, Y.; Ong, B. S., Facile Synthesis of Silver Nanoparticles Useful for Fabrication of High-Conductivity Elements for Printed Electronics. *J. Am. Chem. Soc.* **2005,** *127*, 3266-3267.
189. Shipway, A. N.; Katz, E.; Willner, I., Nanoparticle Arrays on Surfaces for Electronic, Optical, and Sensor Applications. *ChemPhysChem* **2000,** *1*, 18-52.

190. Michaels, A. M.; Jiang, J.; Brus, L., Ag Nanocrystal Junctions as the Site for Surface-Enhanced Raman Scattering of Single Rhodamine 6G Molecules. *J. Phys. Chem. B* **2000,** *104*, 11965-11971.
191. Maier, S. A.; Brongersma, M. L.; Kik, P. G.; Meltzer, S.; Requicha, A. A. G.; Atwater, H. A., Plasmonics—A Route to Nanoscale Optical Devices. *Adv. Mater.* **2001,** *13*, 1501-1505.
192. Magdassi, S.; Bassa, A.; Vinetsky, Y.; Kamyshny, A., Silver Nanoparticles as Pigments for Water-Based Ink-Jet Inks. *Chem. Mater.* **2003,** *15*, 2208-2217.
193. Rai, M.; Yadav, A.; Gade, A., Silver Nanoparticles as a New Generation of Antimicrobials. *Biotechnol. Adv.* **2009,** *27*, 76-83.
194. Lee, K.-S.; El-Sayed, M. A., Gold and Silver Nanoparticles in Sensing and Imaging: Sensitivity of Plasmon Response to Size, Shape, and Metal Composition. *J. Phys. Chem. B* **2006,** *110*, 19220-19225.
195. Magdassi, S.; Grouchko, M.; Kamyshny, A., Copper Nanoparticles for Printed Electronics: Routes Towards Achieving Oxidation Stability. *Materials* **2010,** *3*, 4626-4638.
196. Fievet, F.; Lagier, J. P.; Figlarz, M., Preparing Monodisperse Metal Powders in Micrometer and Submicrometer Sizes by the Polyol Process. *MRS Bull.* **1989,** *14*, 29-34.
197. Chokratanasombat, P.; Nisaratanaporn, E., Preparation of Ultrafine Copper Powders with Controllable Size *via* Polyol Process with Sodium Hydroxide Addition. *Eng. J.* **2012,** *16*, 39-46.
198. Park, K. H.; Im, S. H.; Park, O. O., The Size Control of Silver Nanocrystals With Different Polyols and its Application to Low-Reflection Coating Materials. *Nanotechnology* **2011,** *22*, 1-6.
199. Wiley, B.; Sun, Y.; Mayers, B.; Xia, Y., Shape-Controlled Synthesis of Metal Nanostructures: The Case of Silver. *Chem. Eur. J.* **2005,** *11*, 454-463.
200. Jianfeng, Y.; Guisheng, Z.; Anming, H.; Zhou, Y. N., Preparation of PVP Coated Cu NPs and the Application for Low-Temperature Bonding. *J. Mater. Chem.* **2011,** *21*, 15981-15986.
201. Skrabalak, S. E.; Wiley, B. J.; Kim, M.; Formo, E. V.; Xia, Y., On the Polyol Synthesis of Silver Nanostructures: Glycolaldehyde as a Reducing Agent. *Nano Lett.* **2008,** *8*, 2077-2081.
202. Zhang, L.; Wang, Y.; Tong, L.; Xia, Y., Seed-Mediated Synthesis of Silver Nanocrystals with Controlled Sizes and Shapes in Droplet Microreactors Separated by Air. *Langmuir* **2013,** *29*, 15719-15725.
203. Miyamoto, R. Silver Wire and Its Manufacture by Reduction. Japanese Laid Open Patent Publication 2008-190006, Aug 21, 2008.
204. Zhang, Q.; Li, W.; Moran, C.; Zeng, J.; Chen, J.; Wen, L.-P. W.; Xia, Y., Seed-Mediated Synthesis of Ag Nanocubes with Controllable Edge Lengths in the Range of 30-200 nm and Comparison of Their Optical Properties *J. Am. Chem. Soc.* **2010,** *132*, 11372–11378.
205. Habas, S. E.; Lee, H.; Radmilovic, V.; Somorjai, G. A.; Yang, P., Shaping Binary Metal Nanocrystals Through Epitaxial Seeded Growth. *Nat. Mater.* **2007,** *6*, 692-697.

206. Nandanwar, S. U.; Chakraborty, M.; Mukhopadhyay, S.; Shenoy, K. T., Stability of Ruthenium Nanoparticles Synthesized by Solvothermal Method. *Cryst. Res. Technol.* **2011,** *46*, 393-399.
207. Donnabelle, M. L. B. Syntheses of Metallic Cobalt Nanoparticles and Nanowires by Electroless Deposition. PhD. Thesis [Online]. Kyoto University, September 2011. http://repository.kulib.kyoto-u.ac.jp/dspace/bitstream/2433/151979/2/D_Mary%20Donnabelle%20Lirio%20Balela.pdf (September 12, 2015).
208. Balela, M. D. L.; Yagi, S.; Lockman, Z.; Aziz, A.; Amorsolo, A. V. J.; Matsubara, E., Electroless Deposition of Ferromagnetic Cobalt Nanoparticles in Propylene Glycol. *J. Electrochem. Soc.* **2009,** *159*, E139- E142.
209. Steinfeldt, N., In Situ Monitoring of Pt Nanoparticle Formation in Ethylene Glycol Solution by SAXS—Influence of the NaOH to Pt Ratio. *Langmuir* **2012,** *28*, 13072-13079.
210. Boita, J.; Nicolao, L.; Alves, M. C. M.; Morais, J., Observing Pt Nanoparticle Formation at the Atomic Level During Polyol Synthesis. *Phys. Chem. Chem. Phys.* **2014,** *16*, 17640-17647.
211. Mowery, K. A.; Schoenfisch, M. H.; Baliga, N.; Wahr, J. A.; Meyerhoff, M. E., More Biocompatible Electrochemical Sensors Using Nitric Oxide Release Polymers. *Electroanalysis* **1999,** *11*, 681-686.
212. De Beer, D., Potentiometric Microsensors for In Situ Measurements in Aquatic Environments. *IUPAC Ser. Anal. Phys. Chem. Environ. Syst.* **2000,** *6*, 161-194.
213. Jain, A.; Gupta, V. K.; Singh, R.; Khurana, U.; Singh, L. P., Nickel(II) -selective sensors based on heterogeneous membranes of macrocyclic compounds *Sens. Actuators* **1996,** *40*, 15-20
214. Chumbimuni-Torres, K. Y.; Bakker, E.; Wang, J., Real-Time Probing of the Growth Dynamics of Nanoparticles Using Poteniometric Ion-Selective Electrodes. *Electrochem. Commun.* **2009,** *11*, 1964-1967.
215. Adams, B. A.; Holmes, E. L. Method of and Means For Effecting Anionic Exchanges in Solutions. U.S. Patent 2,151,883, Mar. 28, 1939.
216. Bergin, M. J.; Heyn, A. H. A., Electrochemical Behavior of Cation Exchange Membranes in Liquid Ammonia. *J. Am. Chem. Soc.* **1954,** *76*, 4765–4769.
217. Schmidt-Rohr, K.; Chen, Q., Parallel Cylindrical Water Nanochannels in Nafion Fuel-Cell Membranes. *Nat. Mater.* **2008,** *7*, 75-83.
218. AGC Engineering. Selemion Ion Exchange Membranes. http://www.selemion.com/SELC.pdf (accessed July 2, 2015).
219. Membranes International INC. AMI-7001 Anion Exchange Membranes Technical Specifications. http://www.membranesinternational.com/tech-ami.htm (accessed July 2, 2015).
220. Brockis, J. O. M.; Reddy, A. K. N., *Modern Electrochemistry 1 Ionics*. 2 ed.; Plenum Press: New York, NY, 1998; p 767.
221. Bard, A. J.; Faulkner, L. R., *Electrochemical Methods: Fundamentals and Applications*. 2 ed.; Wiley: New York, NY, 2001; p 833.

222. Bühlmann, P.; Pretsch, E.; Bakker, E., Carrier-Based Ion-Selective Electrodes and Bulk Optodes. 2. Ionophores for Potentiometric and Optical Sensors. *Chem. Rev.* **1998,** *98*, 1593−1687.
223. Bae, S.-E.; Stewart, K. L.; Gewirth, A. A., Nitrate Adsorption and Reduction on Cu(100) in Acidic Solution. *J. Am. Chem. Soc.* **2007,** *129*, 10171–10180.
224. Hong, G. H.; Kang, S. W., Synthesis of Monodisperse Copper Nanoparticles by Utilizing 1-Butyl-3-methylimidazolium Nitrate and Its Role as Counteranion in Ionic Liquid in the Formation of Nanoparticles. *Ind. Eng. Chem. Res.* **2013,** *52*, 794-797.
225. Agnihotri, S.; Mukherji, S.; Mukherji, S., Size-controlled silver nanoparticles synthesized over the range 5-100 nm using the same protocol and their antibacterial efficacy. *RSC Adv.* **2014,** *4*, 3974-3983.
226. Ogawara, S.; Carey, J. L.; Zou, X. U.; Bühlmann, P., Donnan Failure of Ion-Selective Electrodes with Hydrophilic High-Capacity Ion-Exchanger Membranes. *ACS Sens.* **2015**. DOI: 10.1021/acssensors.5b00128.
227. Wendt, K., *QuikChem Method 10-107-04-1-A Determination of Nitrate/Nitrite in Surface and Wastewaters by Flow Injection Analysis*. Instraments, L., Ed. Milwaukee, WI, 2000; pp 1-17.
228. Rasband, W. S., *ImageJ,*. 1st ed. ed.; U.S. National Institutes of Health: Bethesda, MD, 1997.
229. Shvarev, A.; Bakker, E., Pulsed Galvanostatic Control of Ionophore-Based Polymeric Ion Sensors. *Anal. Chem.* **2003,** *75*, 4541-4550.
230. Hodgson, T. H., The Chloride Content of Blood Serum and Aqueous Humour. Its Relation to Glaucoma and to the Formation of Intra-Ocular Fluid. *J. Physiol.* **1938,** *94*, 118-123.